T STUDIES ON THE PRIMARY PHLOEM OF GOMPHOCARPUS PHYSOCARPUS

/ by

A CHRISTIAAN EDWARD JOHANNES BOTHA. —

M.Sc. (Natal)

Submitted for the degree of
Doctor of Philosophy in the
Faculty of Science,
University of Natal,
Pietermaritzburg.

October, 1974.

To my Mother, Cynthia Marjorie Botha, who in the latter years of her life made many personal sacrifices for, and displayed an active interest in my progress.

CONTENTS

TABLES

ABSTRACT

Penetration of the stems and leaves of Gomphocarpus physocarpus by the aphid, Aphis nerii was studied with light and phase microscopes. Penetration of the epidermis and ground tissue was largely intercellular, that of the phloem tissues partly intercellular and in part intracellular. Of 75 pairs of stylet tips encountered in presumably functional sieve tubes 73 were lodged in sieve tubes of the internal and adaxial phloem. Light and electron microscope investigation of the ontogeny and differentiation of the primary phloem revealed that the internal and adaxial phloem attains a more advanced stage of maturity earlier than the corresponding external and abaxial strands. Furthermore, the protoadaxial phloem sieve tubes remain functional throughout the primary stages of growth, whereas the corresponding abaxial phloem sieve plates are associated with massive deposits of definitive callose during the latter stages of primary growth. The internal and adaxial phloem was found to be capable of independent assimilate translocation in plants which had the external phloem experimentally ringbarked. Translocation in the internal and adaxial phloem of such plants was unaffected by ringbarking. The results are interpreted as indicating that a greater proportion of assimilates is translocated in the internal and adaxial phloem sieve tubes than in the external and abaxial sieve tubes. It is concluded that this governs A. nerii's preference for the internal and adaxial phloem as a prime feeding site.

1. INTRODUCTION

Plants containing internal phloem are not common amongst the Dicotyledons. Metcalfe and Chalk (1950) list 13 familes in which internal phloem occurs commonly, amongst which are the Asclepiadaceae. Internal phloem occurs infrequently to rarely in a further 14 Dicotyledonous families.

Very little is known about phloem translocation of assimilates and other organic substances in plants which contain both external and internal phloem. Much of the present state of knowledge of the mechanisms involved in the translocation of assimilates and other dissolved organic constituents of phloem sap has been worked out from plants which have external phloem only. It is easier to work with such plants, as damaging manipulative techniques are kept to a minimum.

Autoradiographic techniques have long been used in an effort to reduce the damage caused by manipulation of the plants during translocation experiments. With few exceptions, such investigations have been confined to plant species lacking internal phloem or bicollateral bundles. Webb and Gorham (1964) using tissue autoradiographic techniques, demonstrated that distribution of ^{14}C after a 30 minute assimilation period was equally heavy in adaxial and abaxial phloem of bicollateral bundles in petioles of mature leaves of Cucurbita melopepo. Later, Tripp and Gorham (1968) suggested that bidirectional transport of tritiated glucose and ^{14}C assimilate took place in the phloem of C. melopepo. Their autoradiographic results further suggested that under the experimental conditions, the internal phloem carried no radioactive assimilate. In other words, under the experimental conditions, the results of Webb and Gorham (1964) and Tripp and Gorham (1968) would seem to

indicate that the external and internal phloem in stems and the adaxial and abaxial phloem in petioles of C. melopepo may be capable of performing different translocatory functions. However, it must be borne in mind that early results such as those of Webb and Gorham (1964) and Tripp and Gorham (1968) are subject to criticism in the light of more refined techniques used in the autoradiography of water and soluble substances (Fritz and Eschrich, 1970). More recently, Sheldrake (1972), using liquid scintillation techniques, demonstrated that polar transport of auxin was confined mainly to the internal phloem of Nicotiana tabacum (cv. Java). He suggested that the increasing ability of the internal phloem to transport auxin is probably associated with the progressive secondary development of the internal phloem.

The technique of using feeding aphids and severed aphid mouthparts was used by Kennedy and Mittler (1953) to study the nutrition of Tuberolachnus salignus (Gmelin). Weatherley, Peel and Hill (1958) applied this technique to study the sieve tube physiology of Salix viminalis. Subsequently, an increasing number of investigators have adopted this technique in attempts to rationalize some of the many problems and major controversies associated with phloem translocation. The reason for the adoption of aphid feeding techniques is simply that the relatively narrow diameter of the piercing organs of aphids (5,0 to 3,0 µm and less) are likely to cause less substantial damage to the sieve tubes than other known techniques. However, all investigations have been confined to plant species with external phloem only. Many of the aphid species used were large, and could consequently damage the sieve tubes after prolonged periods of feeding (Evert et al., 1968, and the literature cited therein).

If meaningful results were to be obtained from a study of the trans-

location of assimilates in the phloem of a plant which contained both external and internal phloem, aphid feeding experiments would have to be incorporated in the experimental procedures. The use of live, feeding aphids was thought to be preferable to severed stylets, as the latter could well be responsible for the formation of a local sink, towards which the assimilates would be attracted.

The problem was to find a plant with external and internal phloem, which was the host of a suitable small aphid. Further the aphid would have to have piercing organs of small diameter, so as not to appreciably damage the sieve elements. Aphis nerii is a small yellow aphid, which ranges in size from 1,0 to 1,5 mm in length. The aphid was observed to feed on Gomphocarpus physocarpus, a member of the Asclepiadaceae, or milkweed, which is a family of shrubs and herbs occurring mainly in warm countries and numerous in South Africa. G. physocarpus is a shrub which may attain a height of about four to five feet and lives usually for about two to four years.

Some of the plant material with attached aphids was collected, hand-sectioned and observed under a microscope. A stylet sheath was seen to traverse the stem tissue, terminating in the internal phloem of the plant. Of great interest was the fact that the stylet track had passed through an external phloem bundle. Further investigation revealed a similar pattern of penetration. In other words, it appeared that the aphid fed preferentially on the internal phloem. Did the aphid feed on the internal phloem by chance or by choice? If by choice, then what factors influenced its choice? As far as could be ascertained, no other observations of preferential feeding by aphids on internal phloem of bicollateral bundles had been recorded. The literature revealed one very important and well-documented point, which seems to have been overlooked by investigators of

phloem translocation. Hanstein (1864) recognised internal phloem in the Apocynaceae, Solanaceae, Cichoreae and the Asclepiadaceae. Moreover, Hanstein conducted ringbarking experiments which revealed that the organic materials continued to move through the ringed portion of the stem. These early observations can give no indication if, on reaching the ring, the organic materials bypass it via the internal phloem. Equally important, Hanstein's observations do not yield information on the fate of the organic material in the external phloem above the ringed portion of the stem, and also whether the internal phloem is damaged in any way due to ringing. To date, the answers to these questions remain unsolved.

The aphid's apparent preference for internal phloem as a food source, coupled with Hanstein's findings seemed to indicate that the internal phloem may continue to function in the long distance translocation of assimilates even when the bark is completely removed over part of the stem.

The primary aim of this study was twofold: firstly to determine the relationship of the external and internal phloem in the translocation of assimilates in Gomphorcarpus physocarpus, and secondly to determine the anatomical, ultrastructural, and physiological factors which influenced the choice of feeding site of Aphis nerii. Further, it was hoped that the information gained would be of use to other investigators of phloem translocation and that this study would stimulate further research on the minority group of Dicotyledons which have both external and internal phloem.

2. MATERIALS AND METHODS

2.1 Light and Electron Microscopy

Suitable stem segments, apicies and leaves of varying morphological age were excised from vigorous Gomphocarpus physocarpus (E. Mey) plants and immediately transferred to either FAA (Sass, 1958) or to 0,05 M cacodylate buffer pH. 7,0. After the plant material was placed in the buffer the median portion was removed under buffer and immediately transferred to 6% gluteraldehyde in cacodylate buffer, pH 7,0. Fixation and further processing was according to the method of Evert et al (1973a) .

The stem segments which were placed in FAA were fixed under low vacuum and dehydrated in an alcohol series and embedded in paraffin wax, to which 20% (w/w) of ceresin had been added. Sections were cut at 4 - 8 µm. The sections were variously stained in either safranin-fast green (Sass, 1958), or in periodic acid-schiff (PAS) and counter-stained with toluidine blue, pH 4,5 (Feder and O'Brien, 1968).

The gluteraldehyde-fixed stem and leaf segments were embedded in Epron-Araldite. Sections were cut on an LKB Ultrome II at 0,25 - 0,5 µm and stained in PAS- toluidine blue. Selected sections were photographed under phase and transmitted light.

For electron microscopy, ultrathin sections were poststained in uranyl acetate and lead citrate prior to viewing with a Hitachi HU-11E electron microscope (Reynolds, 1963).

2.2 Light Microscopy of Stylet Penetration

Colonies of the aphid, Aphis nerii (B. de F.) were established on G. physocarpus plants ranging in age from six to twenty weeks and older. Plants with suitably established aphid colonies were selected for light microscope investigation of stylet penetration . The aphids were killed in situ by exposing them to 100% acrolein vapour. Leaves and stem segments to which aphids remained attached, were immediately

transferred to FAA and were fixed under low vacuum for 24 hours, after which the tissue was diced into smaller more manageable pieces, and dehydrated through an alcohol series. Embedment procedure was as described in 2.1 above. Sections 12 µm thick were variously stained. Safranin-fast green proved to be the most suitable staining combination.

With this stain combination the stylets stained a golden brown colour and the salivary sheath a dark red. Selected sections were photographed under phase and transmitted light.

2.3 Preparation of Stock ^{14}Carbonate and Generation of $^{14}CO_2$

5,0 mg of $Ba^{14}CO_3$ (Radiochemical Centre, Amersham), specific activity 61,1 mCi/mM, was blended with 5,0 g of $BaCO_3$. The activity of the resulting mixture was approximately $6,47 \times 10^5$ dpm/mg. 10,0 mg of the stock carbonate was added to 2,0 ml test-tubes, which were positioned on lengths of dowelling with the mouth of the test-tube being in close proximity to the abaxial leaf surface. One ml of 0,5 N H_2SO_4 was carefully added to the test-tube, in such a way that the acid ran down the wall of the tube. Before the acid reached the carbon source, the mouth of the tube was sealed onto the abaxial leaf surface with strips of masking tape.

At termination of the experiments, 1,0 ml of 100% ethanol was added to scintillation vials, to which was added the plant material, or in the case of the aphid feeding experiments, the segments of cellophane disc. After cold extraction for a period of from 0,5 to 4,0 h, 15 ml of scintillation fluid was added and the amount of ^{14}C present in each vial determined in a Unilux II Nuclear Chicago liquid scintillator, by standard channels ration methods to determine the quench correction values. Radioactivity, in terms of dpm, was computed on a desk-top computer.

2.4 Experiments With Aphid Colonies

Colonies of the aphid A. nerii were established on 20-week-old Gomphocarpus plants, usually four to seven days before the plants were used experimentally. The technique used to collect honeydew was essentially similar to that of Eschrich (1966) with the exception

that the radioactive honeydew was collected on a cellophane disc, which was placed on the face of a clinostat. At termination, the cellophane discs were cut into their respective hr segments, placed in scintillation vials and treated as described in 2.3 above.

2.5 Determination of ^{14}C-Assimilate in the Bark and Pith: Bark-stripping technique

A 10 cm portion of the stem of selected plants was marked into 1 cm sections with India ink, 5 cm above and below the mature leaf which was to be exposed to $^{14}CO_2$. At termination, the stems were rapidly debladed and cut into their respective 1 cm segments.

The bark, consisting of epidermis, cortex, primary phloem fibres, external phloem and cambium, was carefully excised from the rest of the stem, which included the xylem, internal phloem and pith (this central core will henceforth be referred to merely as the "pith"). The excised bark and pith were placed in separate scintillation vials and treated and assayed for radioactivity as described previously.

2.6 Import/Export Relationships in Young and Mature Leaves

In order to facilitate easy identification of individual leaves after they were removed from the stems of experimental plants, all less mature leaves to the right of the mature leaf exposed to $^{14}CO_2$ (one of leaf pair nine) were lightly spotted with India ink.

Treatment was as follows. Some of the plants were ringbarked, either 1 cm above or 1 cm below the node of the feeder leaf. Other untreated plants served as intact controls. The ringbarked and control plants were allowed to stand in the greenhouse for 1 h. All plants which showed signs of wilting during this time were discarded. Exposure to $^{14}CO_2$ was as previously described. At termination, the apical meristem and first pair of leaves were removed and placed in a scintillation vial. Leaf pairs two to six were placed seperately in scintillation vials, dissected into smaller pieces and cold extracted for a period of 4 h prior to assay of radioactivity.

3. PENETRATION OF EXTERNAL AND INTERNAL PHLOEM BY STYLETS OF APHIS NERII

3.1 Results and Discussion

3.1.1 Brief Description of Stem and Leaf Segments Examined

As mentioned, the stems ranged in age from six to 20 weeks, and older. Both young and mature leaves were examined.

Most aphid feeding occurred on young stems, consisting almost entirely of primary tissues. As seen in Figs. 1-4, the six week old stem consists of a uniseriate epidermis, a cortical region of 1-3 layers of partly differentiated collenchyma cells and several layers of parenchyma, a ring of primary vascular bundles of varying age associated with relatively narrow parenchymatous interfasicular regions, and a pith. In the stem of Figs. 1-4 the external and internal phloem is entirely primary; that is, it is procambial in origin.

In both the external and internal primary phloem the sieve elements and associated parenchymatous elements, including the companion cells, occur in more or less distinct groups, the number of groups per vascular bundle being directly proportional to the size of the bundle. The external phloem bundles contain 2 - 10 sieve tubes. The internal generally contain more sieve tubes (range 1 - 20 or more) than the external bundles. Articulate laticifers occur throughout the stems, but are associated mainly with the external and internal phloem.

The larger vascular bundles of the leaf are bicollateral i.e. they contain both adaxial and abaxial phloem (Figs. 15 and 16). The bundle of the petiole and midrib exhibits a limited amount of secondary growth through

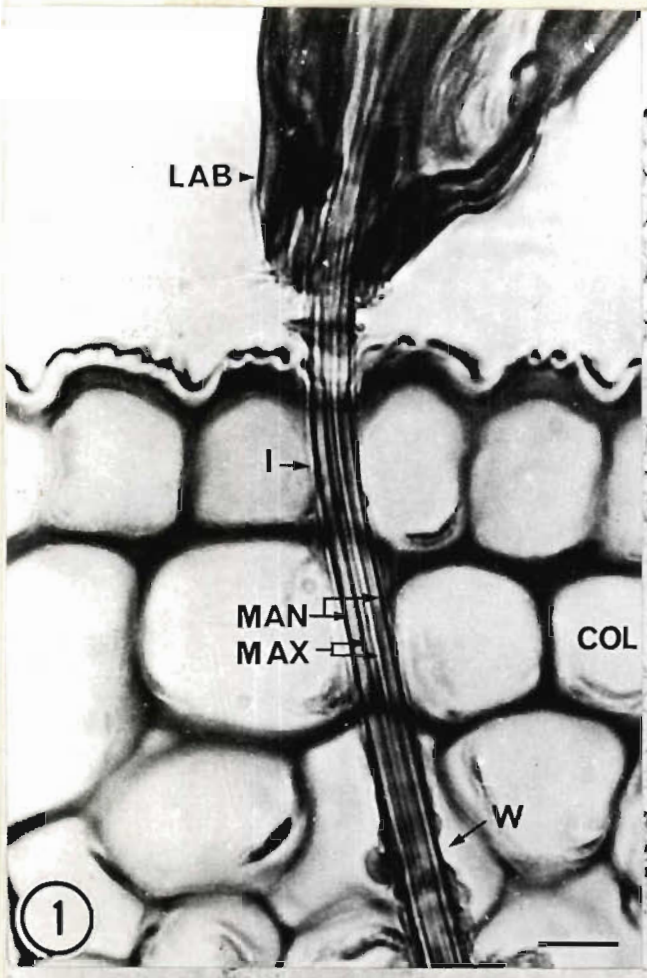
LAB
I
MAN
MAX
COL
W
1

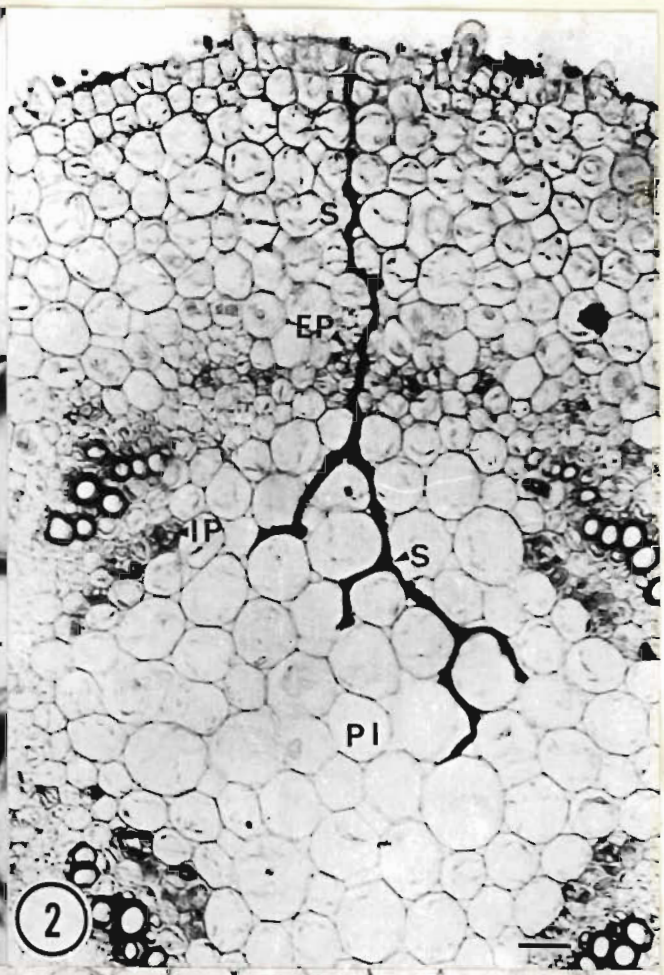
S
EP
IP
S
PI
2

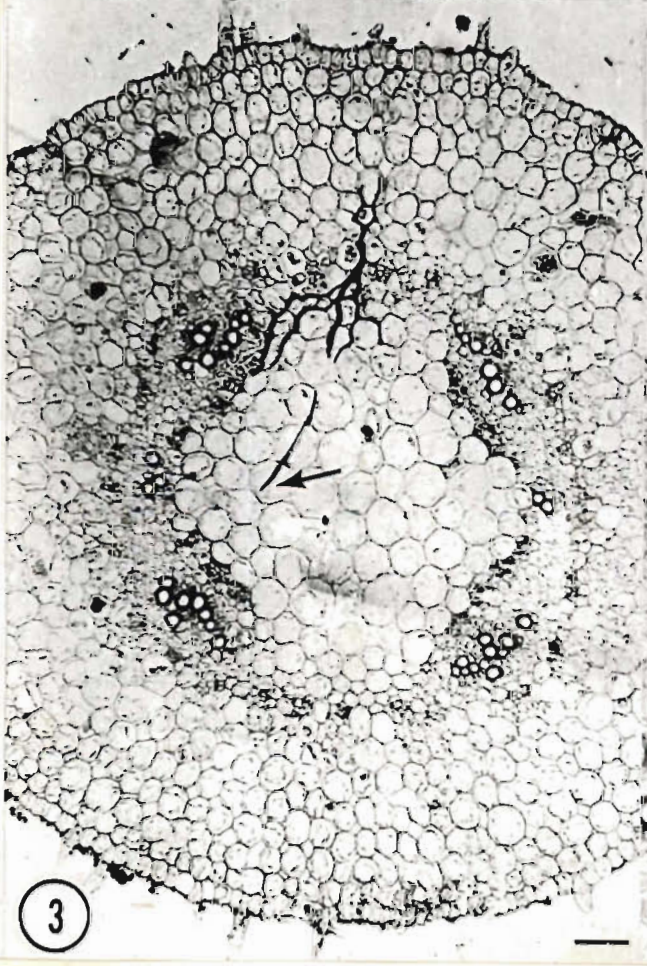
3

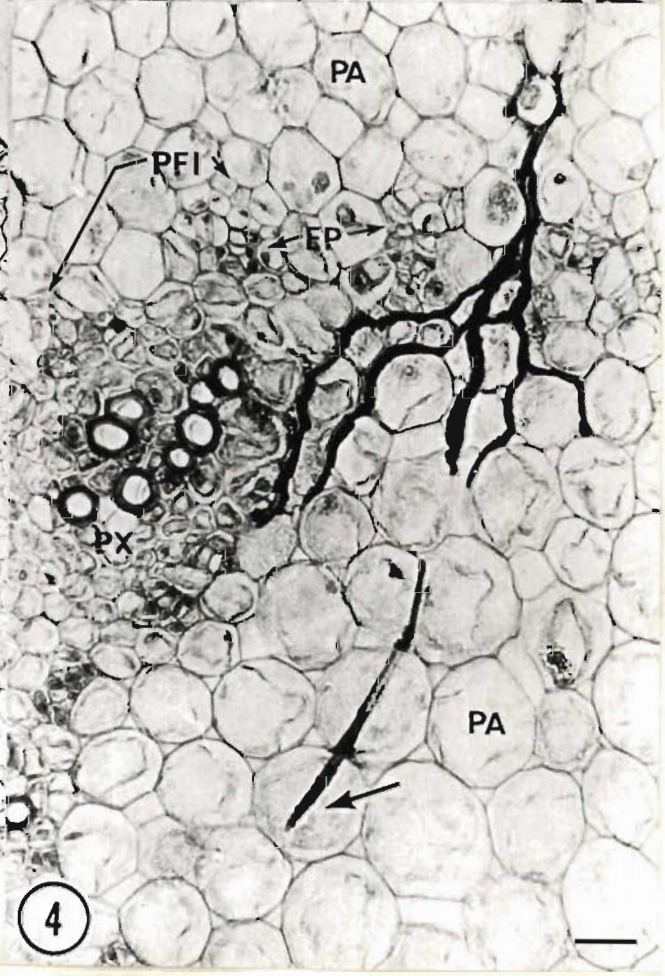
PA
PFI
EP
PX
PA
4

Figs. 1-4. Transections of six week old stem tissue, showing several attempts at phloem probes . Fig. 1. Shows penetration of a stylet group through the uniseriate epidermis and underlying partly differentiated collenchyma. Penetration is predominantly intercellular, except for the lower, partly differentiated collenchyma cell which has been penetrated intracellularly and contains salivary material . LAB = labium, MAN = mandibular stylets, MAX = maxillary stylets, COL = collenchyma, I = intercellular penetration, W = intracellular penetration . Scale line represents 6 µm.

Fig. 2. Shows branched stylet sheath running through cortical tissue and external phloem and terminating after four unsuccessful probes for internal phloem in pith . EP = external phloem, IP = internal phloem, PI = pith parenchyma, S = stylet sheath. Scale line represents 60 µm.

Fig. 3. Shows a branched stylet sheath terminating in the internal phloem. The stylets are lodged within the pith (unlabelled arrow) . Scale line represents 80 µm.

Fig. 4. At higher magnification it can be seen that during the course of penetration, the stylets shown in Fig. 3 . passed in close proximity to an external phloem bundle without signs of feeding on these external sieve tubes. PFI = immature primary phloem fibres, EP = external phloem, PX = protoxylem, PA = parenchyma, unlabelled arrow = stylet group. Scale line represents 40 µm.

activity of a vascular cambium located between the xylem and the abaxial phloem. Differentiation of the adaxial phloem lags behind that of the abaxial.

3.1.2 Penetration of the Stem

Information on the manner of penetration of the stem was obtained primarily by the study of serial sections of sheaths or stylet tracks in host tissues. Seventy-five of the sheaths examined contained stylets, the majority of which were associated with feeding aphids identified as such by the presence of the stylet tips within apparently functional sieve tubes (Evert et al., 1968).

As with most relatively small aphids (see literature cited in Auclair, 196 Evert et al., 1968), penetration of the stem by A. nerii was largely intercellular (Figs. 1-4). The stylets entered the stem between epidermal cells (Figs 1 and 2) and proceeded in a more or less zig-zag pathway along the surfaces of the collenchyma cell walls of the cortex to the vascular tissues and pith (Figs. 2-4). Only occasionally were cortical cells punctured by the aphid's stylets. One such case is shown in Fig. 1, where the lower, partly differentiated collenchyma cell is traversed by the stylets and contains salivary material of the sheath.

Branched stylet tracks were seldom encountered in the cortical region, but were common in and near the vascular tissues and pith (Figs. 2-4). The frequency of branching was greater in the vicinity of the internal phloem bundles and pith (Figs. 3 and 4). As shown in Fig. 2, in the younger stems the stylet tracks ran more or less directly to the inner tissues. In this case the stylet track traversed an external phloem bundle and ended in the pith where the aphid tried probing in several directions.

This resulted in a branched stylet track, no branch of which terminated in the phloem. Although the much branched track in Figs. 3 and 4 approached sieve tubes of the internal phloem (on the left), none were punctured. At the time the tissue was collected, the pertinent aphid apparently was probing deeper into the pith (unlabelled arrows point to the stylet tips in Figs. 3 and 4).

Stylet tracks terminating at the external phloem were more frequent in older than younger stems. Although largely intercellular, intracellular penetration of phloem cells of the external bundles was not uncommon, including penetration of differentiating primary phloem fibres (Fig.6) and of immature as well as mature sieve elements and parenchymatous elements (Figs. 5 and 6). Despite the relatively high numbers of penetrations of the external phloem by aphid stylets in older stems, only two pairs of stylet tips were encountered in sieve elements of the external phloem. In a few cases, stylet-containing sheaths ran more or less directly to the external phloem and ended at sieve tubes (Figs. 7 and 8). However, as in Fig. 8, the tips of the stylets were not discernible within the sieve tubes of these external phloem bundles. Possibly the aphids had withdrawn their stylets during manipulation of the stem. Nevertheless, even with this taken into consideration, the overwhelming majority of the stylet tips occurred in the sieve tubes of the internal phloem.

3.1.3 Penetration of the Internal Phloem

Passage of the stylets through the cambial zone, where present, and the xylem was mostly intercellular (Fig. 9). Figures 9 and 10 show a stylet track traversing the xylem and ending in an internal phloem bundle. The stylets are clearly visible within the sheath, which

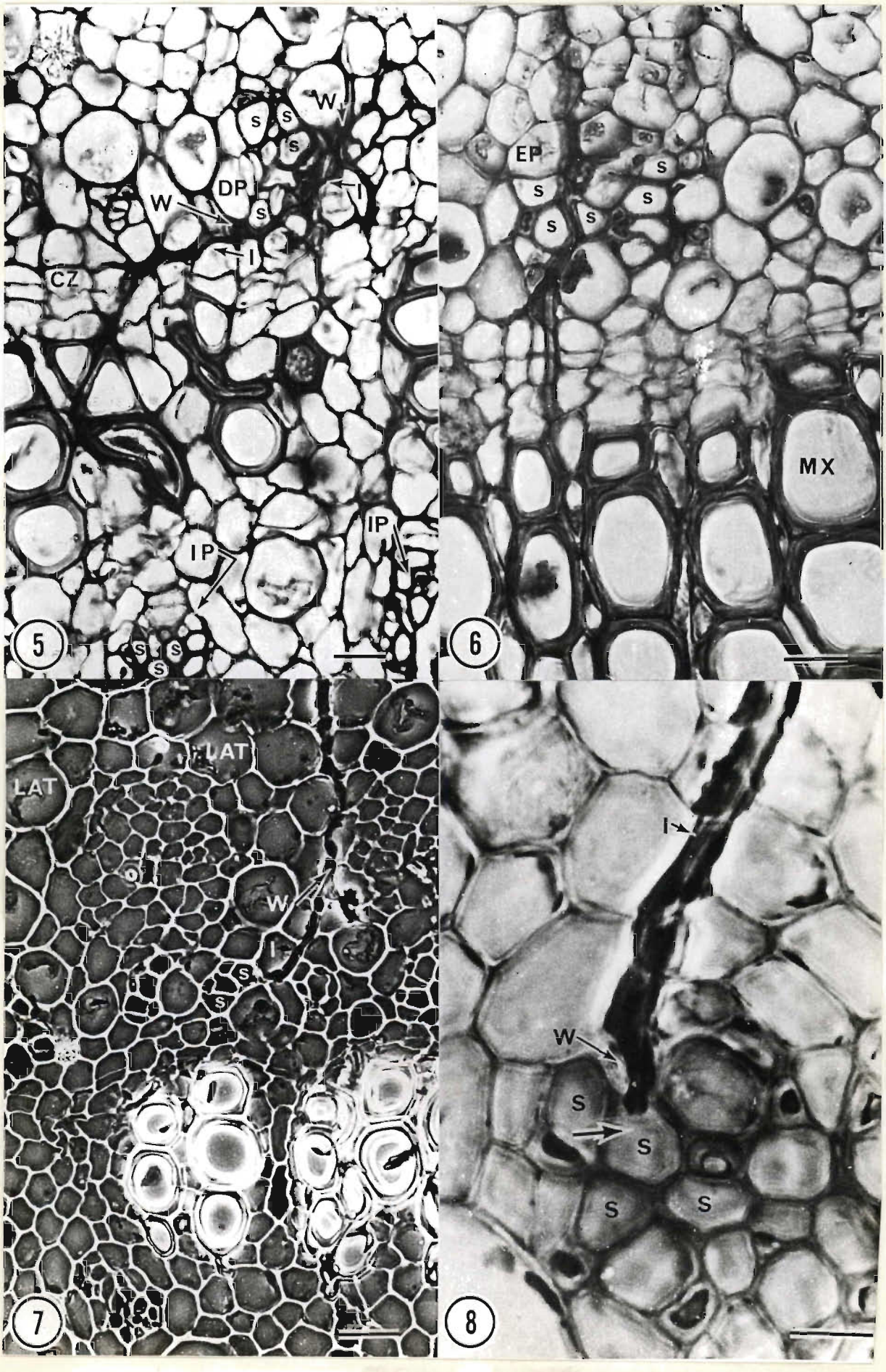
W
S
S
S
DP
W
S
I
I
CZ
IP
IP
5
S
S
S
S
EP
S
S
S
S
S
MX
6
LAT
LAT
W
I
S
S
7
I
W
S
S
S
S
8

Figs. 5 - 8. Transections showing penetration of external phloem.

Fig. 5. Shows a stylet track passing both intercellularly and intracellularly, through the external phloem of a young stem. Passage of the stylets through the cambial zone was predominantly intercellular, and through the primary xylem as well. S = sieve element, DP = dividing external phloem procambial cell, CZ = cambial zone, I = intercellular penetration, W = intracellular penetration, IP = internal phloem. Scale line represents 20 µm.

Fig. 6. Shows the predominantly intracellular passage of stylets through the primary phloem fibres, external phloem and cambial zone. There is no evidence for feeding on this bundle, during passage of the stylets. EP = external phloem, MX = metaxylem vessel. Scale line represents 20 µm.

Fig. 7. Phase contrast photomicrograph showing penetration by stylets of an external phloem bundle. Note that the stylet tips are obscured, presumably by sheath material. LAT = laticifer, W = intracellular penetration, S = sieve tube, unlabelled arrow = punctured sieve tube. Scale line represents 20 µm.

Fig. 8. Another example of penetration of external phloem bundle. Passage of the stylets through the surrounding parenchyma was both intercellular and intracellular. As in Fig. 7, the stylet tips are masked by sheath material. I = intercellular penetration, W = intracellular penetration unlabelled arrow = punctured sieve tube . Scale line represents 10 µm.

terminates at the wall of the punctured sieve tube. Passage of the stylet tips through the sieve element wall can be seen in Fig. 10. The tips of the maxillary stylets entered the sieve tube below the sieve plate shown here, and are thus not visible. Whether aphids ingest food through an open or closed sheath has long been of concern to a number of investigators (Miles et al., 1964, Kinsey and McLean, 1967). These results strongly support earlier reports that aphid feed through an open sheath (Evert et al., 1968, Evert et al., 1973b).

Only the tips of the maxillary stylets penetrated sieve tubes being fed upon. Figure 11 shows a stylet sheath with stylets traversing the xylem and ending at a sieve tube of a small internal phloem bundle. At higher magnification (Fig. 12) it can clearly be seen that the tips of the maxillary stylets have entered the sieve tube and that they are free of any salivary material.

Figures 13 and 14 further illustrate the presence of unoccluded maxillary stylet tips in sieve tubes of the internal phloem. In Figure 13 the stylet tips have barely entered the sieve tube and are still close together. Passage of the stylets through neighbouring parenchymatous tissue was largel intercellular. Within the bundle penetration was in part intercellular and in part intracellular. A sieve tube contiguous to the one containing the stylet tips is occluded with sheath material. In Figure 14 the stylets can be seen following an intercellular pathway to the punctured sieve tube. Within the sieve tube the stylets are free of any salivary material and are separated from one another, as are those in the sieve tube of Figure 12.

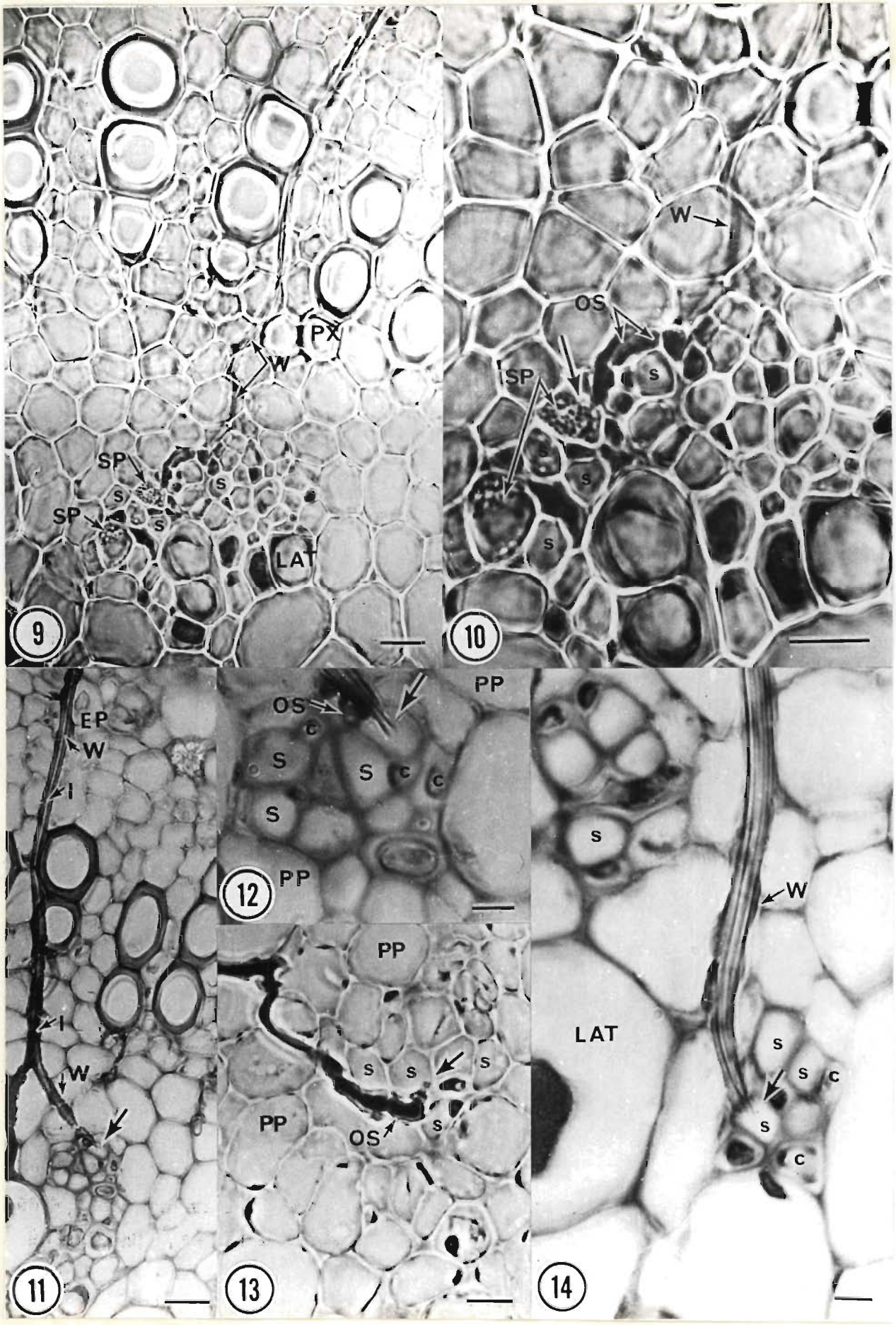
PX
W
SP
SP
S
S
S
LAT
9
W
OS
SP
S
S
S
10
EP
W
I
I
W
11
OS
C
S
S
S
C
C
PP
PP
12
PP
S
S
S
PP
OS
S
13
S
W
LAT
S
S
C
S
C
14

Figs. 9-14. Transections showing stylet penetration of internal phloem.

Figs. 9-10. Phase contrast photomicrographs showing example of direct penetration of internal phloem by aphid stylets. The passage of the stylets was both intercellular and intracellular. At higher magnification (Fig. 10) it is apparent that the aphid fed sequentially on the smaller sieve tubes, which were subsequently obliterated by sheath material, prior to the penetration of the large metaphloem sieve tube. W = intracellular penetration, PX = protoxylem, LAT = laticifer, SP = sieve plate, S = sieve tube. Scale lines represent 40 and 15 µm respectively.

Fig. 11. Illustrates direct penetration of the internal phloem. A metaphloem sieve tube has been punctured by stylets (unlabelled arrow). Note that the external phloem (above) was penetrated intracellularly. I = intercellular penetration, W = intracellular penetration, EP = external phloem, unlabelled arrow = stylet tips within sieve tube. Scale line represents 25 µm.

Fig. 12. At higher magnification, the maxillary stylet tips can be seen to project beyond the salivary sheath and the wall of the sieve tube. The stylets are separated, and apparently free of any muscilaginous deposits. The punctured sieve tube appears uninjured. OS = occluded sieve tube, C = companion cell, PP = phloem parenchyma, unlabelled arrow = maxillary stylet tips within the sieve tube. Scale line represents 7 µm.

Fig. 13. Phase contrast photomicrograph showing predominantly intracellular penetration of the phloem parenchyma bordering internal phloem bundle. Note maxillary stylets (unlabelled arrow) projecting beyond salivary sheath into lumen of sieve tube. As in Fig. 12, the stylets and the lumen of the punctured sieve tube are unoccluded. Details as per Fig. 12. Scale line represents 15 um.

Fig. 14. Shows penetration by stylets of sieve tube of small internal phloem bundle. Note that passage of the stylets through the surrounding parenchyma was mostly intracellular, and that the tips of the stylets are again free of muscilaginous deposits or salivary material. Details as per Fig. 12. Scale line represents 7 µm.

3.1.4 Penetration of Leaves

Figures 15 to 19 illustrate some aspects of stylet penetration of mature leaves or more specifically, of the petioles of mature leaves.

The probes in leaves were frequently unsuccessful. Two apparently unsuccessful probes can be seen in Fig. 15. Originating from the abaxial surface of the leaf, both probes traversed the abaxial phloem in search of a suitable feeding site and both ended in the xylem. Neither probe reached a sieve tube of the adaxial phloem. It will be noted that, as in the stem, penetration of the petiole was largely intercellular. Note that a laticifer above the xylem on the right was completely circumscribed during one of the probes. This is a reflection of the extreme flexibility of the stylets.

Unbranched tracks frequently bypassed the abaxial phloem, traversed the xylem, and terminated in the adaxial phloem (Figs. 16 and 17). Although penetration of the xylem was largely intercellular, occasional tracheary elements were occluded with sheath material (e.g. the third tracheary element from the bottom in Fig. 17).

Only three pairs of stylet tips were observed within sieve tubes of leaves, and all of these were in sieve tubes of the adaxial phloem, which is homologous and continuous with the internal phloem of the stem. In other cases, the stylet tips were about even with the sheath, as shown in Figs. 18 and 19. Possibly the aphid withdrew its stylets at the time of sampling. However, Fig. 19 shows that the end of the sheath is still open.

In its initial probe of the region above the xylem, the aphid completely missed the adjacent group of sieve elements.

Most workers have suggested that aphids and other suctorial insects they have studied find their objectives by trial and error (Painter 1928,

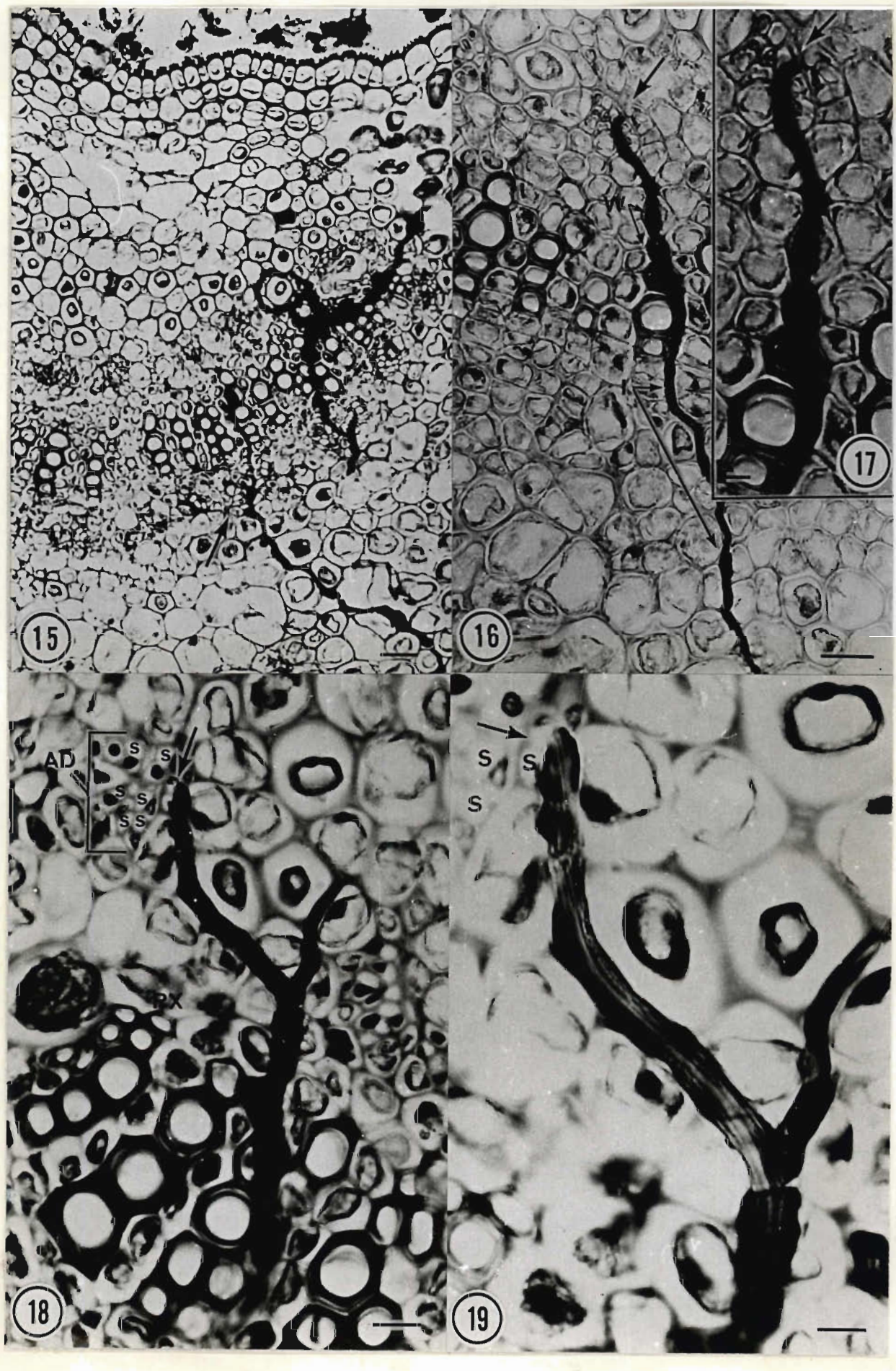
15
16
17
18
19
AD
S
S
S
S
S
S
S
S
S

Figs. 15 - 19. Transections showing penetration of phloem of petioles of mature leaves.

Fig. 15. Shows two stylet tracks originating on abaxial surface of petiole. The stylets traversed the abaxial phloem in search of a suitable feeding site. Both end in the xylem. The laticifer on right, above the xylem was completely circumscribed during one of the probes. Unlabelled arrow = adaxial phloem bundle. Scale line represents 30 µm.

Figs. 16 - 17. Show passage of stylet track through abaxial phloem and xylem . Note tracheary element obliterated by salivary material. I = intercellular penetration, W = intracellular penetration, unlabelled arrow = adaxial phloem probe. Scale lines represent 35 and 15 µm respectively.

Figs. 18 - 19. Show passage of stylets through xylem and termination in adaxial phloem. During this probe, the aphid completely missed the adjacent adaxial phloem bundle on right. The stylet tips are about even with end of sheath, which terminates at wall of sieve tube. At higher magnification (Fig. 19) the stylets are clearly visible within the sheath. AD = adaxial phloem, S = sieve tube, PX = protoxylem, unlabelled arrow = probed adaxial sieve tube. Scale lines represent 20 and 10 µm respectively.

Balch 1952, Day et al., 1952, Evert et al., 1968). Although A. nerii feeds preferentially on the internal phloem of the stem and, apparently on the adaxial phloem of the leaf, it appears that the aphid locates the internal and adaxial phloem with some degree of precision in that the stylets are directed towards a particular strand in some instances (Figs. 10, 13, 14 and 16) and in others, largely by chance (Figs. 2, 4, 11, 15 and 18). However, it would seem that the chance location may be more frequent in the younger stem and leaf material examined. This is suggested by the configuration of the aphid tracks within the stem and leaf, by the frequency of branching near the vascular tissues and within the pith, and by the near misses of sieve tubes in both external and internal phloem bundles.

Auclair (1963) records that in some 46 species of aphids, used in histological investigations, 19 are reported to reach their objective by predominantly intercellular penetration; 8 by both intercellular and intracellular penetration and some, notably lachnids feeding in woody stems, penetrate by a predominantly intracellular path.

Several reasons have been suggested for the predominance of intercellular penetration: e.g. that intercellular penetration follows the line of least resistance (Büsgen, 1891); that the cell walls may offer support to the stylets (Davidson, 1923); that smaller aphids are unable to penetrate the tissue by pressure alone and that their saliva is not strong enough to enable them to take a straight course to their objective. With regard to the last explanation, the stylets of the larger aphid species, for example, Lachnus pinicola (Kltb.), (Büsgen, 1891), Macrosiphum solanifolia (Ashmead) (Smith, 1926); Tuberolachnus salignus (Gmelin) (Mittler, 1957); Longistigma caryae (Harr.), (Zimmerman, 1961, 1963; Evert et al., 1968) have been reported to penetrate host tissues either mainly intracellularly, or both intracellularly and intercellularly.

A. nerii penetrates its host tissue in a predominantly intercellular manner, although intracellular penetration does occur to some extent (Botha et al., 1972).

If the size of the stylets governs the mode of penetration of the host tissue, thenit is logical that A. nerii would tend to penetrate in a predominantly intercellular manner.

Miles et al., (1964), reported that during ingestion of phloem sap, the stylets of the aphid, Acyrthosiphum pisum remained motionless, and that the tips were either level with the end of the salivary sheath, or that they projected a few microns beyond it. Zimmerman (1961, 1963), and Evert et al., (1968) demonstrated that the maxillary stylet tips of L. caryae projected beyond the salivary sheath during penetration of linden phloem. In this present study, it has been demonstrated that the tips of the maxillary stylets of A. nerii in most cases project beyond the salivary sheath and are open within the sieve-tube being tapped. It would seem then, that the presence of stylet tips, and the lack of associated sheath material in living sieve-elements, constitutes sufficient criteria to identify such sieve-elements as functional.

A most intriguing, unanswered question is: "Why do the aphids feed almost exclusively on the internal phloem?" Possibly the internal sieve tubes contain some substance or substances either lacking in the external sieve elements or present in lesser amounts in the latter - substances which are highly desirable to the aphid. This possibility would be difficult to confirm. Both the external and internal phloem are associated with articulate laticifers, the contents of which would interfere with any chemical separation of the phloem sap constituents.

Possibly the external sieve tubes are more easily damaged during penetration by the aphid's stylets than are the internal sieve tubes, rendering the

former non-functional. However, in this regard, it must be borne in mind that the greater majority of stylet tips and tracks bypass the external phloem, without any evidence of penetration of the external phloem sieve tubes.

A further possibility is that greater quantities of assimilates are transported in the internal phloem than the external phloem.

With regard to all the possibilities mentioned above it must be kept in mind that the aphids more often bypass the external phloem than penetrate it

3.2 Morphology of A. nerii and its Stylets

Aphids (Homoptera, Aphididae) are well adapted to exploit their host plants. One of the first approaches to a plant is made by the specialized mouthparts, consisting of an attenuated labial proboscis (Figs. 20, 21 and 23) from which the piercing stylets (Fig. 22) are extruded. Figure 21 reveals that the proboscis of A. nerii is jointed, as in most Hemiptera, thus rendering it flexible, a function which allows for its shortening during stylet penetration and probing of the plant tissues.

In Figures 20 and 21, the attenuated labial proboscis is shown closely appressed to the ventral surface of the aphid. The stylets, mandibular and maxillae, are not usually visible in non feeding aphids, but are withdrawn within the proboscis, where they lie within the labial groove. The labial groove is situated anteriorly in the proboscis (Figs. 21 and 23 The distal tip of the proboscis is surrounded by usually two rings of sensory bristles (Figs. 22 and 23). The stylet group, upon extrusion from the proboscis, (Fig. 22) appears to be controlled to some extent by the muscular collar, from which the sensory bristles protrude.

Apart from A. nerii, the anatomy and morphology of the stylets of

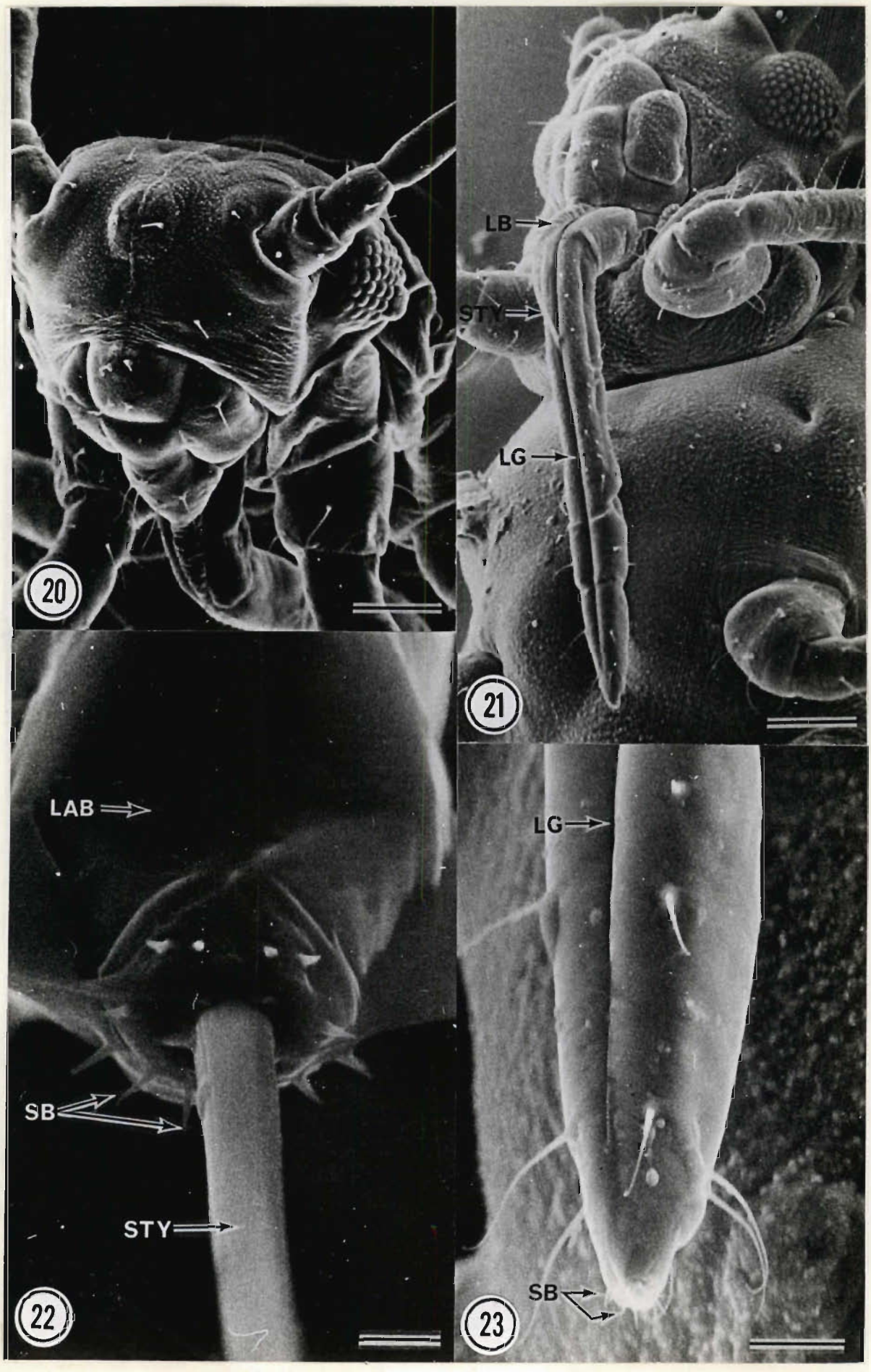
20
LB
STY
LG
21
LAB
SB
STY
22
LG
SB
23

Figs. 20-23. Scanning electron micrographs of aspects of the morphology of Aphis nerii. Figs. 20 and 21 show the aphid in non-feeding position, with the labium carried closely appressed to the ventral surface of its body. The stylets are retracted and lie within the labium. The distal part of the labium thro which the stylets project during penetration of plant tissue is shown in Figs. 22 and 23. A muscular clamp, surrounded by a ring of sensory bristles is situated at the distal end of the labium. Proximally, the stylets lie within the labial groove. LG = labial groove, LAB = labium, LB = labrum, SB = sensory bristles, STY = stylet group. Scale lines represent 70, 80, 3 and 20 μm respectively.

Tuberolachnus salignus (Adams and Fyfe, 1970), Myzus persicae (Van Hoof, 1958; Forbes, 1969; Adams and Fyfe, 1970), Adelges piceae (Forbes and Mullick, 1970). Macrosteles fascifrons (Forbes and Raine, 1973), Macrosiphum euphorbiae (Adams and Fyfe, 1970) and Rhopalosiphum maidis (Parrish, 1967; Evert et al., 1973b) have been investigated using light, transmission and electron microscopy.

The stylets of A. nerii are 3,0 to 3,8 µm in diameter for most of their exposed length. Towards the tips, the stylets taper gradually; the maxillae being about 0,03 µm or less in diameter at their tips. The sharp point formed by the tips would seem to be ideal for piercing and penetrating plant tissues and at the same time, causing as little damage as possible to the penetrated cells. Scanning electron microscopy of the stylets of A. nerii (Botha et al., 1972) indicated that the mandibular stylets closely envelop the maxillary stylets for most of their length. Note the presence of barb-like ridges along the concave edges of the mandibular stylets (Fig. 28, small arrow). These ridges are about 0,5 um apart. Unlike those occuring on the mandibular stylets of M. persicae (Forbes, 1969), those on the mandibles of A. nerii extend for at least the distal 60 - 70 µm of the stylets. However, as in M. persicae, these ridges extend from 0,03 to 0,1 µm from the body of the stylets. These ridges were frequently observed during the anatomical investigation of stylet penetration of C. physocarpus phloem. Each of the mandibular stylets possesses a horn-like projection, about 2,5 to 3,5 µm from the distal end of the stylet (Fig. 27).

The maxillary stylets are interlocked except for the distal 2,5 to 4 µm (Figs. 24, 25 and 26), and possess a series of tooth-like projections (large arrows, Figs. 26 and 28), the first about 3,5 µm from the tip, the second 0,6 µm from the first, and the third, about 0,6 µm from the

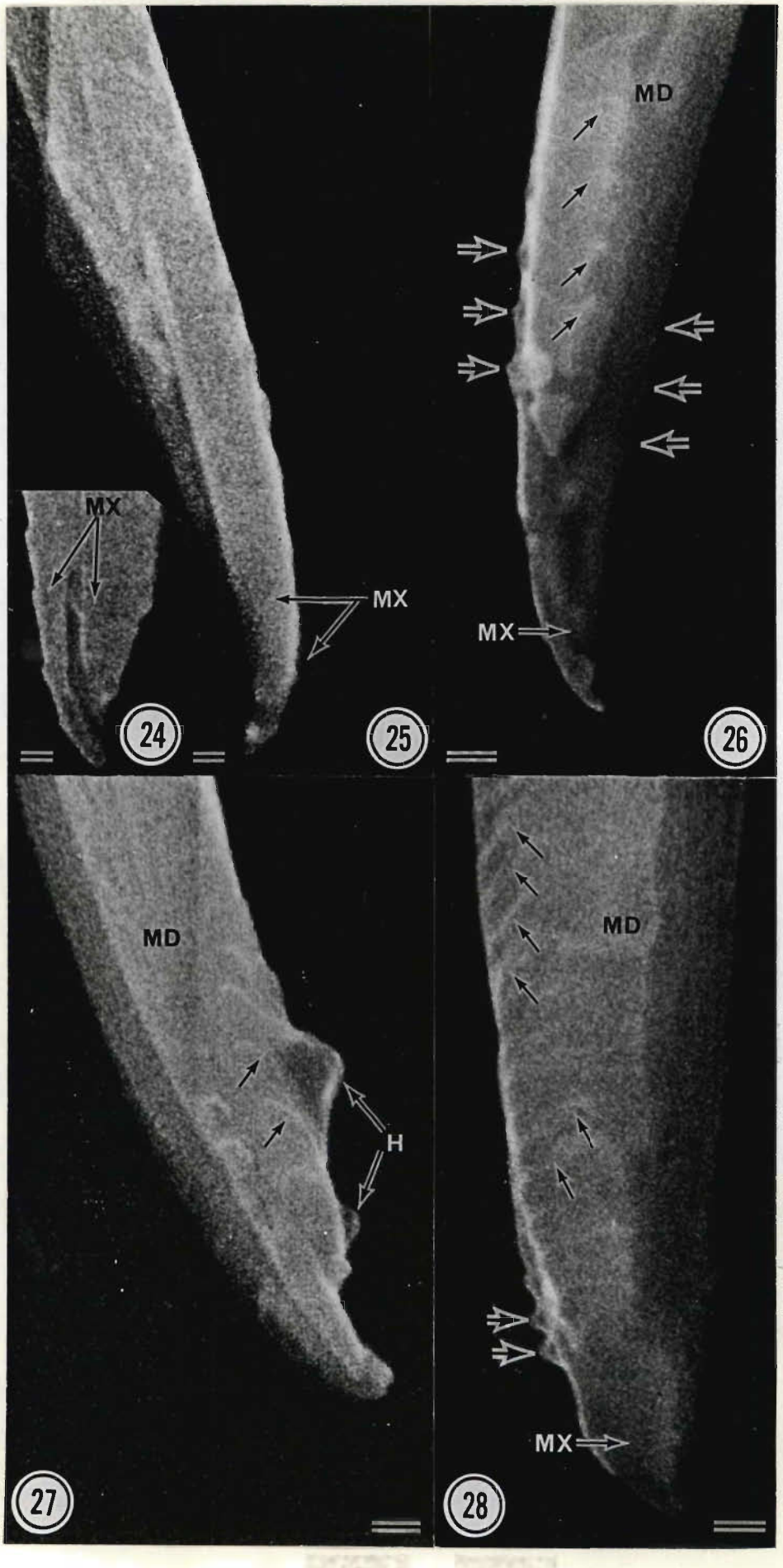
MX
MX
24
25
MD
MX
26
MD
H
27
MD
MX
28

Figs. 24–28. Scanning electron micrographs showing aspects of the mandibular and maxillary stylet tips. The concave surface of the mandibular stylets (Figs. 26 and 28) possess a series of barb-like ridges about 0,5 µm apart. Note the presence of a horn-like projection on both mandibular stylets, viewed from above in Fig. 26 and laterally in Fig. 27. The lateral edges of the maxillary stylets (Figs. 24–27) possess a series of tooth-like projections on their surfaces. Figs. 24 and 25 are two views of the same stylet excised from leaf material. Note the small barbs on the lateral edges of the maxillary stylets in Fig. 24. Figs. 26–28 are representative of stylets excised from the labial groove. Small arrow = barb-like ridges on mandibular stylets, large arrows = tooth-like projections on lateral edges of maxillary stylets, MX = maxillary stylets, MD = mandibular stylets, H = horn-like projection. Scale lines represent 0,5 µm.

second. Both the barb-like ridges and tooth-like projections are assumed to play a part in stylet penetration by bracing and clamping, during alternate protractions of the mandibular and maxillary stylets. The tooth-like projections are located along one edge of the stylet where they cannot be covered by the mandibular stylets, in other words, one set of projections is located on the anterior edge of a maxillary, and the other set on the posterior edge of the second maxilla.

A notable feature is that the tips of the maxillary stylets were often overlapped (Figs. 24 and 25). Overlapping was observed in most of the stylets which had been withdrawn from leaf tissue after the aphids had been killed, and not in stylets which had been excised from the labial groove. Stylets which exhibited overlapping were compared to photo-micrographs of stylets in the process of being withdrawn from the sieve tubes; the comparison of which revealed a distinct similarity. It would seem that overlapping of the tips of the maxillary stylets must precede the withdrawal of the stylet group from plant tissue, perhaps this functions in the release of the barb-like ridges of the mandibles and the tooth-like projections on the edges of the maxillary stylets, thus allowing for easy withdrawal of the stylet group.

3.3 Summary

Penetration of the stems and leaves was studied with light and phase microscopes. Penetration of the epidermis and ground tissues was largely intercellular, that of the phloem tissues partly intercellular and in part intracellular. In the large majority of penetrations the external phloem was bypassed, and the stylet tracks terminated in the internal phloem. Of 75 pairs of stylet tips encountered in presumably functional sieve tubes, 73 were lodged in sieve tubes of the internal and adaxial

phloem. This confirms observations of a preliminary study which indicated that A. nerii feeds preferentially on sieve tubes of the internal phloem.

The stylets of A. nerii are 3,0 to 3,8 µm in diameter for most of their exposed length, tapering gradually toward the tips of the maxillae which measure 0,03 µm or less in diameter. The sharp point formed by the tips would seem to be ideal for piercing and penetrating plant tissues, causing little visible damage.

4. LIGHT MICROSCOPE INVESTIGATION OF PHLOEM ONTOGENY AND DIFFERENTIATION

4.1 Results and Discussion

4.1.1 Brief Description of the Stem

At the end of primary growth the stem of G. physocarpus consists of a uniseriate epidermis, a cortical region of 1 - 3 layers of collenchyma cells and several layers of parenchyma, a ring of primary vascular bundles and pith (Fig. 34). Each vascular bundle is eventually capped by primary phloem fibres (Figs. 36 and 37). External and internal strands of phloem are more or less uniformly distributed around the circumference of the stem. Relatively narrow parenchymatous interfasicular regions separate the vascular bundles.

The external and internal phloem strands consist of sieve elements and associated parenchymatous elements, including companion cells. The number of strands per vascular bundle is directly proportional to the size of the bundle.

As the stem ages a vascular cambium arises between the metaxylem and external phloem and produces some secondary phloem on its outer face and secondary xylem on its inner face. At maturity the stem is hollow-centered.

4.1.2 The External Phloem

Figs. 29 and 30 show transverse and longitudinal views of external phloem strands, respectively. As seen in Fig. 29, the strands are surrounded by relatively large parenchyma cells. The strand in Fig. 29 consists almost entirely of sieve elements and companion cells. A vascular cambium has been

initiated external to the phloem strand, but has not yet produced any secondary tissues.

Comparison of Figs. 29 - 30 and 31 - 32, and examination of the data recorded in Table 1, shows that the sieve elements of the external phloem strands are both longer and wider than those of the internal strands. Conversely, the walls of the external sieve elements are generally narrower than those of the internal sieve elements. Nacreous thickening of the lateral walls of the sieve elements is evident in Fig. 30. Initiation of differentiation of the external phloem strands precedes that of the internal strands.

TABLE I

MEASURED PARAMETERS OF THE EXTERNAL AND INTERNAL PHLOEM[1]

	EXTERNAL[2]	INTERNAL[3]
Mean length, μm	253	200
Diam. Sieve Plate, μm	15,1	14,6
Cross-sectional Area of Sieve Plate, μm^2	179,2	167,0
Perimeter of Sieve Plate, μm	47,5	45,6
Volume, Sieve Tube Member, μl	$4,54 \times 10^{-5}$	$3,33 \times 10^{-5}$

1. Based on intact, randomly selected sieve tube members.
2. Mean of 40.
3. Mean of 28.

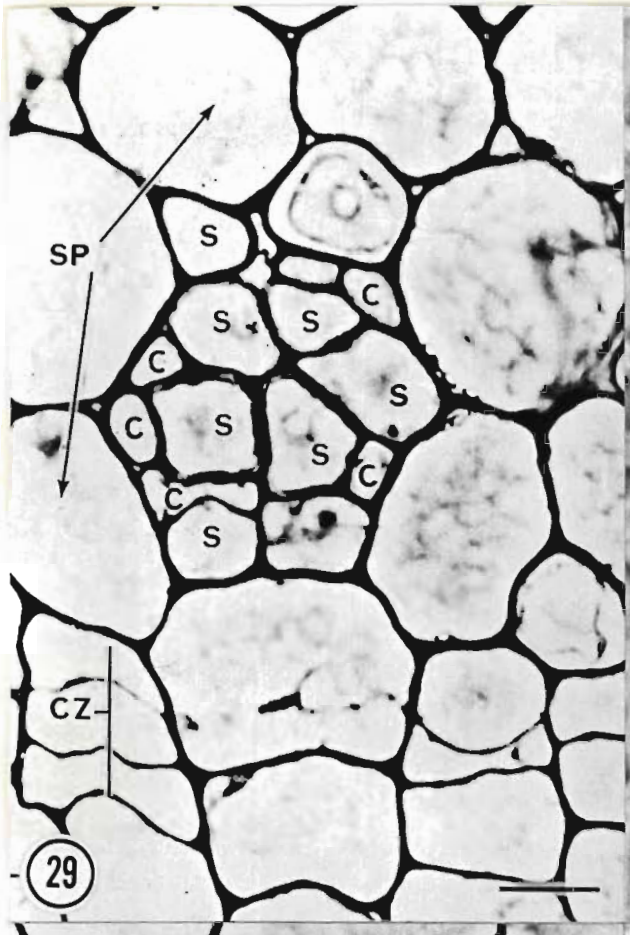

29

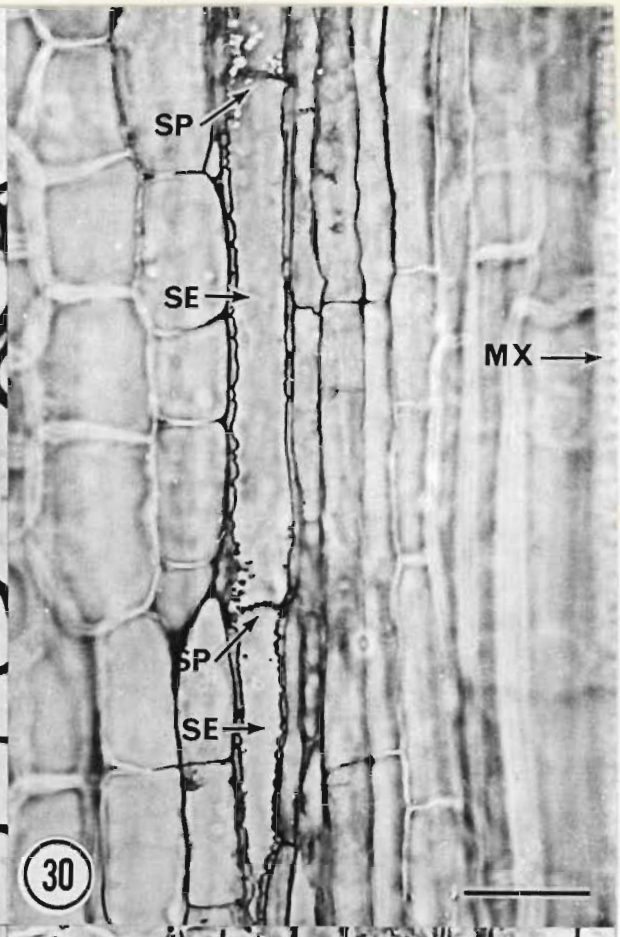

30

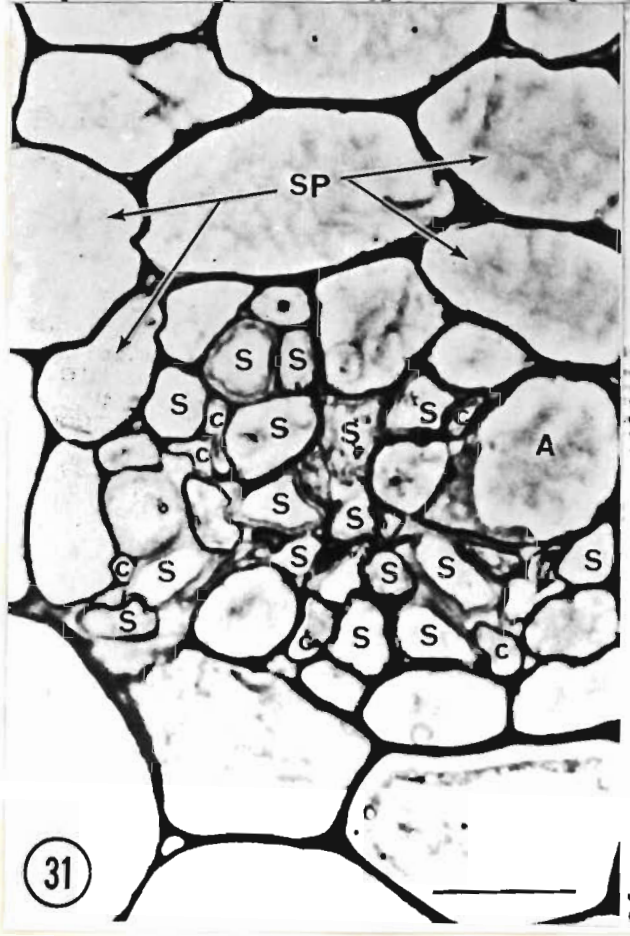

31

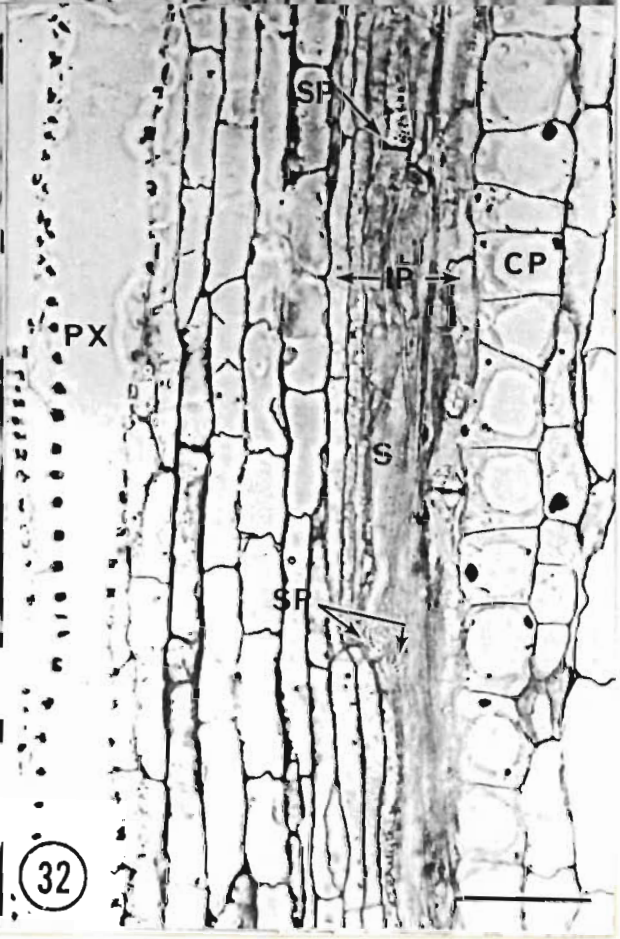

32

Figs. 29–32. Transections (Figs. 29 and 31) and longisections (Figs. 30 and 32) of primary external and internal bundles.

Fig. 29. Transection of mature external phloem bundle. The cambial zone below has not yet become active in the production of secondary phloem or secondary xylem. SP = sheath parenchyma, C = companion cell, S = sieve tube, CZ = cambial zone. Scale line represents 15 μm.

Fig. 30. Phase contrast photomicrograph of longitudinal section through bark, cambial zone and metaxylem of stem at same stage of differentiation as that in Fig. 29. Portions of several files of sieve tubes are visible. Note nacreous thickening on lateral walls of sieve elements. MX = metaxylem, SE = sieve element, SP = sieve plate. Scale line represents 30 μm.

Fig. 31. Transection of an internal phloem bundle. Compare widths of sieve elements in this bundle with those of the external phloem bundle of Fig. 29. C = companion cell, S = sieve tube, A = procambial cell, SP = sheath parenchyma. Scale line represents 30 μm.

Fig. 32. Phase contrast photomicrograph of a longitudinal section of stem showing primary internal phloem strand from similar portion of stem as in Fig. 31. Several inclined sieve plates are visible in the plane of the section. Much of the phloem is immature. The file of stubby parenchyma cells are undergoing crystal formation. PX = protoxylem, SP = sieve plate, IP = internal phloem, S = sieve tube, CP = crystal-containing parenchyma. Scale line represents 48 μm.

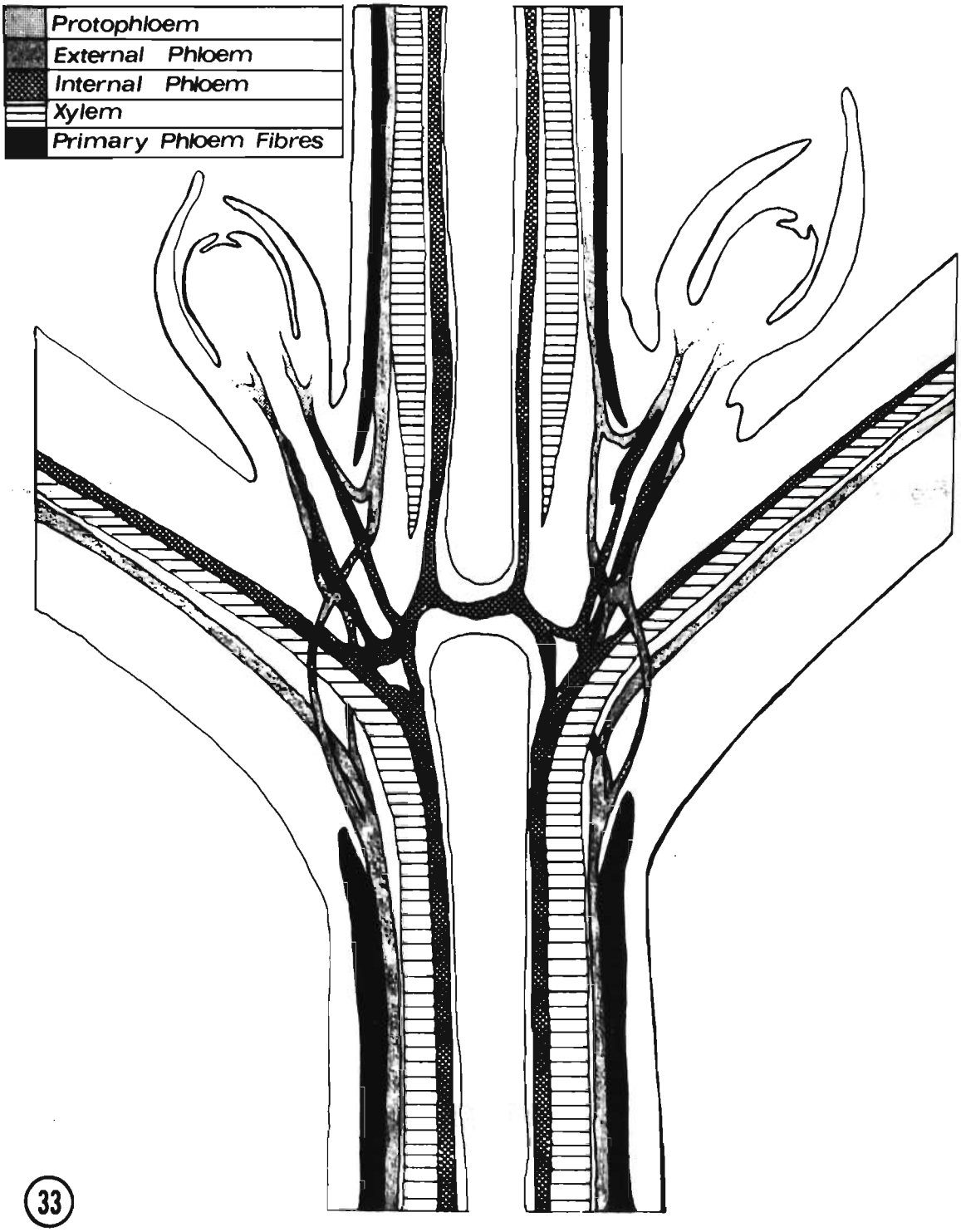
Protophloem
External Phloem
Internal Phloem
Xylem
Primary Phloem Fibres

Fig. 33. Camera lucida reconstruction of the vascalature of the nodal region of the stem at the end of primary growth, showing the relationship of the external and internal phloem in stem, leaf gaps and axillary buds.

4.1.3 The Internal Phloem

Figs. 31 and 32 are transverse and longitudinal views, respectively, of internal phloem strands. As mentioned, the sieve elements of the internal phloem strands are narrow, shorter and more numerous than those of the external strands. The narrow size and greater numbers of sieve elements of the internal strands is quite obvious when the representative internal strands of Figs. 31 and 32 are compared with the respective external strands of Figs. 29 and 30.

As pointed out by Esau (1969), the size of individual phloem strands is dependent upon two factors: the initial number of cells that undergo division to make up a strand and the duration of meristematic activity within each strand. The same two factors are operative in Gomphocarpus, the precursors (procambial cells) of the external strands being fewer in number and undergoing relatively fewer divisions than in the case of the internal strands. As in Tobacco (Esau, 1938, 1969) meristematic activity within external strands of Gomphocarpus is largely confined to periclinal divisions resulting in centripetal production of derivatives. In contrast, the phloem mother cells of the internal phloem strands in Gomphocarpus divides mostly radially. As a consequence, the internal strands become wider tangentially than radially.

Cell division in the earliest phloem strands is of short duration. As a result of prolonged meristematic activity, the latter-formed strands may attain considerably size. The internal phloem bundles in Gomphocarpus may be arbitarily divided into three size classes:

Class A - 20 or more sieve tubes per strand

Class B - 10-19 sieve tubes per strand, and

Class C - 1-9 sieve tubes per strand.

As might be expected, class C represent the earliest-formed (older) phloem strands and class A, the last-formed (youngest) strands.

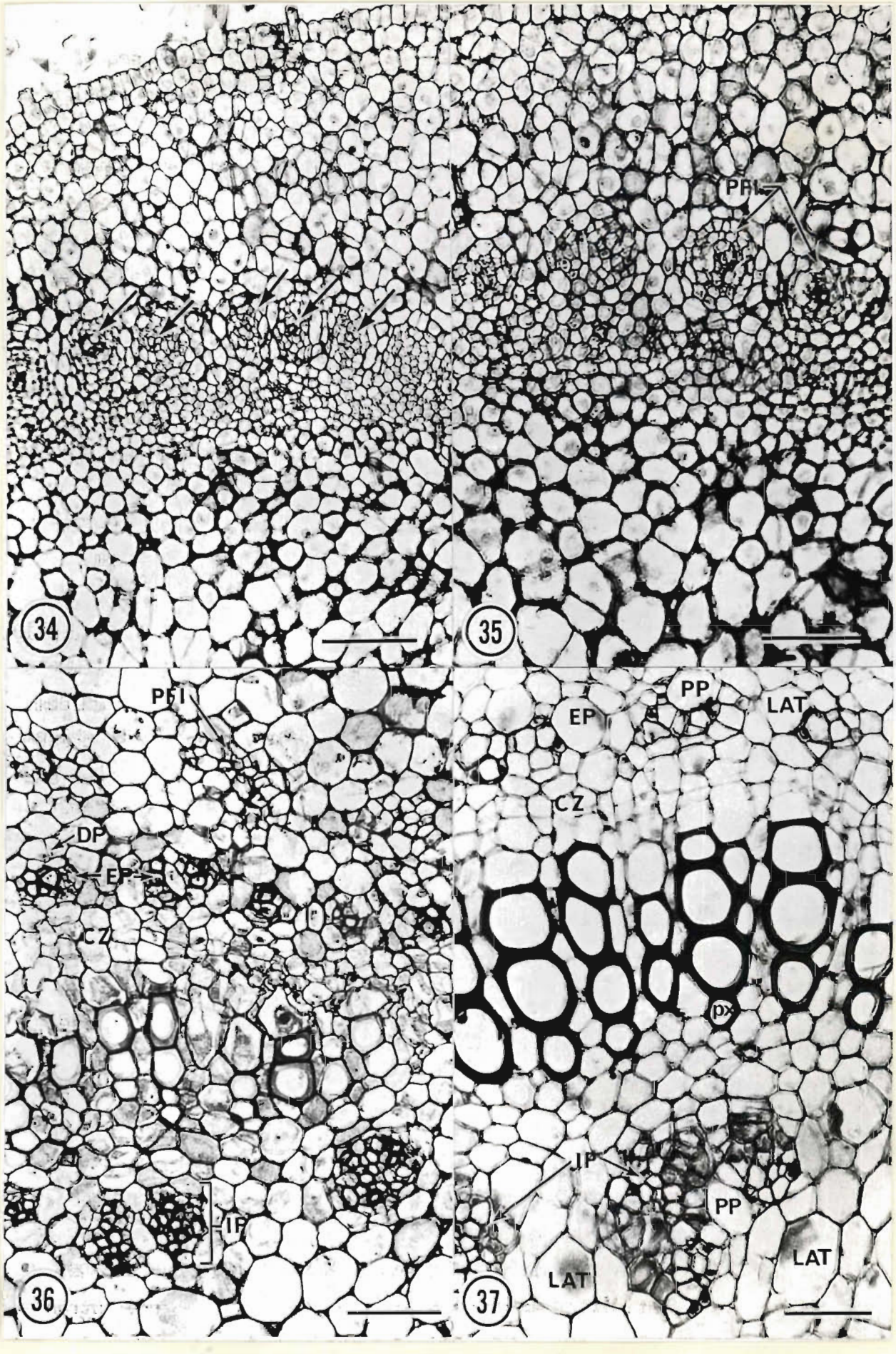
34
35
PFI
36
PFI
DP
EP
CZ
IP
37
EP
PP
LAT
CZ
px
IP
PP
LAT
LAT

Figs. 34-37. Transections 80 µm below the shoot apex (Figs. 34 and 35); between nodes 4-5 (Fig. 36); and in the region of mature primary tissues (Fig. 37), illustrating the sequence of differentiation of the external primary phloem, the primary xylem, and the internal primary phloem in the stem.

Figs. 34 and 35 show portions of a young stem, which has a uniseriate epidermis, a cortical region of 1-3 layers of partly differentiated collenchyma cells, and several layers of parenchyma. The pith is parenchymatous. Laticifer develop-ment has as yet not taken place. At this level vascular differentiation is limited to single protophloem sieve tubes of the external phloem. At higher magnification (Fig. 35) the external protophloem strands can be seen to be associated with immature primary phloem fibres. Neither the xylem nor internal phloem is visible in Fig. 35.

Unlabelled arrows = external protophloem, PFI = primary phloem fibres. Scale line represents 80 and 65 µm respectively.

Fig. 36. At this level, the differentiating primary phloem fibres are clearly discernible. Parenchymatous elements occupy the region between the fibres and the metaphloem. Meristematic activity within the external primary phloem has resulted in an increase in the number of sieve tubes and companion cells per strand. The cambial zone is clear, but has not produced any secondary phloem. Of interest is the rapid appearance and maturation of the internal phloem, which took place between nodes 3-4. In the plane of section of Fig. 36 (between nodes 4-5) the internal phloem is already the quantitatively dominant phloem.

EP = external primary phloem, CZ = cambial zone, IP = interr primary phloem. Scale line represents 60 µm.

Fig. 37. The metaphloem of the external strands is mature. The cambial zone as in Fig. 36, is well-formed, but apparently has formed no secondary phloem. Continued meristematic activity of the internal phloem strands has resulted in the lateral expansion of the strands, and rapid increase in the number of sieve tubes and companion cells per strand. Note laticifers associated with external and internal strands. LAT = laticifer, PX = protoxylem. Scale line represents 60 µm.

4.2 Arrangement and Spatial Relationship of External and Internal Phloem in Nodal Regions

Serial longitudinal sections of the nodal regions of numerous shoots of differing morphological ages were examined in order to determine whether the external phloem and the internal phloem were interconnected in the nodal regions, or whether they constituted separate systems. No evidence could be found for the union of external and internal phloem in either internodal regions or at the nodes (Fig. 33). The vasculature in the nodal regions is complicated, owing to the presence of a glomerulus, from which strands of internal phloem, together with their associated articulate laticifers diverge from the stem to the petiolar trace, where they are continuous with similar tissues on the adaxial side of the petiole.

Examination of serial sections revealed that whereas the main portion of the external phloem diverged into the petiole, before doing so branches from it bypassed the internal phloem acutely and continued on up the stem, portions of them feeding the axillary buds along the way. The leaf traces were found to be unilacunar, and exhibited no evidence of mergence of the adaxial with the abaxial phloem. The nodal plexus in Gomphocarpus appears ring-shaped in transection, with interspersed articulat laticifers and parenchymatous elements, effectively bridging the otherwise hollow-centered stem.

4.3 Ontogeny of the Primary Phloem

4.3.1 The Internal and External Phloem

Serial transverse and longitudinal sections of the apical portion of stems of G. physocarpus were studied in order to elucidate the ontogeny of the

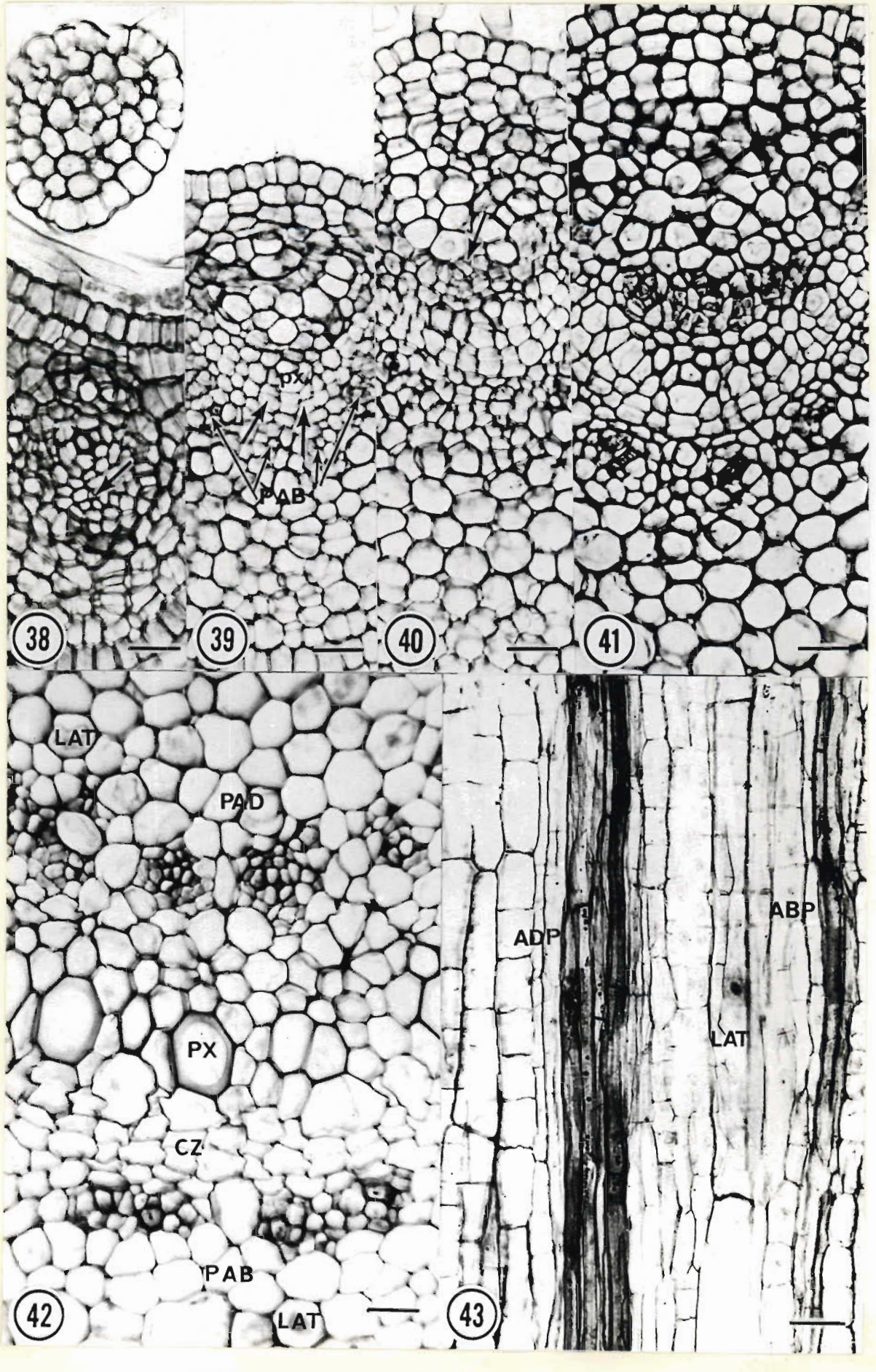
38
39
PX
PAB
40
41
LAT
PAD
PX
CZ
PAB
LAT
42
ADP
ABP
LAT
43

Figs. 38-43. Transections (Figs. 38-42) and longisection (Fig 43) showing stages of differentiation of the vascular system of petioles of leaf pairs (LP) 1-2, (Fig. 38); LP 3, (Fig. 39); LP 4, (Fig, 40); LP 5, (Fig. 41); and LP 6 (Figs. 42-43). Arrow points to single protophloem sieve tube of abaxial phloem in LP 2 (Fig. 38). The tissue which comprises the midrib consists of small, dense, undifferentiated cells. No vascular differentiation was evident in LP 1. In LP 3, (Fig. 39) a single protoxylem element is evident at PX. Four protophloem elements are now evident in abaxial phloem. Future site of cambial zone is evident. LP 4 (Fig. 40) show first protophloem sieve element of adaxial phloem which by LP 5 (Fig. 41) is rapidly becoming the dominant phloem in the midrib. In the petiole of LP 6 (Fig. 42) both the adaxial and abaxial phloem are at an advanced stage of differentiation, with lateral spreading of the strands becoming more obvious, compared with LP 5. Although evident only in Fig. 43, the adaxial phloem is the dominant phloem. Unlabelled arrows: Fig. 38 = protophloem sieve element of abaxial phloem; Fig. 39 = developing cambial zone; Fig. 40 = protophloem sieve element of adaxial phloem. PX = protoxylem, PAD = adaxial protophloem, PAB = abaxial protophloem, CZ = cambial zone, ADP = adaxial phloem, ABP = abaxial phloem, LAT = laticifer. Scale lines: Figs. 38-41 represent 60 µm, Figs. 42-43 represent 30 µm.

external and internal phloem Figures 34 - 37 illustrate the developmental sequence in the stem, and Figures 38 - 43 that in the leaf. At a distance of 80 µm below the shoot apex (Fig. 34), vascular differentiation is confined to protophloem sieve tubes of the external phloem (arrows). At higher magnification (Fig. 35) it is clear that neither protoxylem nor internal phloem differentiation has begun at this stage.

Between nodes 4 - 5 (Fig. 36) precursors of the primary phloem fibres are discernible, but their walls have not begun to thicken. Most of the external sieve tubes are now mature and a well-defined cambial zone is established between external phloem strands and the xylem. Maturation of the primary xylem has not been completed. Narrow zones of interfasicular parenchyma cells are visible between the bundles. At this level the internal phloem strands contain relatively numerous, small diameter sieve tubes.

The transection of Fig. 37 is representative of those examined between nodes 5 - 15. It is obvious that meristematic activity of the internal phloem strands continued after cessation of meristematic activity of the external strands. As a result the internal phloem strands are much larger than the external strands. Although the vascular cambium in Fig. 37 is completely formed, it has not yet produced any recognizable secondary tissue.

4.3.2 The Adaxial and Abaxial Phloem

Representative transverse sections of young leaves (Figs. 38 - 42), cut approximately 80 - 100 um above the apex, illustrate the sequence of differentiation and maturation of the vascular tissue in that part of the shoot. Figure 38 illustrates part of the leaf and leaf base of leaf

pair 1 - 2 (LP 1-2). No vascular differentiation was evident in LP 1, but in LP 2, the first protophloem sieve tube could be distinguished in the abaxial phloem. Organization of the vascular bundle was more conspicuous in LP 3 (Fig. 39). The precursor of the vascular cambium was already evident (arrowheads), the protoxylem had begun to differentiate, but was unlignified. Several protophloem sieve tubes are evident in the abaxial phloem of Fig. 39. The mesophyll is still poorly differentiated in this immature leaf.

In LP 4 a single protophloem sieve tube (arrow) is discernible in the adaxial phloem (Fig. 40). The vascular bundle is still poorly defined in this leaf pair, but it is beginning to assume a bicollateral form. In comparison, LP 5 (Fig. 41) has several distinct strands of adaxial phloem. The cambium is clearly formed in this leaf pair, separating the abaxial phloem from the protoxylem, which is beginning to develop secondary walls. The protophloem sieve tubes of the adaxial phloem are wider than those of the abaxial phloem. Figure 43 is a longitudinal view of the ad- and abaxial phloem in LP 6. Differentiation of the midrib in LP 6 (Fig. 42) is considerably advanced when compared to that in either LP 4 or LP 5 (Figs. 40 and 41). Especially conspicuous is the increase in numbers of sieve tubes per adaxial phloem strand compared with the abaxial phloem strands of LP 4 and LP 5. In LP 6 the lumina of both ad- and abaxial sieve tubes are clear, which suggests that the sieve tubes of both adaxial and abaxial phloem are mature and may function in the export of photosynthates to the still immature leaves.

It has been shown that Aphis nerii tends to feed on the internal and adaxial phloem of stems and leaves below node 5. The greater numbers of sieve tubes per strand in the internal and adaxial phloem might provide the aphids with greater quantities of assimilate than available in the

external and abaxial phloem.

As mentioned, the larger numbers of internal and adaxial strands, and the greater numbers of sieve tubes per strand are due in part to the greater longevity of meristematic activity associated with these strands, and partly to the belated differentiation of the internal phloem, compared with that of the external and abaxial phloem. Calculation of the changing ratio of external to internal phloem, e/i (Table II), based on observations of numerous transverse sections, indicates that the e/i ratio increases gradually basipetally in the primary axis. A fairly rapid increase in the e/i ratio occurs with the advent of the initiation and differentiation of the secondary phloem, which is initiated between nodes 15 - 16. The e/i ratio then continues to increase until death of the plant, usually 2 - 4 years after germination. Sections cut of mature two year old stems indicated that the internal phloem was still intact in such aged stems, but it could not be determined whether the internal phloem was still functional.

TABLE II

CHANGE IN e/i RATIO IN INTERNODES OF INCREASING MORPHOLOGICAL AGE

INTERNODE N^{o}.	e/i
Apex	
2	
3	1,5-1,8:1
4	0,30:1
5	0,32:1
7	0,54:1
9	0,62:1
15	0,90:1
Mature, 20-25	1,9-2,0:1
Two year	2,2:1 or more

PROTOPHLOEM CRUSHED

CAMBIAL ACTIVITY ↓

INTERNAL PHLOEM DOMINANT ↓

Inasmuch as the internal phloem begins to differentiate after the external phloem and the primary xylem, one may question whether the internal phloem should be considered as part of the original primary vascular bundle or as a separate tissue originating in the ground tissue. Jean (1926) in his examination of the origin of the internal phloem in the Solanaceae, Apocynaceae, Convolvulaceae, Onagraceae, Cucurbitaceae, Lythraceae, Compositae and Asclepiadaceae, suggested that within the leaf traces the internal phloem arose from procambium contiguous with the first xylem elements. This is the case in Gomphocarpus (Figs. 40 - 41). Jean (1926) further suggested that in the interfasicular region the differentiation of the internal phloem was delayed, but that at least the first elements in this part of the phloem arose from procambium.

The quantitative dominance of the internal and adaxial phloem may in itself provide part of the answer to the feeding habit of A. nerii. It may be that the internal/adaxial system translocates more assimilate than does the external/abaxial system. If this is the case, then more of the desired substances on which the aphid feeds would in all probability be present in the former than in the latter. Part of the answer may lie in ultrastructural and/or physiological differences between the two systems.

4.4 Summary

Investigation of the ontogeny and differentation of the primary phloem indicates that the external phloem and internal phloem do not begin to differentiate and mature at the same time. The external primary phloem begins to differentiate first, followed by xylem differentiation, and then by the internal phloem. Once differentiation of the internal primary phloem commences, which is between nodes four and five, it

rapidly becomes the quantitatively dominant phloem. It remains dominant until the vascular cambium commences producing secondary phloem. Investigation of serial transverse and longitudinal sections indicated that the external/abaxial and internal/adaxial primary phloem strands constitute separate systems in stem and leaf.

5. ULTRASTRUCTURE OF THE PRIMARY PHLOEM

5.1 Results and Discussion

It was stressed in section 4 that the internal and adaxial phloem and the external and abaxial phloem are two separate systems, the former anatomically independent of the other. Further, the light microscope study of ontogeny and differentiation indicated that differentiation of the external/abaxial phloem preceeded that of the internal/adaxial phloem, but that the internal/adaxial phloem was the dominant phloem by node five. An electron microscope investigation of the differentiation and maturation sequence within the external/abaxial and internal/adaxial phloem was therefore considered essential to a better understanding of their respective rôles in long-distance translocation of assimilates and hence, A. nerii's choice of feeding site.

Observation of numerous thin sections of stem and leaf material indicated that the ontogeny of the primary external and internal phloem of the stem closely parallels that of the abaxial and adaxial phloem respectively, but with one exception: the adaxial phloem strands do not consist of as large a number of sieve tubes and companion cells as do the internal phloem strands. It is therefore unnecessary to discuss the ontogenetic and developmental sequence in both stem and leaf. The results of the study of phloem differentiation and maturation are thus largely confined to findings in leaf material examined, especially petioles of leaves between nodes three to seven. The electron micrographs are representative of numerous stems and leaves examined.

5.1.1 Internal and Adaxial Sieve Element Protoplast

5.1.2 Protophloem

As mentioned the internal proto- and metaphloem sieve elements are shorter and narrower in cross-section than the corresponding external phloem proto- and metaphloem sieve elements (TABLE I). Figure 44 is an overall view of a typical internal protophloem strand. The sieve elements are surrouned by companion cells, and by procambial and sheath parenchyma cells. Some of the sieve elements in Figure 44 are partly collapsed, due either to pressure during sectioning, or to pressure due to expansion of the bundle. Two apparently functional sieve elements are visible, with parietally dispersed endoplasmic reticulum cisternae (ER). Note that the lumen of these sieve elements is essentially devoid of protoplasm. The companion cells of the protophloem vary in appearance, but all contain mitochondria, which vary in size and show varyin degrees of internal membrane structure, ER, and free ribosomes within their protoplasts.

Figure 45 shows a procambial mother cell which has recently undergone internal division. It is difficult to establish with any degree of certainty at such an early ontogenetic stage, which of these recently-formed phloem mother cells are destined to become sieve elements or companion cells. Part of a differentiating protophloem sieve element is shown at lower left. Although still immature, note the parietal aggregation of the protoplasm, lack of recongisable tonoplast, mitochondria and associated rough ER cisternae and dictyosomes.

The differentiation sequence within protophloem sieve elements is similar to that in the metaphloem sieve elements.

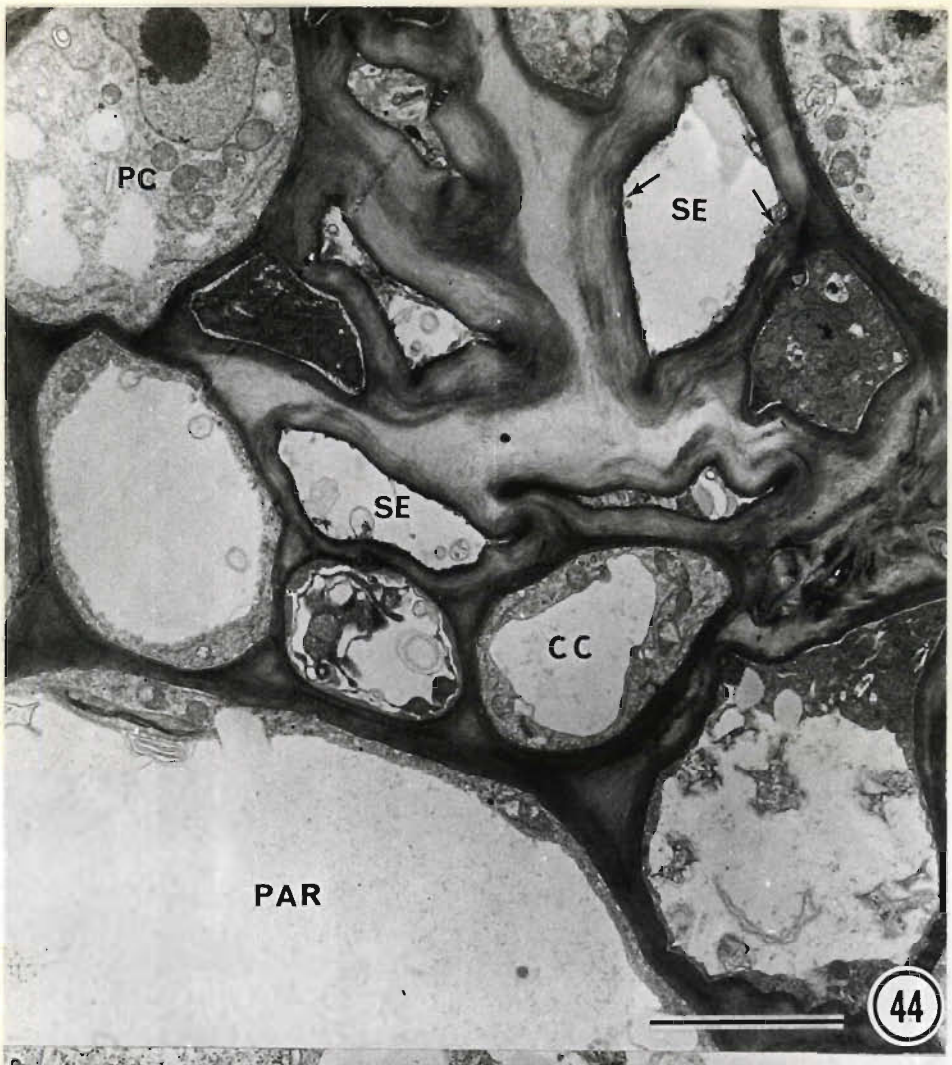
PC
SE
SE
CC
PAR
44

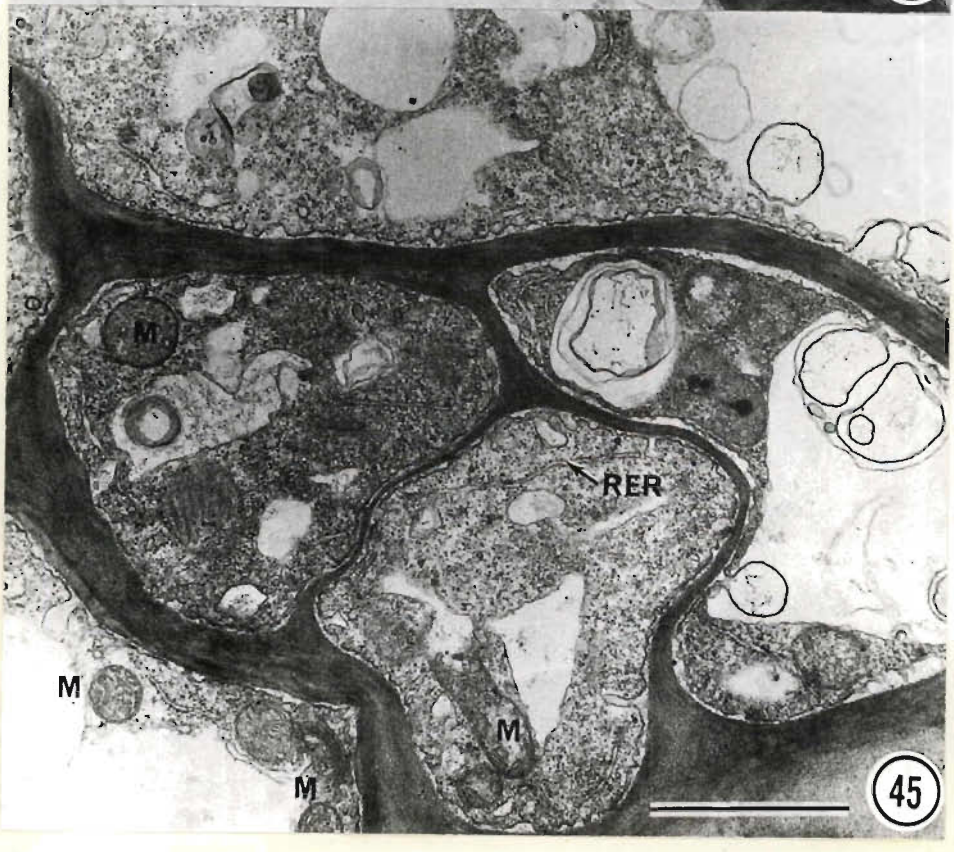
M
RER
M
M
M
45

Figs. 44–45. Transections of internal protophloem strand.

Figure 44. Shows two mature protophloem sieve tubes with parietally-dispersed protoplasm and endoplasmic reticulum (unlabelled arrows), companion cells, procambial and parenchymatous elements. Note partly-collapsed sieve elements. SE = sieve element, CC = companion cell, PAR = parenchyma, PC = procambium. Scale line represents 5 μm.

Figure 45. Shows detail of an internal phloem procambial cell, which has undergone internal division. Three immature procambial derivatives are visible in this section, containing rough endoplasmic reticulum (RER), numerous free ribosomes and mitochondria. The immature sieve tube (lower left) has parietally-dispersed protoplasm. M = mitochondrion, RER = rough endoplasmic reticulum. Scale line represents 3 μm.

5.1.3 Metaphloem

5.1.3.1 The P-Protein

The fibrillar nature of the substance comprising the P-protein bodies is apparent in Figures 47, 48, 55 and 57 - 58. A fibrillar P-protein aggregate occupies much of the lumen of the immature sieve element in Fig. 47 - 48, and are relatively narrow structures, ranging from 70 - 80 A in diameter. The tubular P-protein measures approximately 100 A. Orientation is vertical with respect to the longitudinal axis (Figs. 62 and 64) of the sieve elements during early stages of development as is the tubular P-protein (Fig. 57 and 58). Throughout the stages of development and dispersal of P-protein, the parietal layer of protoplasm is delimited from the vacuole by the tonoplast (Figs. 47 and 55). The maturing sieve element shown in Figure 47 contains a P-protein body which has dispersed. Significantly, the tonoplast is still intact in this sieve element. Evert and Deshpande (1969) reported similar findings in Ulmus americana phloem. It is pertinent to point out that in the mature sieve elements, the P-protein encountered varied both in size and appearance, but was predominantly dispersed around the periphery of the cell wall as indicated in Figs. 62 and 64. In transverse section, some of the sieve elements were almost entirely devoid of P-protein, (Figs. 61-62 and 64); while others contained large amounts of it. It is likely that all the mature sieve elements contained P-protein, but that distribution depended on the proximity of the section to the sieve plates or lateral sieve areas. Portions of slime plugs are shown in longisection in Figs. 74 - 77. It is obvious that the P-protein is aggregated in and near the sieve plate pores. Aggregation of P-protein was often observed in close proximity to lateral sieve areas as well

(Figs. 78 and 79), but not in all cases (Figs. 80 and 82). Where no P-protein was observed near lateral sieve areas, the lateral sieve area pores were often not occluded by P-protein (Figs. 80 and 82). It is therefore quite possible that the fixation technique used during the course of this study was inadequate in preventing disruption of the P-protein in mature, highly vacuolated sieve elements.

5.1.3.2 Organelles and Membrane Systems

During the early stages of development of Gomphocarpus phloem, the nucleate sieve element protoplast is similar in appearance to that of the procambial cells and its other derivatives. During the period of P-protein body development and early stages of dispersal of protoplasmic ground substance, the sieve elements are generally quite dense in appearance, compared with contiguous parenchymatous elements (Figs. 44 - 50 and 55).

The cytoplasm of immature sieve elements contain numerous free ribosomes (Figs. 45, 55 and 60) and many cisternae of mostly rough-surfaced ER (Figs. 47 and 48). Interspersed within the cytoplasm are numerous dictyosomes (Figs. 47 and 55) which, together with the rough ER cisternae, give rise to numerous membrane-coated vesicles (Figs. 48 and 55) and membrane complexes, which are found nearer the plasmalemma as the sieve elements mature (Northcote and Wooding, 1966; Weatherby and Johnson, 1968; Evert et al., 1966, 1969 and 1973a). Buvat (1963 a,b) reported that in sieve lements of Cucurbita pepo the ER forms and presses many vesicles against the cell wall. He suggested that these vesicles may be pinocytotic and accumulate solutions from the nacreous cell walls (see Esau and Cheadle, 1958) or might conversely transfer materials outward to produce callose or cell wall material. The cell walls in mature sieve elements of Gomphocarpus become lined with a layer which

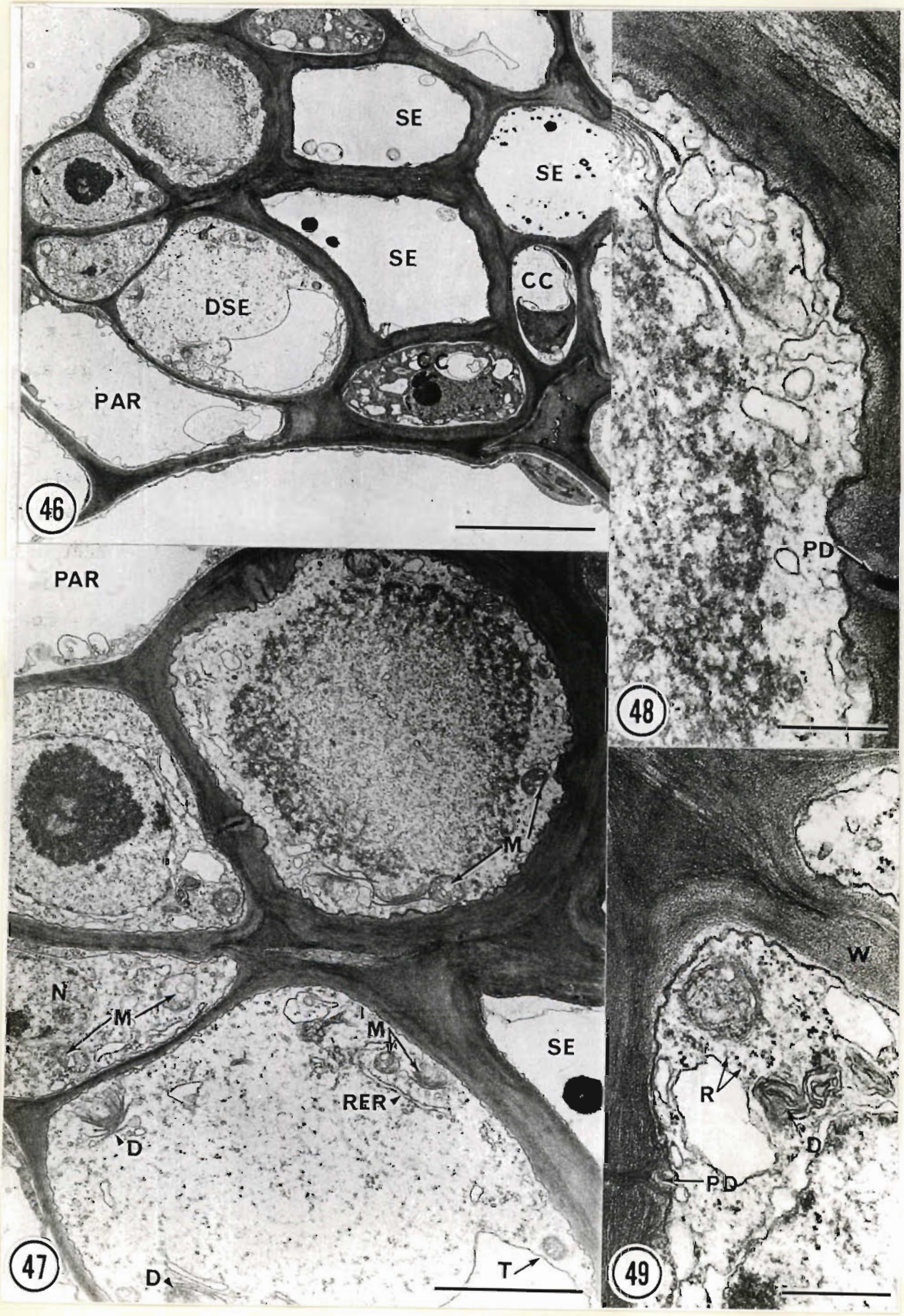
SE
SE
SE
CC
DSE
CC
PAR
46
PD
48
PAR
M
N
M
M
SE
RER
D
D
T
47
W
R
D
PD
49

Figs. 46-49. Transections showing stages of maturation of adaxial phloem strand. Three mature sieve tubes and associated companion cells are visible to the right of a group of immature sieve elements. At higher magnification (Figs. 47-49) two of the immature sieve elements, containing dispersed (Figure 49) and undispersed (Figure 48) P-protein are shown. The tonoplast is still visible, and the organelles are beginning to assume a parietal position. Endoplasmic reticulum closely parallels the P-protein body (Figure 48). Part of a plasmodesmatal connection between this immature sieve element and its contiguous companion cell is callose-free. Figure 49 shows part of the contiguous companion cell nucleus and protoplast. Note numerous free ribosomes. DSE = differentiating sieve element, SE = sieve element, CC = companion cell, PAR = parenchyma, RER = rough endoplasmic reticulum, M = mitochondrion, R = ribosomes, W = wall, PD = plasmodesmata, D = dictyosome, T = tonoplast Scale Lines: Figure 46 = 5 µm; Figure 47 = 3 µm, Figs. 48-49 = 0,5 µm.

contains closely packed membranes and sometimes vesicles (parietal layer, Duloy et al., 1961). Falk (1969 and literature cited therein) states that the membranes of the secretory vesicles are morphologically similar to those of the plasma membranes and are capable of fusing with the plasma membranes. Frequently, segments of endoplasmic reticulum closely parallel the surfaces of dispersed P-protein fibrils and tubes for some distances.

Concomitant with the dispersal of P-protein bodies, certain of the protoplasmic components undergo very marked changes. Especially notable are the changes which occur to the endoplasmic reticulum. In immature sieve elements the endoplasmic reticulum rammifies throughout the protoplasm, and consists predominantly of cisternae of rough ER (Figs. 47 - 48, 52 and 55). As the sieve element approaches maturity, the rough ER cisternae migrate toward the plasmalemma (Figure 56), assuming a parietal position (Fig. 61 and 62). The outermost layer of the ER cisternae becomes firmly attached to the plasmalemma, to the extent that it is often difficult to distinguish between plasmalemma and the contiguous membrane of the endoplasmic reticulum (Figs. 53 - 56, 62 and 64). Various views of these parietally situated membranes indicate that they comprise an extensive and highly complex network.

Often ER cisternae become stacked along the wall, the outermost membrane of each stack being closely appressed to the plasmalemma. In most of the stacks encountered, the cisternae have a very orderly arrangement (Figs. 61 - 64, 65 and 67). Most of these stacks were horizontally orientated with respect to the longitudinal axis of the sieve element, but some (Fig. 64) were vertically orientated. As mentioned, the ER membranes in young sieve elements are generally associated with ribosomes, whilst those in mature sieve elements are entirely smooth-surfaced.

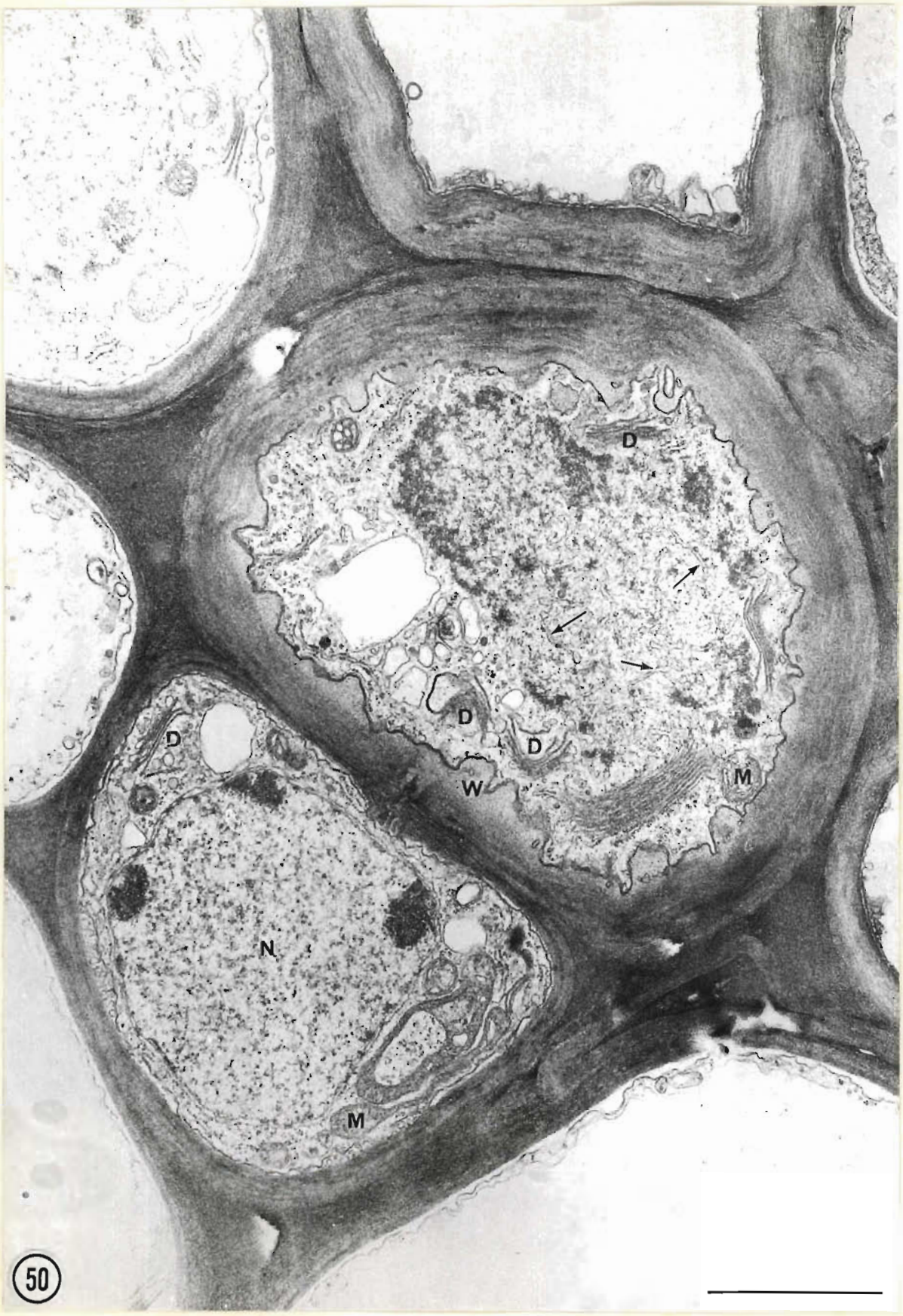

50

Figure 50. Transverse section of immature adaxial metaphloem sieve element (upper) and immature companion cell (lower). P-protein dispersal and parietal dispersal of and distribution of ER is well advanced. Note ramification of ER (unlabelled arrows) within the protoplast, and the distinct inner wall layer (W) of the sieve element. D = dictyosome, N = nucleus, M = mitochondrion. Scale line represents 2.5 μm.

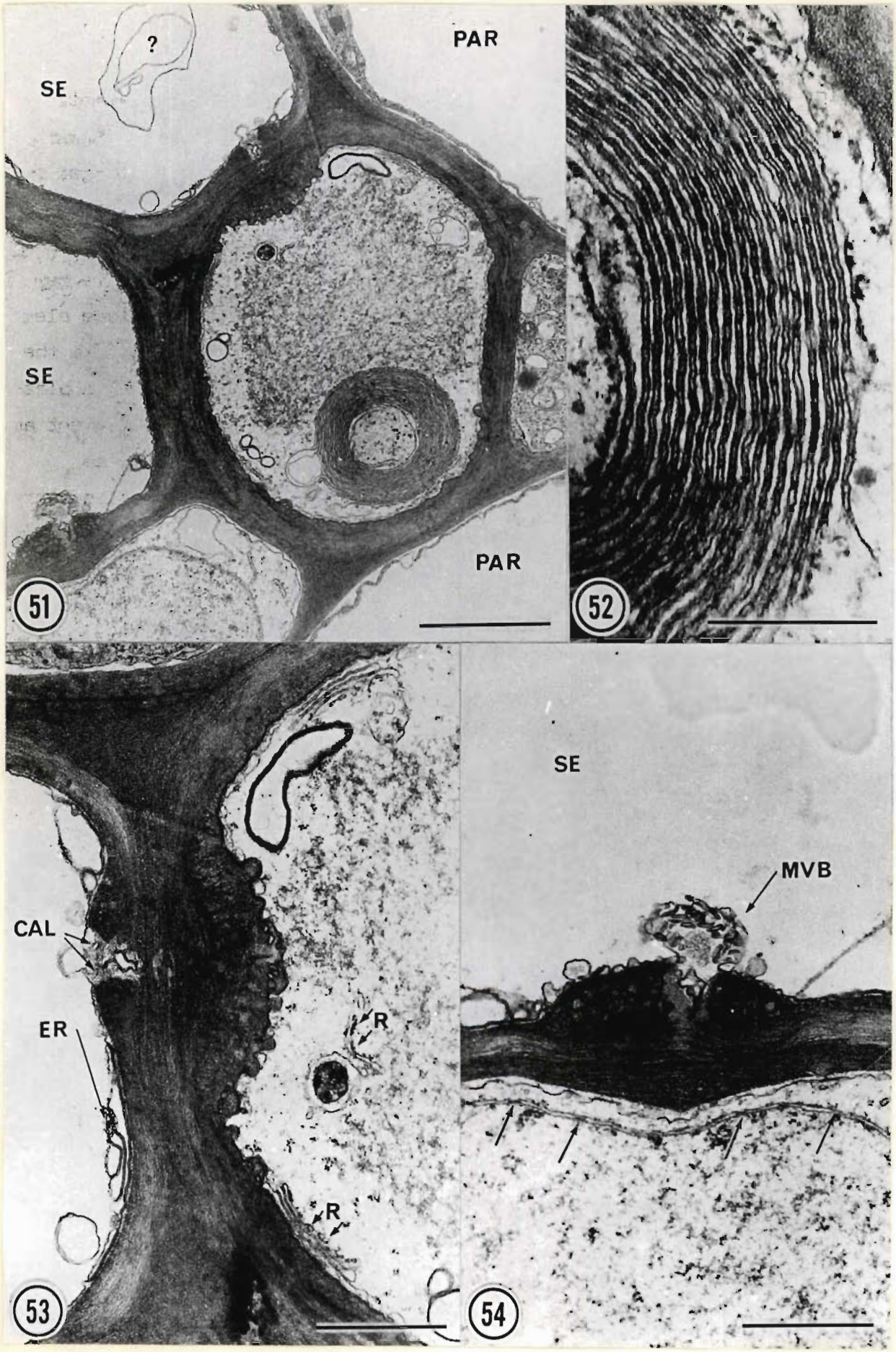
?
SE
PAR
SE
PAR
51
52
CAL
ER
R
R
53
SE
MVB
54

Figs. 51–54. Transverse sections of maturing adaxial sieve elements. Figure 51. Shows dispersing P-protein body in an immature sieve element. Note the large myelin figure, enlarged in Figure 52 to show that it consists of concentric rings of ER, with ribosomes attached to the inner and outer face. Figure 53. Shows developing lateral sieve area pore between a mature sieve element and contiguous immature sieve element. Ribosomes (unlabelled arrows) are still attached to the ER. Figure 54. Shows glancing section through part of a plasmodesmatal pore between mature metaphloem sieve element and contiguous companion cell. A multivesicular body is associated with the pore. Nuclear pores (unlabelled arrows) are evident in the nuclear membrane. MVB = multivesicular body, R = ribosomes, CAL = callose. Scale lines: Figure 51 = 2,5 μm; Figure 53 = 0,5 μm; Figs. 52 and 54 = 1,0 μm.

During formation of the stacks, the ribosomes are first lost from the surfaces of adjacent cisternae and then from the surfaces of the cisternae facing the plasmalemma (Figs. 52 and 55). Evert and Deshpande (1969) reported a similar sequence of events in the ontogeny of elm phloem.

The endoplasmic reticulum of mature internal and adaxial phloem is fairly uniform in size, mostly about 100 A (range: 95 - 160 A). The intercisternal spaces are uniform, usually 90 A (range: 60 - 120 A). The width of the intracisternal spaces are variable, the average being 160 A (range: 95 - 230 A). The intercisternal spaces contain an electron-opaque substance (Figs. 52, 61 and 65), whereas the intracisternal spaces are relatively clear in appearance.

A feature often observed was that plastids (Figs. 65 and 67) and mitochondria (Figure 66) of both immature and mature sieve elements were often closely associated with endoplasmic reticulum cisterae. Northcote and Wooding (1968) reported that during differentiation of the sieve elements of sycamore, the sieve element plastids were always surrounded or ensheathed by endoplasmic reticulum cisternae during the breakdown of the cell contents. The internal and adaxial sieve elements of Gomphocarpus contain only one type of plastid (Figs. 65 and 67). No plastids were observed which contained recognisable protein. All plastids contained starch, and as these plastids matured, so the proliferation of internal membranes became less obvious in thin sections.

This results in a loss of electron-density of the plastid matrix, (compare Fig. 67 with Figs. 74 - 76), a feature often encountered in maturing sieve tube plastids (see Evert and Deshpande, 1969 and references cited therein). Wooding and Northcote (1965) and Northcote and Wooding (1966 have reported that the plastids of developing sieve tubes of Acer pseudoplatanus are sheathed over all or part of their surfaces by endo-

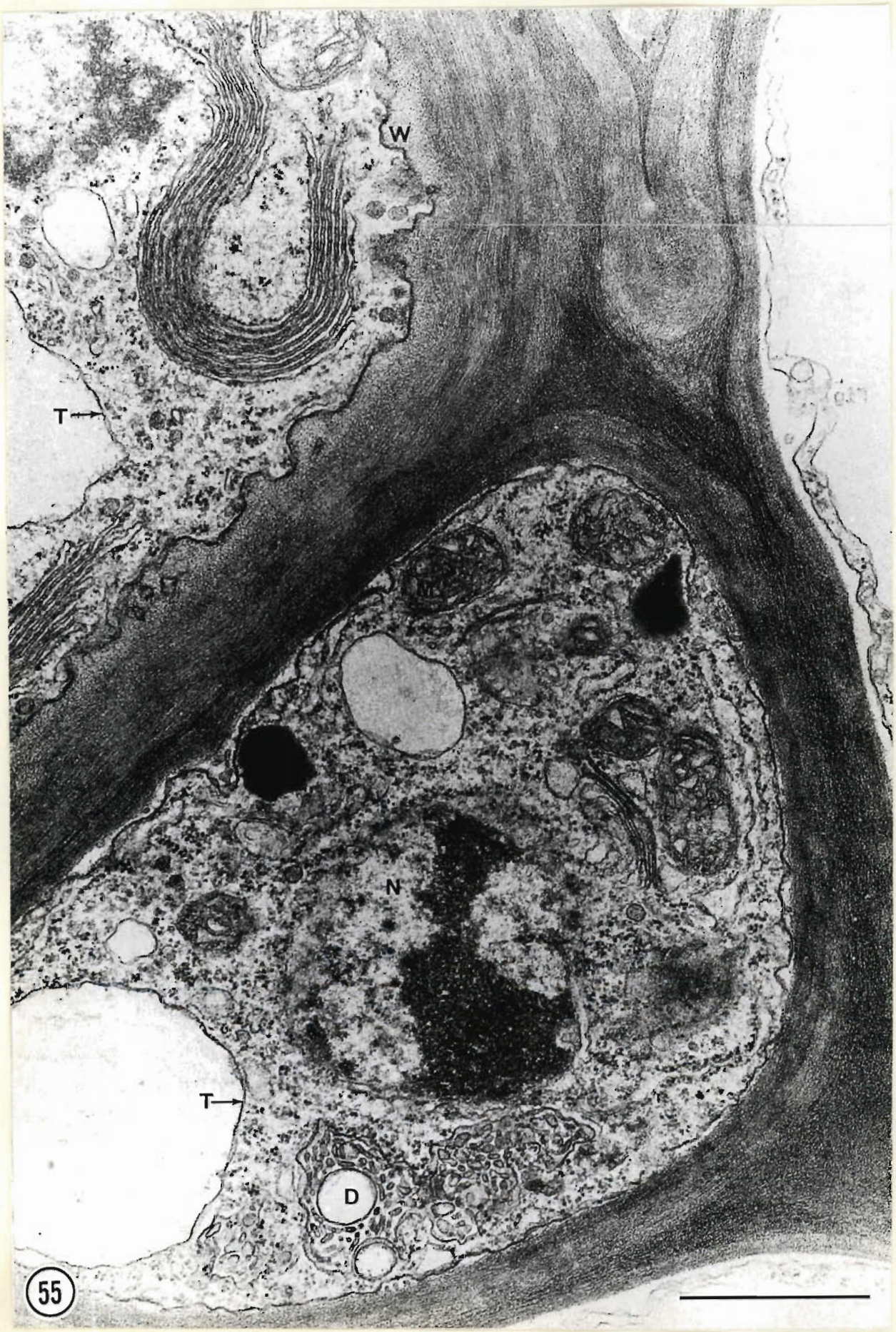
W
T
N
T
D
55

Figure 55. Transverse section of an immature adaxial metaphloem sieve element (upper) and its contiguous companion cell. The large vesiculate body in the companion cell (D) is a transversely-cut dictyosome. Ribosomes have become dissociated from the sieve element ER, except for the inner and outer faces of these bodies, which are at this stage, closely associated with the inner face of the wall (W). N = nucleus, D = dictyosome, M = mitochondria, T = tonoplast. Scale line represents 1,0 µm.

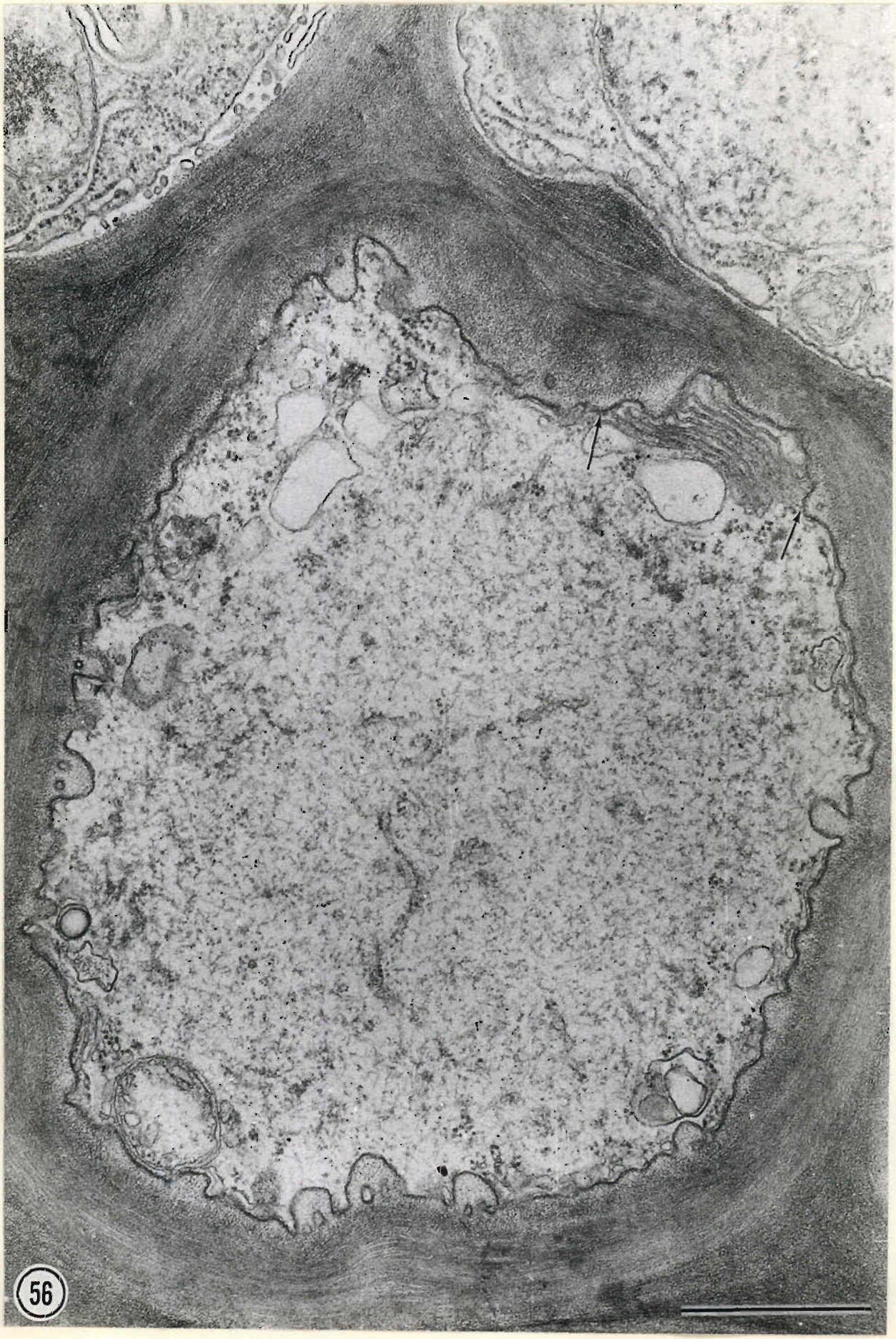
56

Figure 56. Transverse section showing later stage of differentiation of immature adaxial metaphloem sieve element. P-protein dispersal is almost complete, and ER lies closely-appressed to the plasmalemma (unlabelled arrows). Note the distinct inner wall layer. Scale line represents 1,0 µm.

plasmic reticulum, but that plastids of mature sieve elements are not. In Gomphocarpus, plastids from sieve tubes with open pores in adaxial phloem were often seen to have structures resembling transversely cut fibrillar P-protein filaments attached to the outer surface of the plastid membrane (Figs. 74 and 75). Wooding and Northcote (1965) have suggested that sheathing endoplasmic reticulum might play a role in plastid de-differentiation. Whether or not these P-protein filaments associated with plastids from mature Gomphocarpus sieve elements play a role in plastid de-differentiation is not known.

5.1.4 Cell Walls

Although the lateral walls of protophloem sieve elements generally are thickened, their outline is more regular than that of metaphloem sieve elements. The waivy outline of metaphloem sieve elements is evident when Figure 44 is compared with Figs. 47 - 49, 50, 55, 56 and 58. Evert and Deshpande (1969) encountered sieve elements in elm which had a distinct inner wall layer which was loosely lamellate in appearance. Evert and Deshpande described these walls as not being nacreous. Warmbodt and Evert (1974) suggest that irregularities in the inner wall surface of sieve elements of Lycopodium lucidulum arise as a result of "erosion" or hydrolysis of wall material during the late stages of sieve element development. In Gomphocarpus many of the metaphloem sieve elements had walls which consisted of an inner wall layer, which appears to be morphologically distinct from the outer wall layer (Figs. 55 and 56). Dictysome and endoplasmic reticulum vesicles were often appressed to, or in close association with, the plasmalemma, which overlies the morphologically distinct wall layer. As mentioned, the endoplasmic reticulum and dictyosome-derived vesicles have been associated with

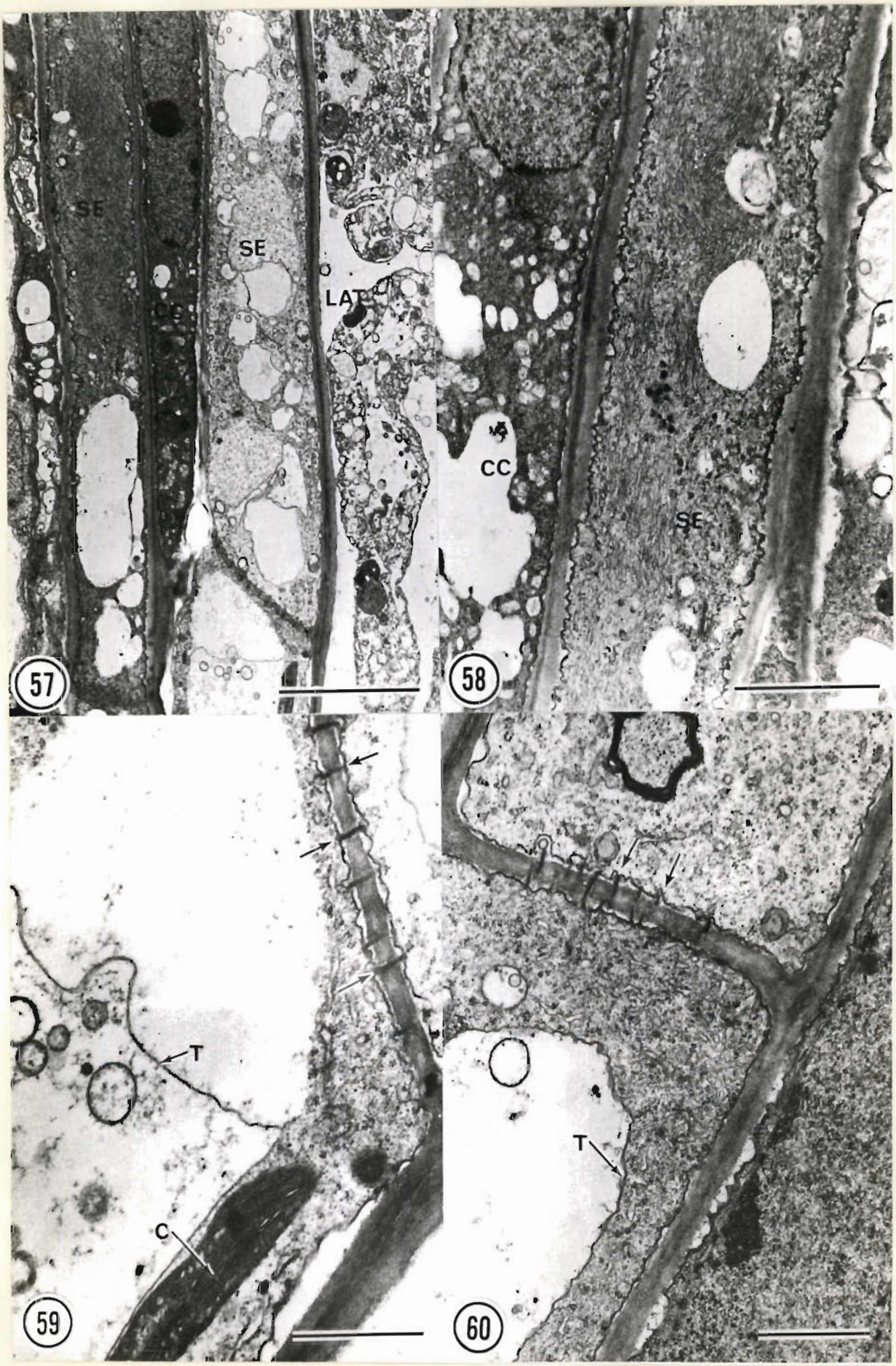
SE
SE
LAT
CC
57
CC
SE
58
T
C
59
T
60

Figs. 57–60. Longitudinal sections through very young adaxial sieve elements.

Figure 57. Shows two immature sieve elements, the younger (to the left) contains a large undispersed mass of longitudinally-oriented P-protein (enlarged in Figure 58).

Figs. 59 and 60. Show differentiating sieve plates from upper (Figure 60) and lower (Figure 59) ends respectively of the same sieve element. The developing pores are still plasmodesmatal. Narrow callose platelets are visible between the plasmodesmal apertures (unlabelled arrows), marking the sites of the future sieve plate pores. Note the chloroplast in the ontogenetically-youngest immature sieve element. CC = companion cell, SE = sieve element, LAT = laticifer, C = chloroplast, T = tonoplast.

Scale lines: Figure 57 = 5μm; Figure 58 = 3 μm; Figs. 59 and 60 = 1 μm.

nacreous wall thickening (see Esau and Cheadle, 1958) or could transfer materials outward to produce callose or cell wall material (Duloy et al., 1961; Northcote and Wooding, 1966).

5.1.4.1 Plasmodesmata

Plasmodesmal connections between immature and mature adaxial sieve elements and their contiguous companion cells were of variable appearance, often occurring in groups (Figs. 69 and 71) or singly (Figs. 70 and 73). Figure 69 is a glancing section through parietal cytoplasm and cell wall of an adaxial phloem companion cell. The callose platelets seen in such views were typically 16 - 20 A thick, with pores ranging in diameter from 300 - 375 A. Figure 71, and at higher magnification in Figure 72, is a glancing section of part of a mature sieve element and contiguous companion cell, which shows typically wide zones of callose deposited around the plasmodesmal pores on the sieve element side. Callose thickness varies from 500 to 1000 A. Figure 70 clearly shows that callose deposition is greatest on the sieve element side, tapering rapidly toward the companion cell. In some instances (Figure. 73) no callose deposition was observed associated with the plasmodesmata.

5.1.5 Sieve Plates and Lateral Sieve Areas

5.1.5.1 Sieve Plates

In immature sieve elements, perforation of the cross-walls between contiguous sieve tube members is initiated early in the differentiation sequence, and prior to the dispersal of P-protein or the disappearance of the tonoplast. Figure 57 and 59 - 60 are views of differentiating sieve plates in immature adaxial phloem. Callose deposition is limited

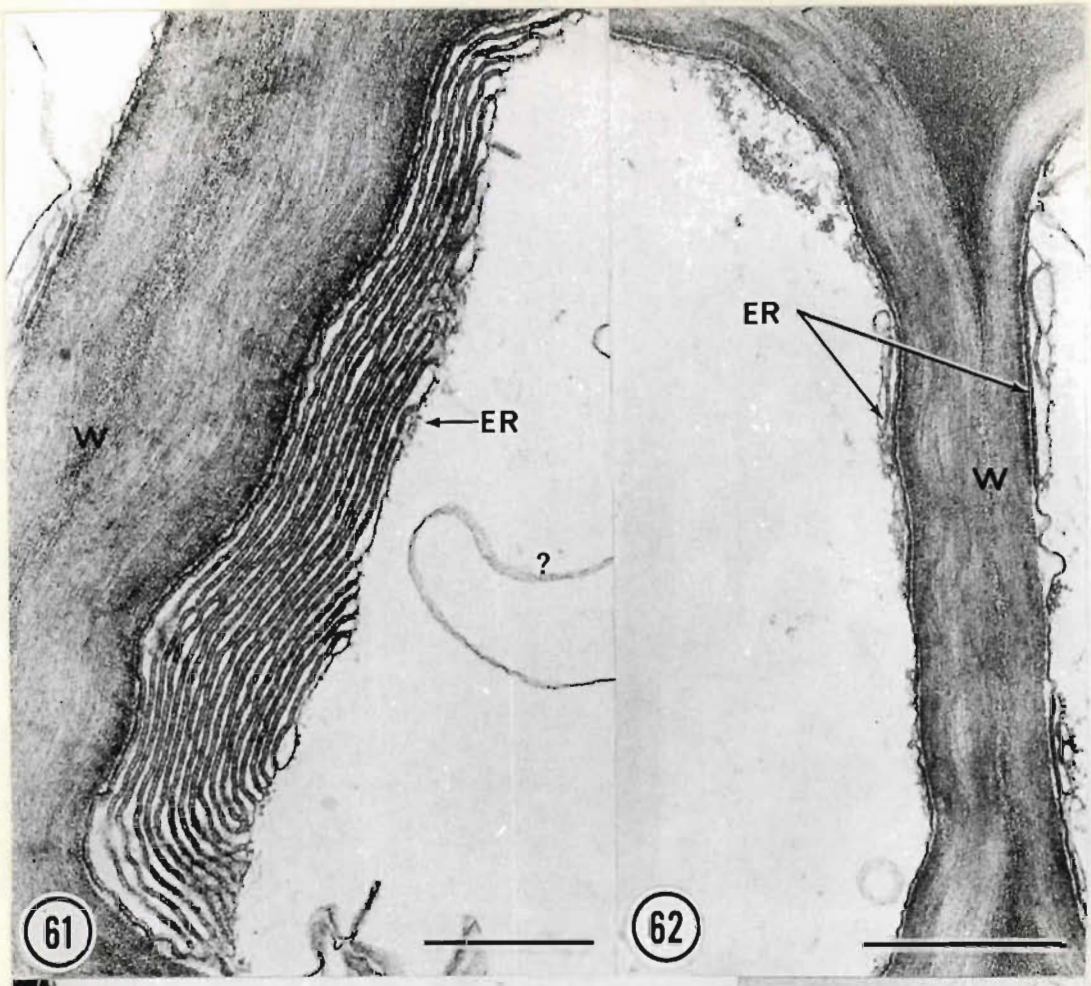
W
ER
?
61
ER
W
62

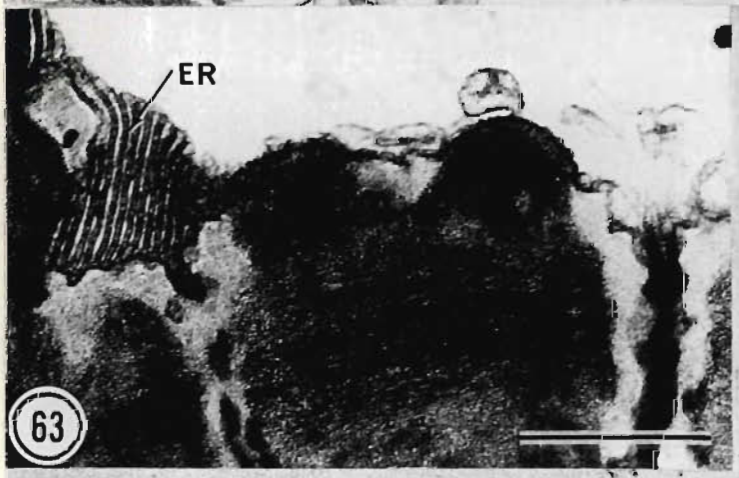
ER
63

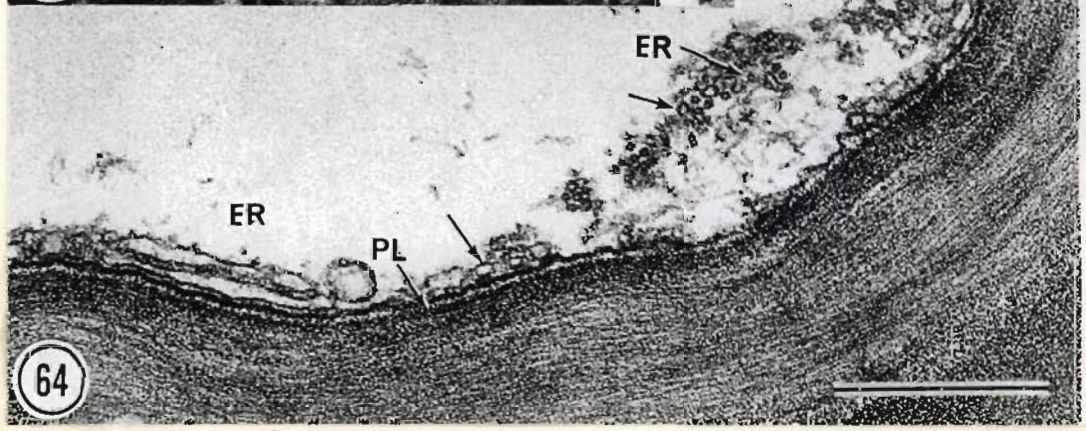
ER
ER
PL
64

Figs. 61-64. Transverse (Figs. 61, 62 and 64) and longitudinal (Figure 63) sections of mature adaxial metaphloem sieve elements, showing ER which exists as a parietal system of smooth cisternae, closely appressed to the plasmalemma. Most of the ER cisternae were horizontally-orientated (Figs. 61, 62 and 64), some vertically orientated with respect to the longitudinal axis of the sieve elements. Some vertically-orientated tubular P-protein (Figure 62, and at higher magnification, in Figure 64) is interspersed with the vertically-orientated ER. W = wall, PL = plasmalemma, unlabelled arrows = tubular P-protein, ? = unidentified component. Scale lines: Figs. 61, 63 and 64 = 0,5 µm; Figure 62 = 1,0 µm.

to narrow platelets between the pores, which, even at this early stage, interconnect the contiguous immature sieve tube members. None of the sieve plate pores in immature or mature adaxial phloem lacked callose. Not only were the pores lined with callose, but all surfaces of the plates were generally lined as well. Figures 74 - 77 are views of mature sieve plates. At maturity, each sieve plate pore is lined by the plasmalemma. In some instances (Figure 77) endoplasmic reticulum cisternae were observed closely appressed to the plasmalemma in close proximity to the sieve plate pores. The sieve plate pores were in all instances, traversed by P-protein (Figure 75), the quantity of P-protein present varying with its distribution within the sieve elements. Sieve elements with slime plugs generally exhibited sieve plate pores plugged with P-protein (Figs. 75 - 76). The contents of such plugged pores was often so dense that no structure could be seen within them. The fact that all sieve plates of the adaxial phloem examined contained varying amounts of P-protein and callose suggests that the fixation (Evert et al., 1973a) was not entirely suitable for the adaxial phloem of Gomphocarpus.

In mature sieve elements, the pores measure approximately 0,07 to 0,10 µ at the narrowest point, and 0,49 to 0,51 µ at the widest. Taking into account the thickness of the callose cylinders (range: 0,13 to 0,17 µ), then they would measure on average, 0,51 µ at their narrowest point (range: 0,43 to 0,59 µ).

5.1.5.2 Lateral Sieve Areas

The lateral sieve areas of the adaxial phloem often extended for more than 15 µ along the walls of contiguous sieve elements. Figure 79 shows a portion of an obliquely cut lateral sieve area. All lateral sieve areas were partly occluded and lined by callose cylinders of variable thickness.

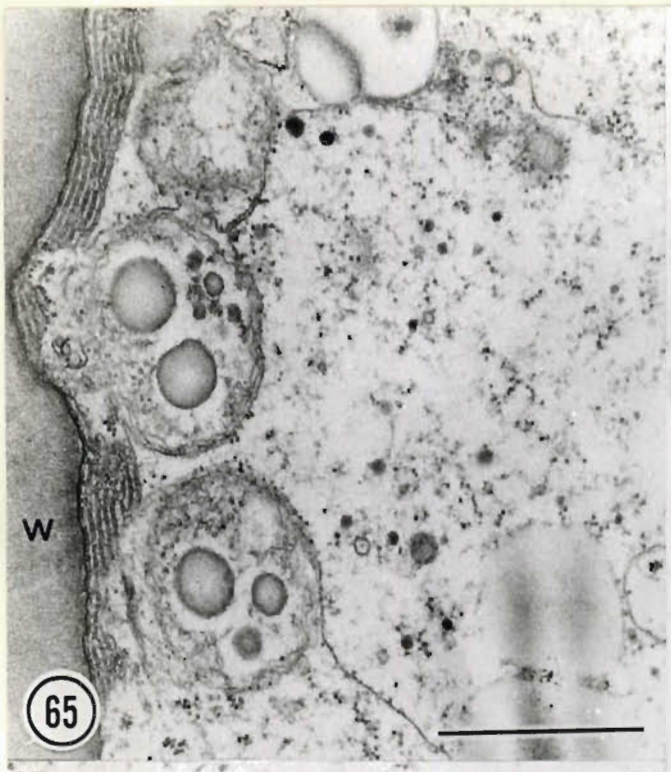

65

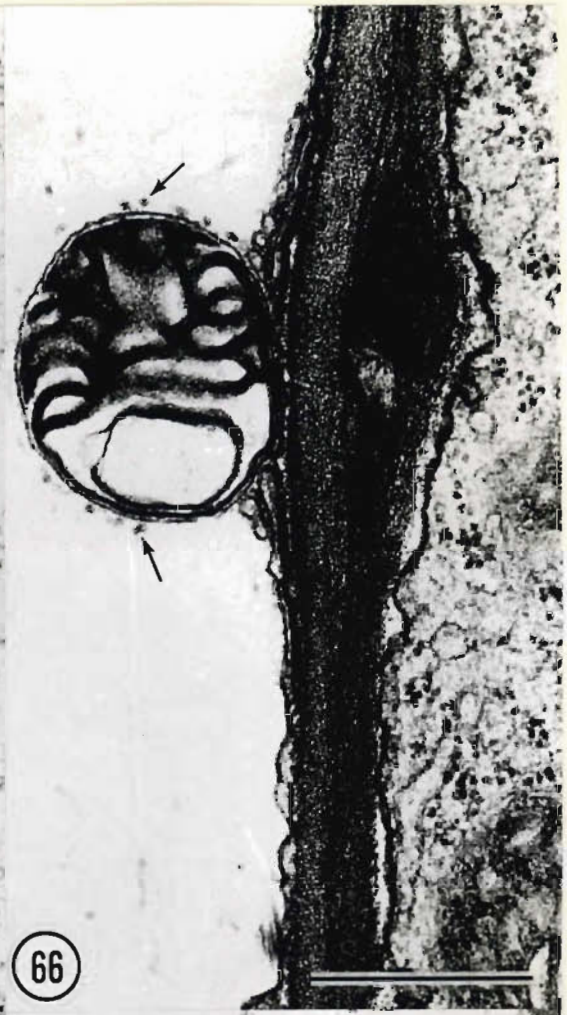

66

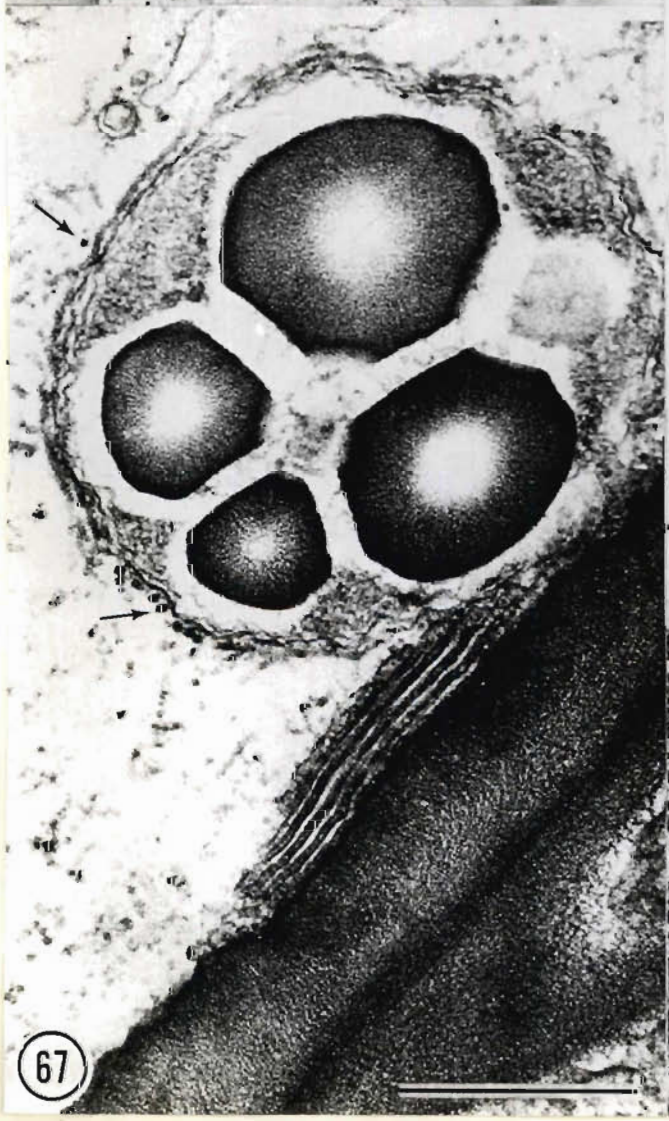

67

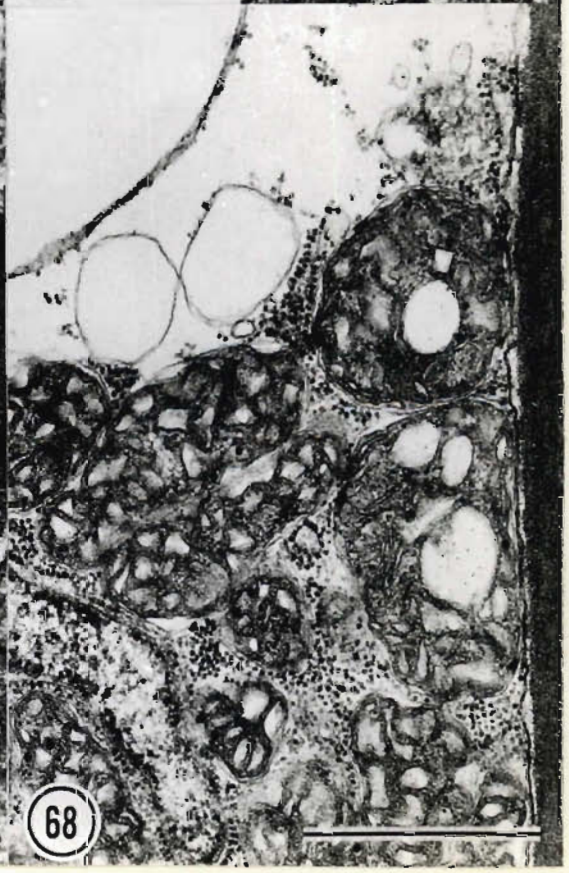

68

Figs. 65 – 68. Longitudinal sections of immature (Figure 65) and mature (Figs. 66 and 67) adaxial metaphloem sieve elements and associated companion cells (Figs. 66 and 68). The plastids are closely-appressed to the plasmalemma and smooth ER cisternae. P-protein is closely-associated with platids and mitochondria in mature sieve elements (Figs. 66 and 67). W = wall, unlabelled arrows = P-protein. Scale lines: Figs. 65 and 68 = 1,0 µm; Figs. 66 and 67 = 0,5 µm.

The width of the pores at their narrowest point was on average 0,044 μ (range: 0,040 to 0,048 μ). As stated, the width of the sieve plate pores was approximately 0,09 to 0,10 μ. The lateral sieve area pores do not fall into the same size range as the sieve plate pores.

Nearly all lateral sieve area pores examined contained P-protein (Figs. 78 - 82). In most pores the P-protein was densely packed (Figure 79) and had an amorphous appearance, except near the apertures of the pores where individual components of P-protein could be seen extending into the lumina of the cells (Figure 79). The degree of P-protein packing was related to the amount of P-protein within the respective sieve elements. Some lateral sieve area pores, notably those from non-plasmolysed sieve elements, contained no P-protein within the pore apertures (compare Figs. 53, 54 and 77 to Figs. 79 and 82). All pores were lined by the plasmalemma, which was contiguous from cell to cell.

The median nodule, which is formed during early stages of perforation of the pore site, is not always apparent in fully-developed pores whilst in others it is easily recognisable (Figs. 78 and 79). The diameter of some of the fully-developed pores is often uniform from one side of the pore to the other (0,18 μ), so that the nodule no longer exists in the region of the middle lamella (Figure 80).

As stated, not all lateral sieve area pores examined were occluded by P-protein. Figure 82 shows an example of a lateral sieve area pore which lacked P-protein. None of the lateral sieve area pores examined contained endoplasmic reticulum. Evert *et al.*, (1971) examined the lateral sieve area pores of seven species of woody dicotyledons and reported that in *Tilia americana* lateral sieve area pores contained vesicular material, tentatively identified as endoplasmic reticulum. In addition, they reported P-protein within the median cavities of *Tilia*, which were occluded by dormancy

callose, indicating that P-protein may normally be present within the pores.

5.1.6 Companion Cells, Procambial Cells and Phloem Parenchyma

5.1.6.1 Companion Cells

The adaxial phloem sieve elements usually have one but sometimes two companion cells per sieve tube member. During early stages of ontogeny, it is difficult to distinguish immature companion cells from immature sieve elements. As the companion cells mature, certain changes take place within the cytoplasm; the nucleus elongates and heterochromatin material becomes peripherally dispersed (Figs. 57 and 58). Mature companion cells contain mitochondria which have highly developed cristae similar to those in adaxial phloem sieve elements, endoplasmic reticulum, and many free ribosomes dispersed throughout the cytoplasm. Mature companion cells have numerous plasmodesmatal connections with their respective sieve elements (Figs. 69 and 71).

5.1.6.2 Procambial Cells

The adaxial protophloem (Figure 44) is surrounded by procambial and sheath parenchyma cells. As stated, the primary phloem is as in other plants, derived from procambium, which divides internally, giving rise to companion cells and sieve elements. After division and during the early stages of phloem ontogeny, the procambial cells are very similar to immature companion cells and immature sieve elements (Figure 45), as they contain free ribosomes, endoplasmic reticulum and mitochondria.

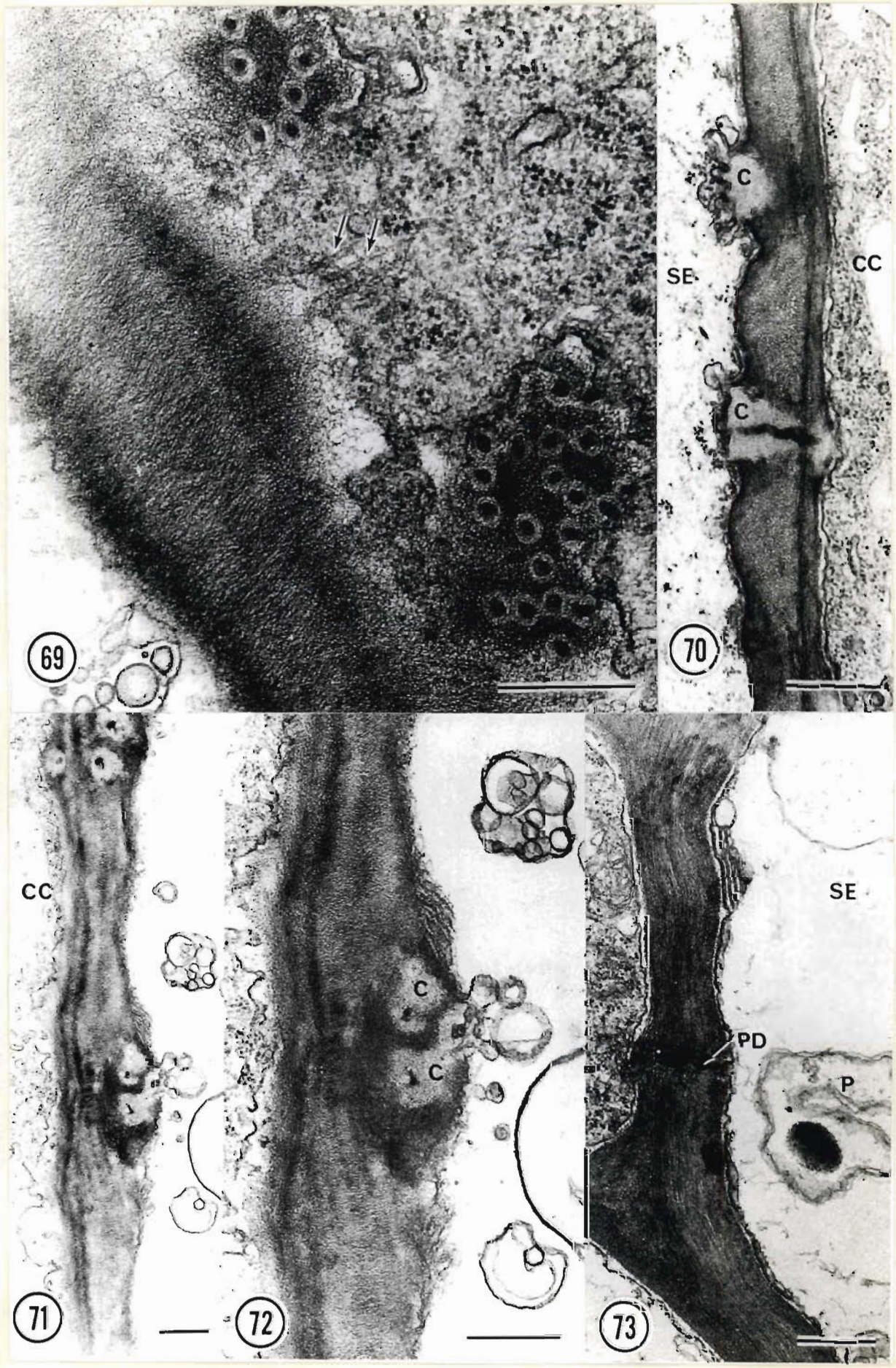
69
70
C
SE
CC
C
71
72
73
CC
C
C
SE
PD
P

Figs. 69–73. Plasmodesmatal connections between mature sieve elements and contiguous companion cells.

Figure 69. Glancing section showing in surface view, two groups of plasmodesmata as seen from companion cell side of pores. Callose is confined to a narrow ring surrounding pores. Note longitudinal micro-tubules (unlabelled arrows).

Figs. 70 and 73. Show longitudinal sections through plasmodesmata surrounded by callose (Figure 70) and plasmodesmatal pore (PD) free of callose (Figure 73).

Figs. 71 and 72. Surface view of pores, showing uneven disposition of callose. CC = companion cell, SE = sieve element, C = callose. Scale lines represent 0,5 µm.

5.1.6.3 Phloem Parenchyma

The parenchymatous elements which surround the primary phloem strands of Gomphocarpus are the widest in cross-section (40 μ and more) of all the phloem components. In comparison to the other phloem components, phloem parenchyma cells are highly vacuolated, and contain mitochondria, chloroplasts, rough and smooth endoplasmic reticulum within the peripheral cytoplasm (Figs. 45, 46, 47, 50 and 51).

5.2 External and Abaxial Sieve Element Protoplast

5.2.1 Protophloem and Metaphloem Origin

The external and abaxial protophloem of Gomphocarpus has a very similar ontogeny and structure compared to the internal and adaxial protophloem, therefore it does not require separate discussion. Light microscopic investigation revealed that like the internal/adaxial phloem, precursors of the external/abaxial phloem was procambium. One major point of difference is that the primary external/abaxial phloem have less procambial cells per strand than the internal. Observations of thin sections indicated that the external/abaxial phloem procambial cells lost their meristematic function after the formation of from 9 - 15 sieve elements per strand.

5.2.2 The P-protein

A major point of difference observed in thin sections was the apparent lack of P-protein in mature abaxial sieve tubes. By comparison, the P-protein within abaxial phloem sieve elements disperses, and becomes more dispersed within the parietal layer than was observed in mature

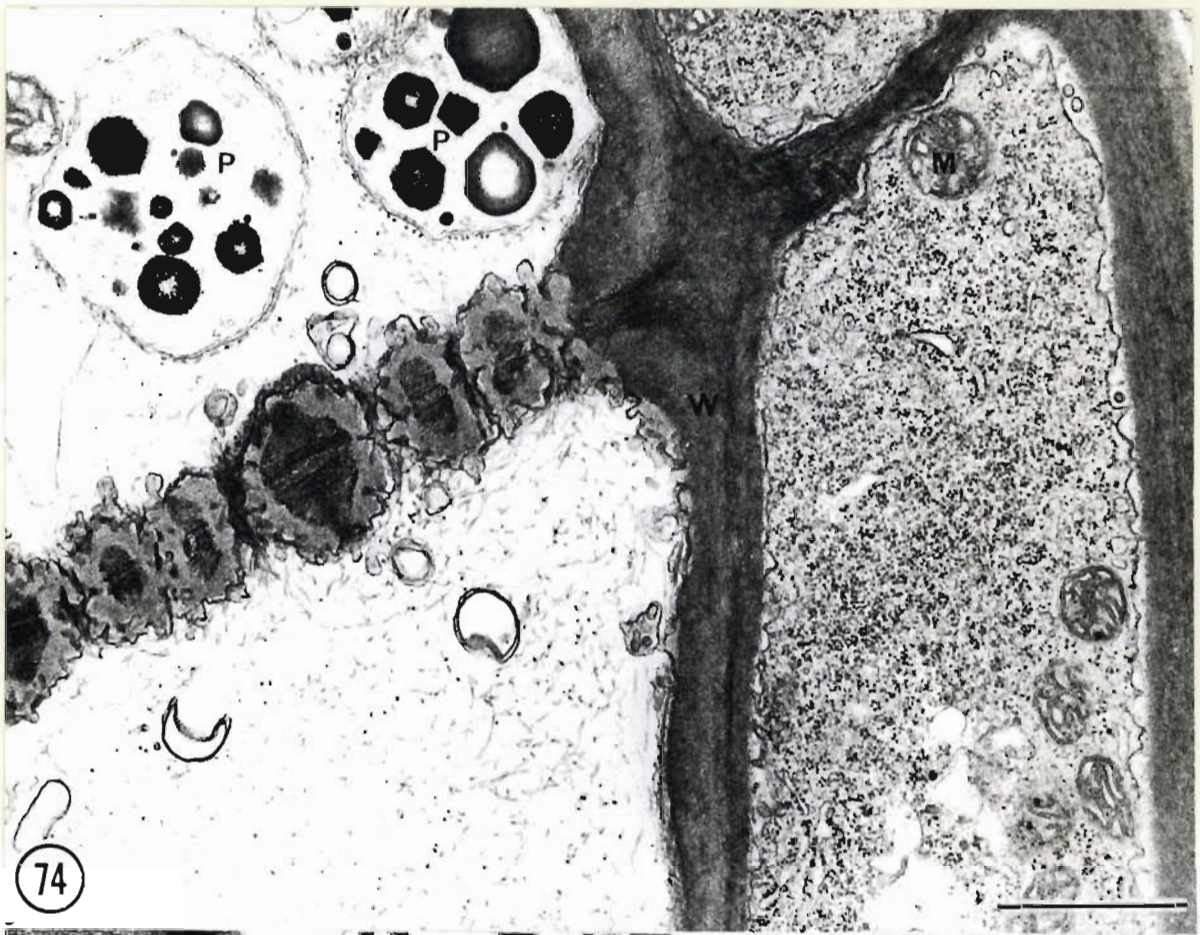

74

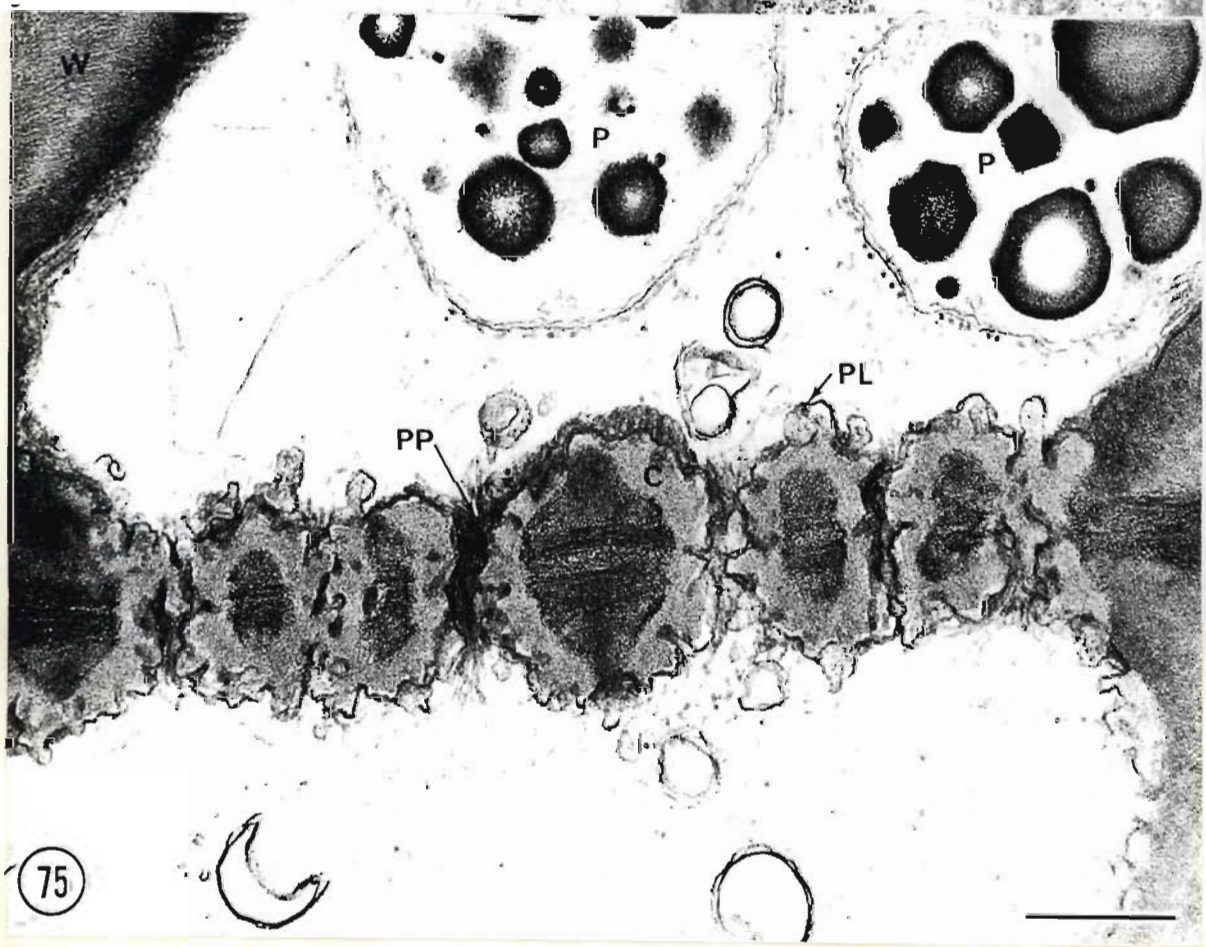

75

Figs. 74-75. Glancing longitudinal section through portion of a sieve plate of mature adaxial metaphloem sieve element and contiguous companion cell. All sieve plate pores are partly occluded by varying amounts of callose and P-protein, the latter due to surging of the sieve element contents. At higher magnification (Fig. 75) variable detail is discernible within the pores. W = wall, P = plastid, M = mitochondrion, C = callose, lining pores of sieve plate, PP = P-protein, PL = plasmalemma.
Scale lines: Figure 74 = 1,0 µm; Figure 75 = 0,5 µm.

adaxial sieve elements (compare Figs. 88 - 90 with Figs. 61 and 62). Of significance was the lack of slime plugs associated with sieve plates and lateral sieve areas compared with the adaxial phloem, and the lack of P-protein within sieve plate pores or lateral sieve area pores (compare Figs. 84 and 88 - 90 with Figs. 63, and 74 - 77).

The extrafasicular sieve elements of Cucurbita (Cronshaw and Esau, 1968, and literature cited therein) contain slime bodies which fail to disperse at maturity, unlike those within the bundles. The sieve plate pores of the extrafasicular sieve elements are usually unobstructed by P-protein (Cronshaw and Esau, 1968; Evert et al., 1973a). P-protein has been reported to be absent from mature sieve elements of a large number of plants (see Evert et al., 1973a, and literature cited therein).

If P-protein plays an essential role in the long distance translocation of assimilates, then this must indicate that more than one mechanism of long distance translocation in sieve elements must be operative. At least one in plants which contain P-protein and at least one or even more, in those plants in which P-protein is lacking. Whilst it may be acceptable that more than one mechanism may be responsible for long distance translocation in different plants, it is unlikely that two independent translocation mechnaisms are operative, one in the external/abaxial phloem and another in the internal/adaxial phloem of Gomphocarpus. It must be assumed that P-protein, or the lack of the substance, is not causative in the preferential feeding of Aphis nerii on the internal/adaxial phloem. However, it cannot be ruled out that lack of or less P-protein within mature abaxial and external sieve elements may exert some effect on the translocation rate compared with that in the adaxial and internal phloem sieve elements.

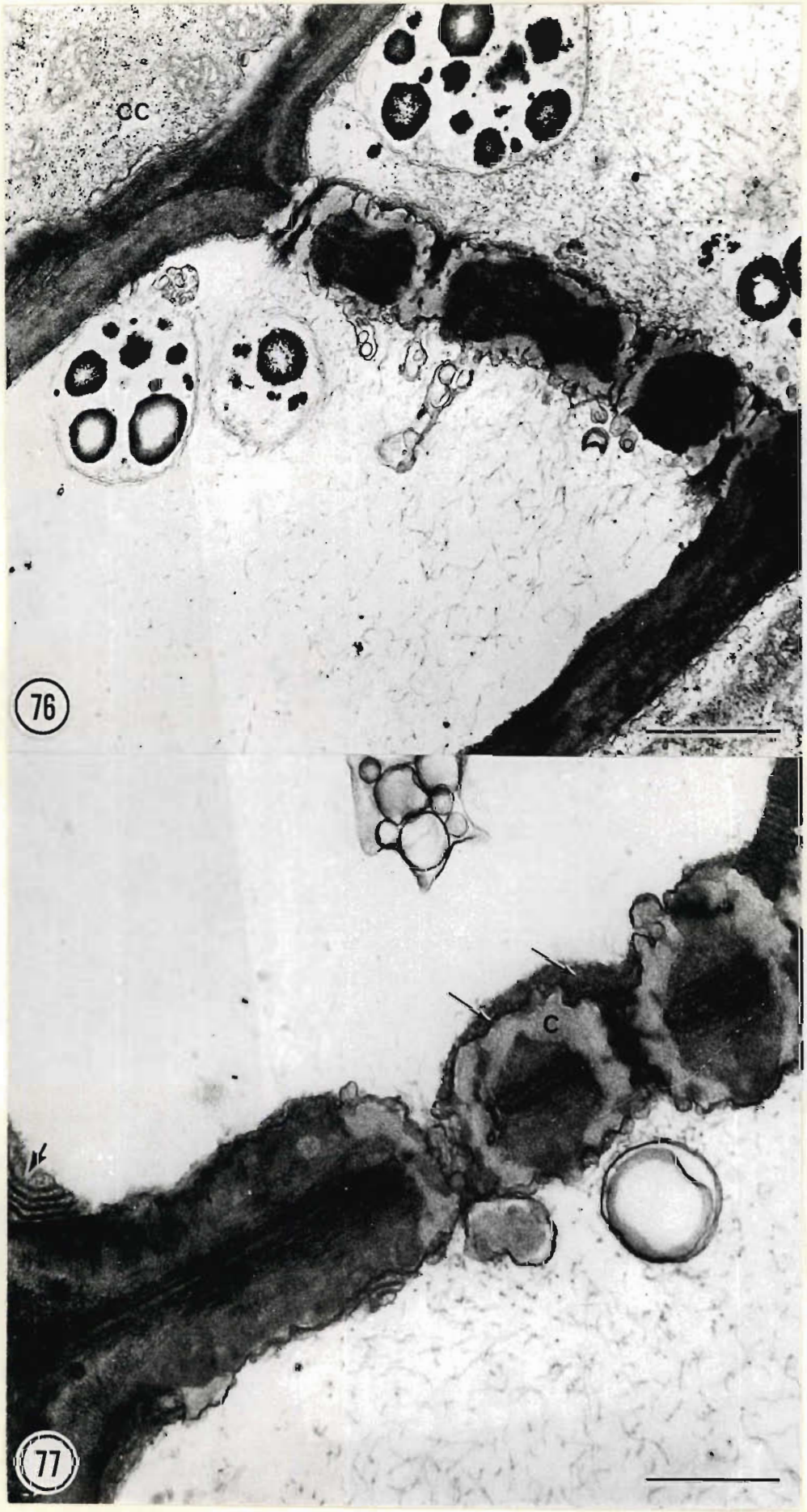
CC
76
C
77

Figs. 76 and 77. Glancing longitudinal sections through portions of sieve plates of mature adaxial sieve elements.
Figure 76. Sieve plate pores plugged with P-protein.
Figure 77. Shows a pore relatively free of P-protein, which covers pores to right (unlabelled arrows). Portions of longitudinally orientated ER cisternae (arrowhead) line wall and on right, and part of sieve plate.
CC = companion cell; C = callose lining pores of sieve plate. Scale lines: Figure 76 = 1,0 µm; Figure 77 = 0,5 µm.

5.2.3 Organelles and Membrane Systems

During the early stages of ontogeny of the abaxial phloem, the nucleate sieve element protoplast is similar in appearance to that of the immature adaxial procambial derivatives. Figures 92 - 95 are longitudinal sections through the metaxylem and cambial zone (Figure 93); procambium and protophloem (Figs. 94 and 95); procambium and metaphloem (Figure 92 Examination of thin sections revealed that the tonoplast, as in the adaxial phloem sieve elements, ruptured after the dispersal of P-protein bodies was completed (Figure 92). At the same time as P-protein body dispersal, as in the adaxial phloem, certain of the protoplasmic components undergo marked changes. The initially rough endoplasmic reticulum migrates toward the plasmalemma, loses its attached ribosomes and lies closely appressed to the plasmalemma, where it either assumes a curvilinear (Figs. 83 and 89 longitudinal (Figure 89) or horizontal form (Figs. 88 and 89) with respect to the longitudinal axis of the sieve element.

As in the adaxial phloem, the endoplasmic reticulum of mature external and abaxial phloem sieve elements is fairly uniform in size, mostly about 130 - 140 A, slightly larger than the endoplasmic reticulum of the adaxial phloem sieve elements (range: 95 - 160 A).

Unlike the plastids of the adaxial phloem sieve elements, those of the abaxial sieve elements (Figs. 83, 86 and 87) were rarely associated with P-protein, although in some instances (Figure 83) the plastids were associated with the parietal ER cisternae. As in the adaxial sieve element plastids, those of the abaxial phloem sieve elements contained only starch. Of note is the fact that many of the mature abaxial phloem sieve elements lacked mitochondria. Those sieve elements which contained mitochondria, did not have as many as those in the adaxial phloem sieve elements; these mitochondria were generally located within the parietal

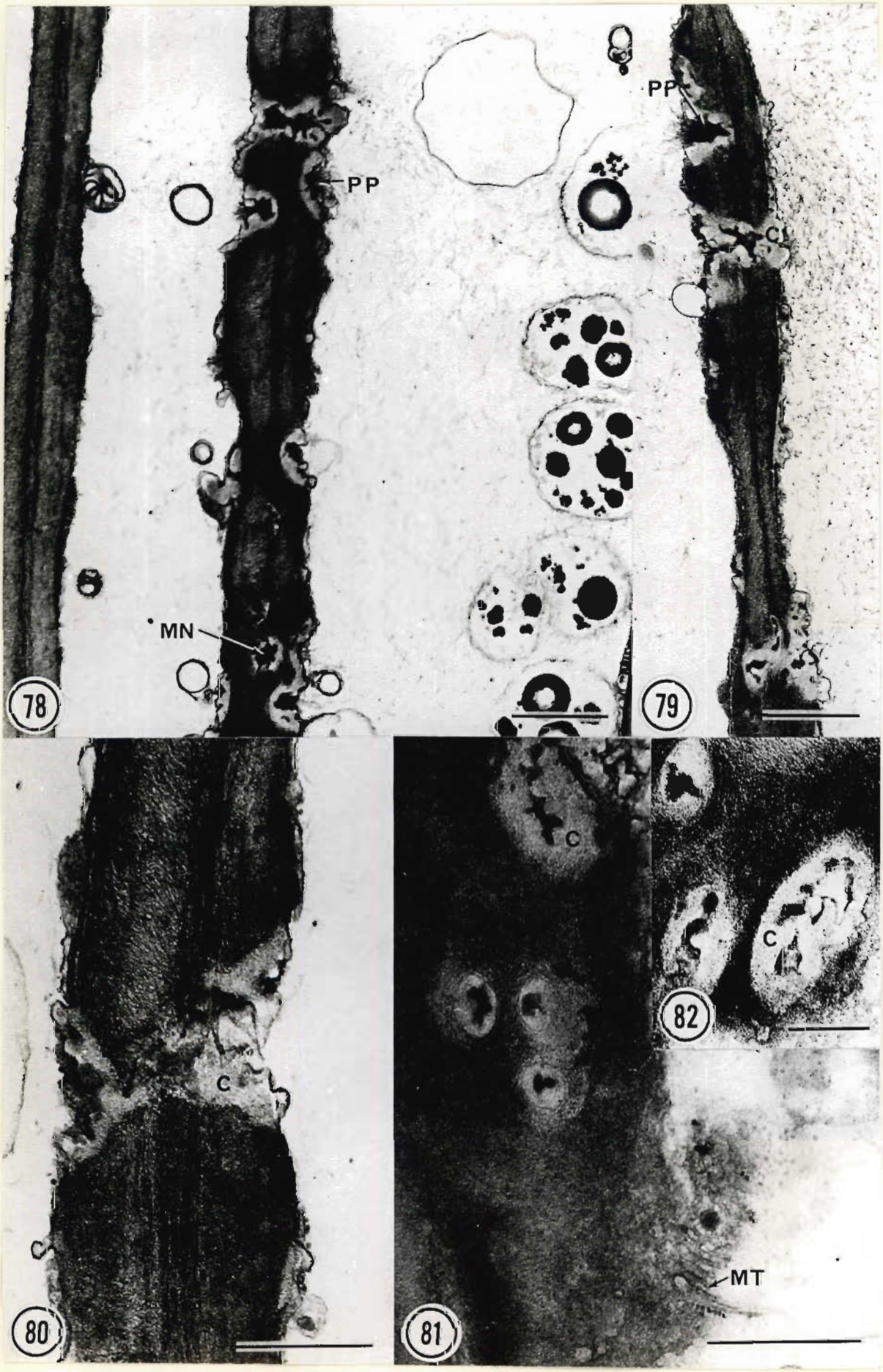
PP
MN
78
PP
CI
79
C
80
C
C
82
C
MT
81

Figs. 78-82. Longitudinal (Figs. 78-80) and surface view (Fig. 81 and 82) of lateral sieve areas in mature adaxial sieve elements. Lateral sieve areas were partly occluded by varying amounts of callose. Few (Figure 82) were free of, or only partly blocked (Figure 80) by P-protein. C = callose lining sieve area pores, MT = microtubules, PP = P-protein, MN = median nodule. Scale lines: Figs. 78 and 79 = 2,0 µm; Figs. 80 and 81 = 0,5 µm; Figure 82 = 0,25 µm.

cytoplasm. P-protein was not observed to be associated with abaxial sieve element mitochondria as was the case in adaxial sieve element mitochondria (compare Figure 66 with Figure 91).

The mitochondria of the abaxial phloem companion cells were variable both in size (range: 0,04 - 0,09 μ) and internal membrane complexity (Figs. 90 and 91), and were fewer in number compared with adaxial companion cells (compare Figure 66 with Figure 90).

5.2.4 Cell Walls

As in the adaxial phloem, the lateral walls of the abaxial metaphloem sieve elements had a wavy outline even when viewed under phase-contrast light (see Figs. 30, 83 and 92). However, when viewed with the electron microscope, the lateral walls of the abaxial and external metaphloem sieve elements do not have an inner wall layer which appears to be morphologically distinct from the outer layer.

5.2.4.1 Plasmodesmata

Plasmodesmal connections between immature and mature abaxial sieve elements and their contiguous companion cells were similar to those encountered in thin sections of adaxial phloem (see Figs. 69 - 73 for reference). On the sieve element side (Figure 92), callose deposition was variable, with very thin callose rings in the companion cell side (Figure 90).

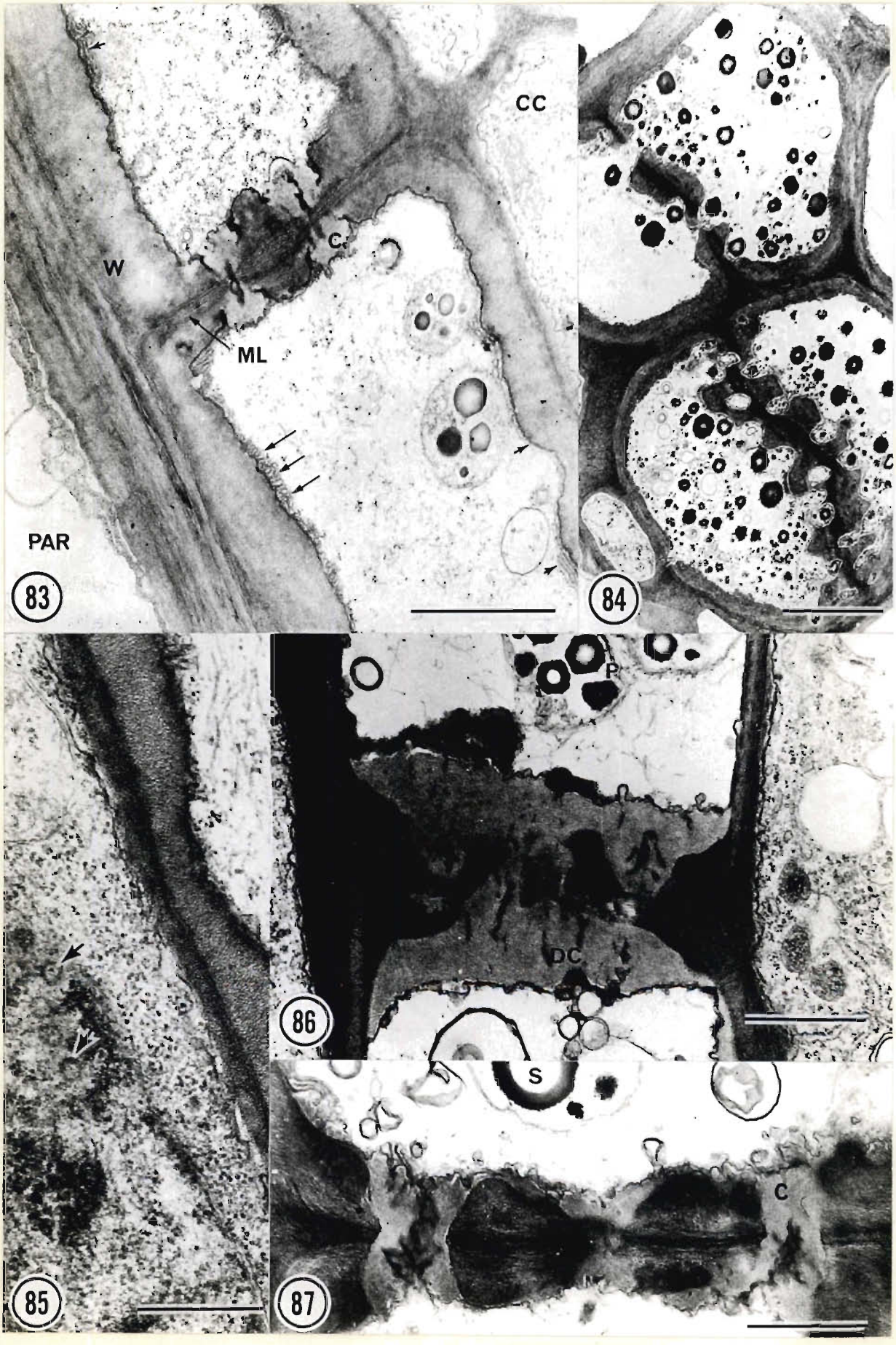
CC
C
W
ML
PAR
83
84
85
P
DC
86
S
C
87

Figs. 83-87. Details of abaxial phloem sieve elements (Figs 83-84 and 86-87) and companion cell nucleus (Figure 85).
Figure 83. Glancing longitudinal section of immature adaxial metaphloem sieve element, with pores lined with thick callose cylinders. ER in concomitant sieve elements is both horizontally (arrows) and vertically orientated (arrowhead). P-protein dispersal completed in lower sieve element.
Figure 84. Transverse section of part of sieve plates of concomitant protophloem sieve elements. Note even though the plastids have ruptured, releasing starch, that sieve plate pores are lined by relatively narrow callose cylinders
Figure 85. Tangential view of portion of nuclear envelope of companion cell showing arrangement of nuclear pores (unlabelled arrowheads).
Figure 86. Longitudinal section of sieve plate between concomitant protophloem sieve elements. Sieve plate pores blocked by definative callose. Note that plastid membranes are intact.
Figure 87. Glancing section through part of sieve plate between concomitant metaphloem sieve elements. Note pores partly restricted by callose. W = wall, P = plastid, S = starch, C = callose lining sieve plate pores, DC = definitive callose, M = mitochondrion, ML = middle lamella.
Scale lines: Figure 83 = 3,0 µm; Figure 84 = 2,5 um; Figure 85 = 0,5 µm; Figure 86 and 87 = 1,0 µm.

5.2.5 Sieve Plates and Lateral Sieve Areas

5.2.5.1 Sieve Plates

The present study added little to the knowledge of sieve plate development in the abaxial phloem of Gomphocarpus, for few developing sieve plates were encountered with the electron microscope. As mentioned the abaxial and external phloem contain less sieve tubes in cross-section compared with the adaxial and internal phloem. In transverse section (Figure 84), part of two concomitant sieve plates of mature abaxial protophloem sieve elements are shown. The sieve plate pores are unobstructed by P-protein, even though the sieve tube plastids are ruptured, indicating severe plasmolysis within these sieve tubes. The pores are surrounded by relatively narrow callose cylinders. The sieve plate pores average 0,53 µ (range: 0,36 - 0,72 µ) in diameter at their narrowest point.

As differentiation and maturation of the abaxial metaphloem sieve elements proceeded, many of the protophloem sieve elements were observed to have massive deposits of definative callose which completely occluded the sieve plate pores. The plastids in such sieve elements were always observed to be intact and to contain variable numbers of starch grains (Figure 86), indicating that plasmolysis was not responsible for the formation and deposition of the definative callose.

Very few of the sieve plate pores of the abaxial metaphloem were observed to be callose-free. The pores were restricted by deposition of callose cylinders of varying thicknesses (Figs. 83 and 87). Of importance is the fact that the sieve plate pores of the abaxial phloem were never as restricted by callose as were those of the adaxial phloem.

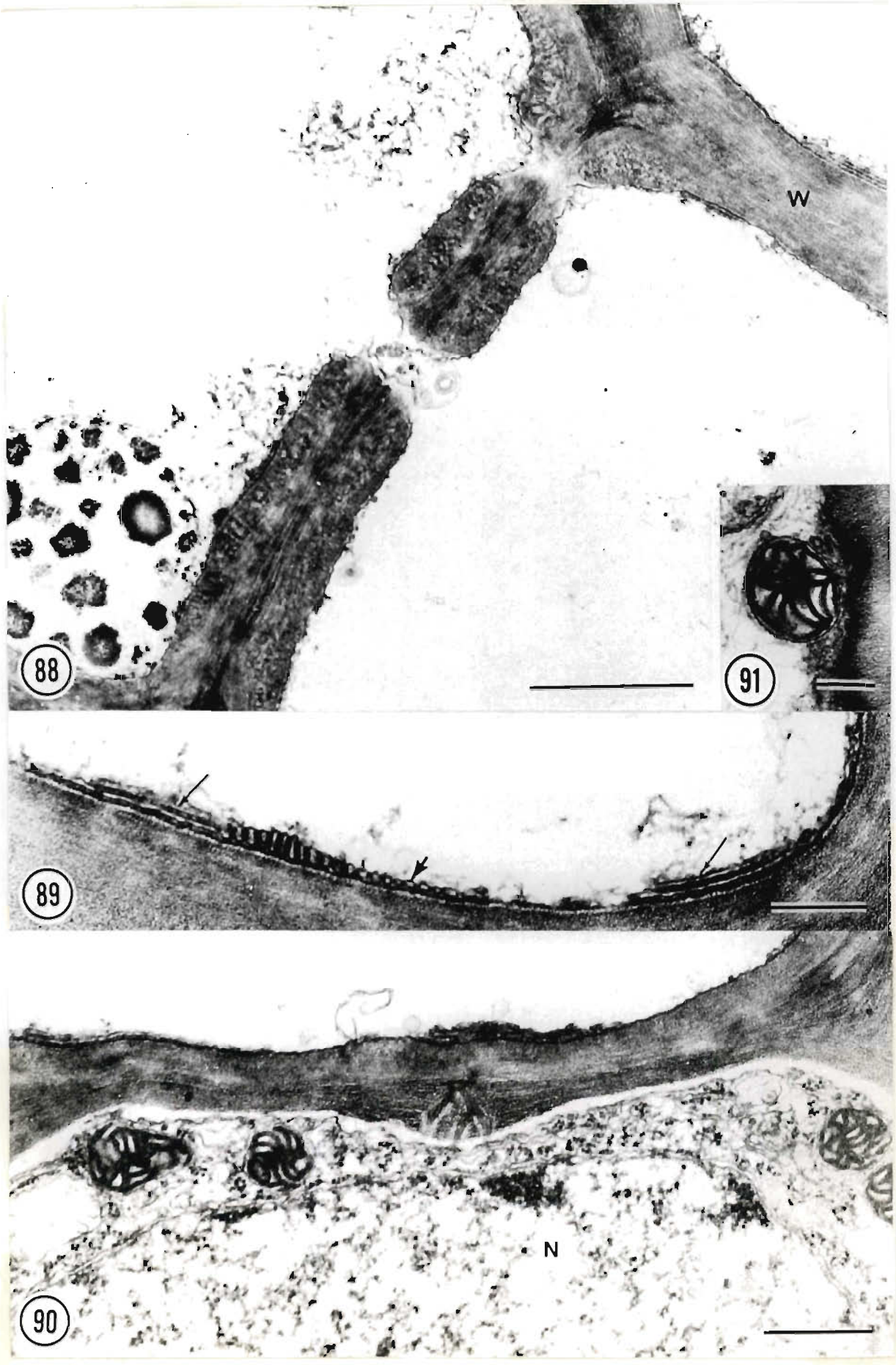
W
88
91
89
N
90

Figs. 88-91. Transverse sections of mature abaxial metaphloem.
Figure 88 shows part of a lateral sieve area. Open pore is free of callose.
Figure 89 shows horizontal and curvilinear ER cisternae closely appressed to the plasmalemma. The lumen of the sieve element contains little P-protein.
Figure 90. Glancing section through branched plasmodesmata between companion cell and concomitant metaphloem sieve element. In cross-section the nucleus occupies much of the companion cell.
Figure 91. Mitochondrion from mature abaxial metaphloem sieve element.
W = wall, unlabelled arrows = horizontal ER, arrowhead = curvilinear ER, N = nucleus.
Scale lines: Figs. 88 and 90 = 0,5 μm; Figure 89 = 0,25 μm; Figure 91 = 0,03 μm.

5.2.5.2 Lateral Sieve Areas

Few lateral sieve areas were encountered in thin section of either abaxial phloem or external phloem. Figure 88 is a transverse section of a callose-free lateral sieve area pore. Another pore site is visible immediately above in the lateral wall of the sieve element. Although the contents of the sieve elements which contained the lateral sieve area pore shown in Figure 88 was poorly fixed, the pore is unobstructed by either P-protein or callose. Lateral sieve area pores of abaxial phloem sieve elements measured on average 0,103 μ, smaller than the calculated values for sieve plate pores (0,36 - 0,72 μ).

5.2.6 Companion Cells, Procambial Cells and Phloem Parenchyma

The abaxial sieve elements usually have one companion cell per sieve element. Figures 92 - 95 are views of the cambial zone and abaxial phloem. As in the adaxial phloem, it is difficult to distinguish between the nucleate, thin-walled procambial cells and their immature derivatives during the early stages of differentiation. Figure 92 is a longitudinal section showing part of a procambial cell, adjacent to which is part of a companion cell, and an immature and mature sieve tube. The nucleus of the procambial cells is usually large (Figure 94 and enlarged in Figure 95), but does not occupy as much of the protoplast as does the nucleus of the abaxial companion cells (Figure 90). Figure 85 is a glancing section through part of the nuclear membrane and nucleus of an abaxial phloem companion cell; several regularly-spaced nuclear pores (arrows) are visible. Burr and Evert (1973) reported similar, regularly-arranged pores in Selaginella kraussiana, and also that ribosomes were always found attached to the nuclear envelope in interpore areas. It was not possible to determine if ribosomes were present in the

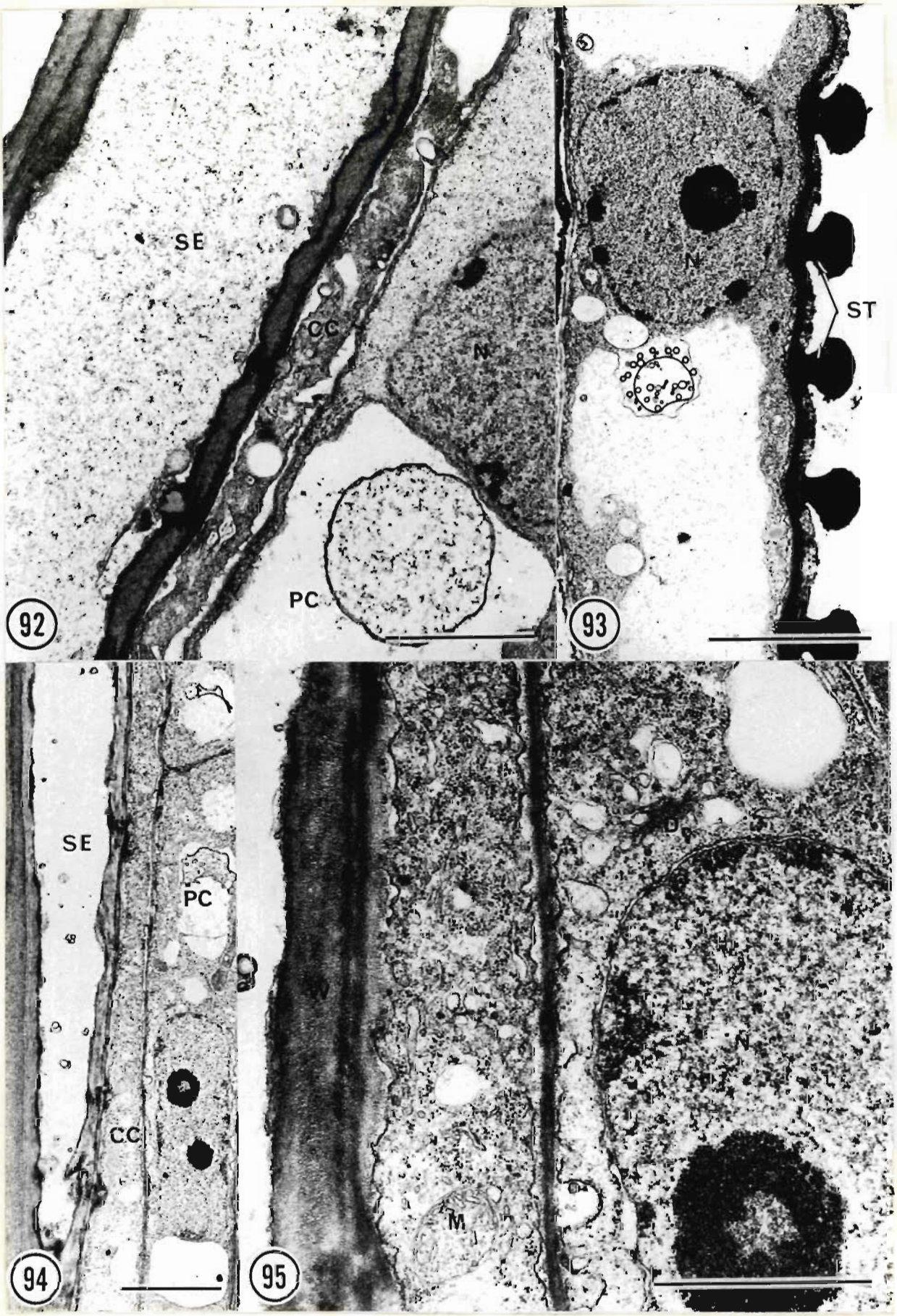
SE
CC
N
PC
92
N
ST
93
SE
PC
CC
94
N
M
95
N

Figs. 92-95. Longitudinal views of cambial (Figure 93), procambial (Figs. 92, 94 and 95) and abaxial sieve elements and companion cells (Figs. 92 and 94).
W = cell wall, ST = metaxylem secondary thickening, SE = sieve element, CC = companion cell, PC = procambial cell, M = mitochondrion, N = nucleus, D = dictyosome.
Scale lines: Figure 92 = 3 μm; Figure 93 = 5 μm; Figure 94 = 10 μm; Figure 95 = 2 μm.

inter-pore areas of the nuclear envelope of Gomphocarpus. Apart from the smaller diameter of the procambial derivatives in the abaxial phloem, their contents were essentially similar to that of the procambial derivatives of the adaxial phloem. Similarly, the external and abaxial phloem parenchyma cells closely resembled the phloem parenchyma of the internal and adaxial phloem.

5.3 Summary

As seen with the electron microscope, the protophloem sieve elements are essentially devoid of protoplasm, and have parietally-dispersed endoplasmic reticulum cisternae, and were mostly partly collapsed, due either in part to pressure during sectioning, or to pressure due to expansion of the bundle. The metaphloem sieve elements have lateral walls which are generally thickened, usually consisting of two distinct layers: the inner wall layer being morphologically distinct from the outer wall layer. Concomitant with the dispersal of P-protein bodies, which occurs prior to the breakdown of the tonoplast, certain of the protoplasmic components of the sieve elements undergo very marked changes. Especially notable are the changes which occur to the endoplasmic reticulum. As the sieve elements approach maturity, the rough endoplasmic reticulum cisternae migrate towards the plasmalemma, assume a parietal position, becomes firmly attached to the plasmalemma, during which process ribosomes are lost from the cisternae. The endoplasmic reticulum of mature internal and adaxial phloem sieve elements is uniform in size, mostly about 120 A; that of the abaxial and external phloem sieve elements mostly 130 - 140 A. Starch-containing plastids and mitochondria were often seen in close association with the ER cisternae, those of the adaxial and internal phloem sieve elements often had fibrillar P-protein attached to their surfaces.

The ER cisternae of mature adaxial and internal phloem sieve elements were mostly horizontally orientated with respect to the longitudinal axis of the sieve elements, associated with which was vertically-orientated tubular and fibrillar P-protein. The ER cisternae of mature abaxial and external phloem sieve elements assume either a curvilinear, longitudinal, or horizontal form with respect to the longitudinal axis of the sieve elements. All sieve plates and lateral sieve areas of adaxial and internal phloem sieve elements were usually associated with P-protein. The degree to which sieve plate and lateral sieve area pores were plugged by P-protein and by callose deposition was variable. A major point of difference observed between adaxial/internal and abaxial/external sieve elements was that the latter contained less parietally-dispersed P-protein at maturity. Significantly, the sieve plate and lateral sieve area pores usually lacked slime plugs or heavy deposits of callose, irrespective of the state of fixation of the sieve element protoplast. Many of the adaxial and internal phloem protophloem sieve elements appeared functional, whereas the sieve plates of many of the protophloem sieve elements of mature abaxial and external phloem bundles were not.

Although the external and abaxial protophloem sieve elements begin to differentiate before the internal and adaxial protophloem sieve elements, the former do not persist as functional elements throughout the life of the plant. In LP 5, the adaxial protophloem is mature, and presumably functions in assimilate translocation, whereas the abaxial protophloem sieve elemets are by this stage, occluded by massive deposits of definitive callose. Concomitantly, most of the abaxial metaphloem sieve elements are not mature, and are fewer in number than the already mature adaxial protophloem sieve elements. The lack of evidence of surging in the external and abaxial phloem coupled with less callose deposition,

and the early occlusion of protophloem sieve elements is taken as evidence that the external and abaxial phloem sieve elements are not as functional in the translocation of assimilates as are the internal and adaxial protophloem and metaphloem sieve elements.

6. PHLOEM TRANSLOCATION OF ^{14}C-ASSIMILATES

6.1 Results and Discussion

The experiments to be discussed are of three types: (1) those in which colonies of A. nerii were used to investigate the effects of ringbarking on the translocation profiles within the internal phloem of stems which contained no secondary phloem; (2) those in which the bark was separated from the pith in order to determine the proportion of ^{14}C-assimilate translocated in the external and internal phloem, respectively; and (3) those designed to investigate the relative roles of external and internal phloem in export/import relationships of young and mature leaves.

6.1.1 Translocation of Assimilates in the Internal Phloem

When a comparison is made of the translocation profiles of control and ringbarked plants (Figs. 96 and 97 respectively), it is apparent that ringbarking below the feeder leaf had little or no effect on the translocation profile of the internal phloem. Acropetal transport of ^{14}C-assimilate was least affected by this treatment. Basipetal transport within the internal phloem of ringbarked plants was similar to that of the intact controls for the first 3 hours. After 4 hours the amount of ^{14}C present in the honeydew began to level off; after 6 hours, a pulse-type of profile was exhibited. The latter was most evident 6 to 8 hours after commencement of the experiments. The slopes of the curves plotted in Figs. 96 and 97 suggest that a difference may have existed in the rate of translocation acropetally and basipetally in the internal phloem, under the experimental condition.

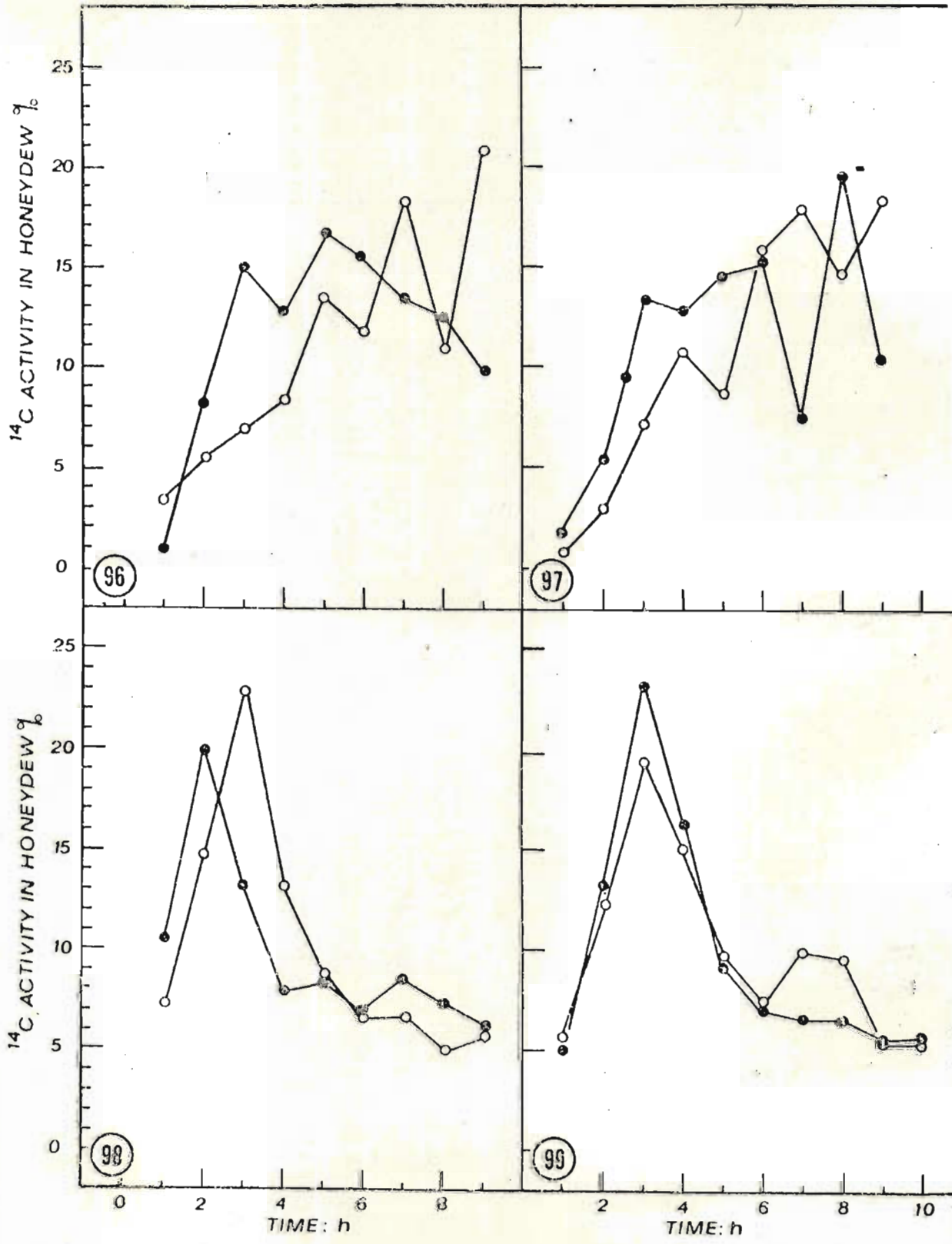
^{14}C ACTIVITY IN HONEYDEW %
25
20
15
10
5
0
96
97
98
99
0
2
4
6
8
10
TIME: h

Figs. 96-99. Translocation of ^{14}C-assimilate in the internal phloem of G. physocarpus. Monitoring by aphid technique.
Figure 96. Acropetal (O-O) and basipetal (●-●) translocation in intact controls. Note that basipetal translocation decreased after 5 hours, whereas the acropetal component did not.
Figure 97. Translocation of ^{14}C-assimilate, showing the effect of ringing on the translocation profile. Plants ringbarked below feeder leaf. Acropetal (O-O); basipetal (●-●). Comparison of Figure 96 with Figure 97 reveals that ringbarking had very little effect on the translocation profile in the internal phloem.
Figure 98. Comparison of translocation (acropetal plus basipetal) in intact control stem (●-●) and stem (O-O) ringed above feeder leaf. Note delay of one hour prior to attainment of maximum translocation of assimilate in ringed plant compared to intact control. Total recovered ^{14}C. t = 4891 and 4024 dpm respectively.
Figure 99. Comparison of acropetal translocation of ^{14}C-assimilate in intact controls (O-O) and stem ringed below feeder leaf (●-●); t = 3226 and 3783 dpm respectively. Note that acropetal translocation is not adversely affected by ringing.

Experiments conducted one month later (in April) resulted in translocation profiles (Figs. 98 and 99) which differed markedly from those of the original experiments (Figs. 96 and 97). Of particular interest was a delay of one hour in the passage of the translocation front in plants ringed above the feeder leaf (Figure 98). Both acropetal and basipetal translocation were monitored for the internal phloem. Apart from the one hour delay, the translocation profile of the ringed plant nearly mirrored that of the intact controls (Figure 98). By comparison, ringbarking of the stem below the feeder leaf resulted in no apparent delay in the passage of the front acropetally in the internal phloem (Figure 99).

These results indicate that removal of the external phloem did not result in any marked depression of the translocation profile in the internal phloem, even though a delay of one hour was noted in plants ringed above the feeder leaves. Although collectively these results indicate that translocation in the internal phloem is independent of that of the external phloem in G. physocarpus, they provide no information on the relative dependence or independence of external phloem transport on that of the internal phloem.

6.1.2 Bark Stripping Experiments

As mentioned, bark stripping experiments were conducted in an attempt to determine quantitatively the ratio of assimilate transported in the external and internal phloem. Figures 100 -105 illustrate the principal results of these experiments.

When experimental plants were subjected to low light intensity (350 ft candles) and a mature leaf of each fed $^{14}CO_2$ continuously for 25 minutes, the total ethanol-soluble ^{14}C-assimilate was greater in the "pith"

segments than in corresponding bark segments (Figure 100). With increasing distances from the feeder leaf, ^{14}C-assimilate declined more rapidly in the pith segments than in those of the bark. In addition, levels of ^{14}C decreased more rapidly acropetally than basipetally in both pith and bark.

The rapid decrease in pith ^{14}C may be indicative of a non-equilibrium translocation state (MacRobbie, 1971) as higher levels of radioactivity are associated with the fed zone. The rate of incorporation of $^{14}CO_2$ and translocation of ^{14}C-assimilates out of the leaf under non-equilibrium conditions, would be low. Indeed, this was the case in these experiments, in which the mean total ethanol-soluble ^{14}C in the fed leaves was 273 315,9 dpm, and 1 989,3 in the stem. In other words, only 0,7% of the total extracted ^{14}C-assimilate was associated with the bark and pith segments. Of special interest was the mean exernal/internal ^{14}C-assimilate (e/i) of 0,42 : 1. Under low light intensity, more assimilate apparently moved within the internal phloem than the external phloem.

Figures 101 - 105 show the results of experiments similar to those just discussed (Figure 100), with the exception that those of Figures 101 - 10 were conducted 1,5 months later and under daylight conditions.

Comparison of the results of the first experiment (Figure 100) with the one conducted under an identical steady-state feeding time of 25 minutes, but with daylight conditions (Figure 101) reveals striking differences. In the low light intensity experiment, 11,0 and 25,8 % of the total radioactivity recovered from bark and pith segments, respectively, were associated with the node of the feeder leaf (the "feeder node"). In those grown under daylight conditions, 64,0 and 54,7 % were associated with the feeder node. The e/i ratio under daylight conditions was 1,51 : 1, which is significantly different from the 0,42 : 1 calculated

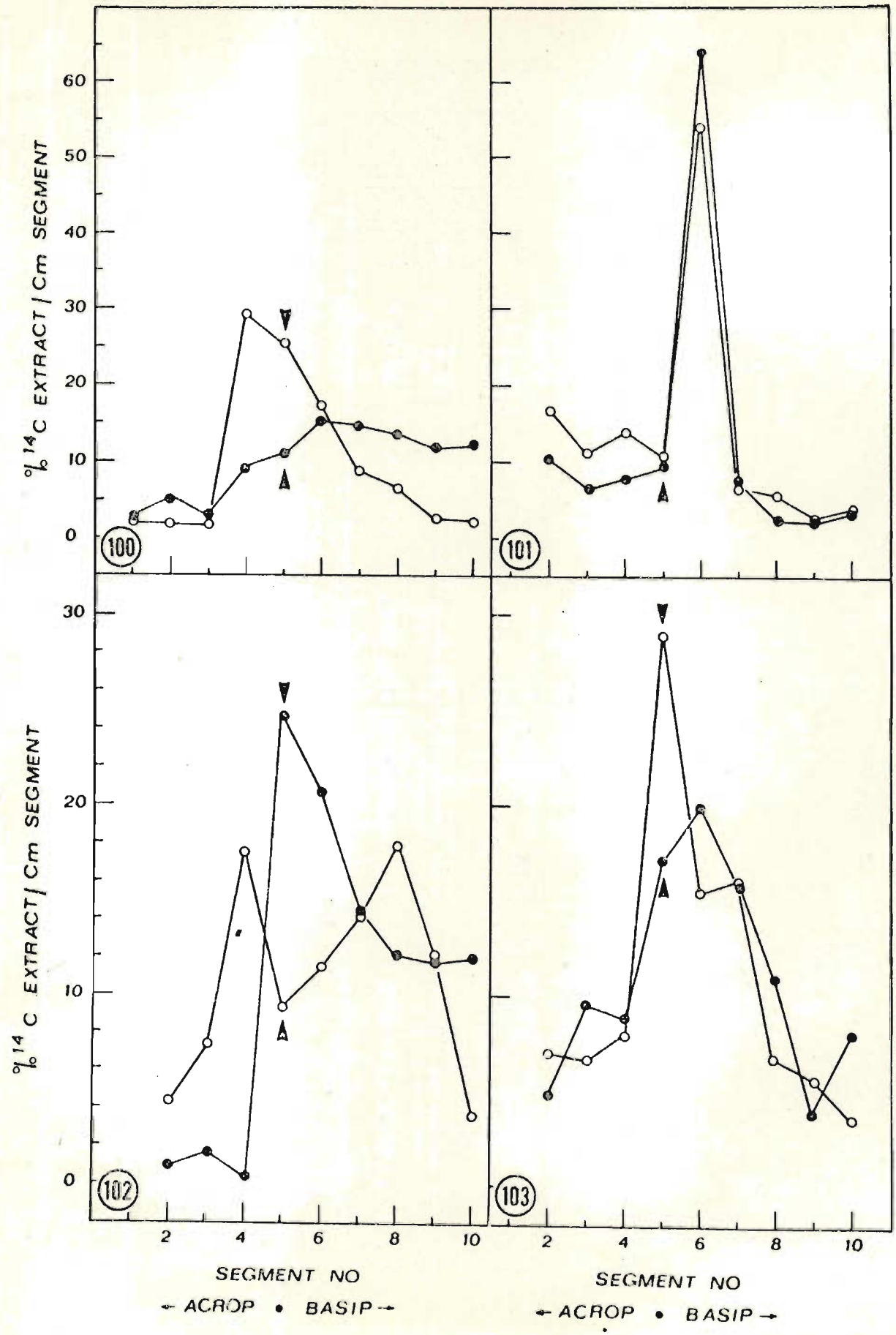
% 14C EXTRACT / Cm SEGMENT
60
50
40
30
20
10
0
100
101
30
20
10
0
102
103
2
4
6
8
10
SEGMENT NO
← ACROP • BASIP →
SEGMENT NO
← ACROP • BASIP →

Figs. 100-103. Comparison of ^{14}C-assimilate distribution as a function of distance along a 10 cm portion of 20-week-old G. physocarpus stems. Figure 100. 25 minutes continuous feeding, under low light intensity. Figure 101. 25 minutes continuous feeding under daylight conditions. Figure 102. 40 minutes continuous feeding. Figure 103. 2,5 hours continuous feeding. Both 40 minutes and 2,5 hours feeding under daylight conditions. Arrowheads correspond to the segment associated with the feeder leaf.

Figure 100. Translocation and distribution of assimilate in the bark (■-■) and pith (O-O) (external and internal phloem respectively). In this experiment, in which the plant was grown under low light intensity, the external phloem translocated less ^{14}C than the internal phloem. Total recovered radioactivity in the bark and pith was 800 and 1 189,5 dpm respectively. Mean external/internal ratio was 0,42 : 1.

Fig. 101. Translocation and distribution of assimilate in the bark (■-■) and pith (O-O). Distribution of radioactivity in the bark and pith were similar to each other. Total recovered radioactivity in the bark and pith was 1 699,3 and 1 124,6 dpm respectively. Mean e/i ratio was 1,51 : 1, which indicates an increase in the external phloem translocation component.

Figure 102. Translocation and distribution of assimilate in the bark (■-■) and pith (O-O). Note that more ^{14}C is present in the lower pith segments than in the lower bark segments. Total recovered radioactivity in the bark and pith was 99 380,4 and 58 635,0 dpm respectively Mean e/i ratio was 1,69 : 1.

Figure 103. Translocation and distribution of assimilate in the bark (■-■) and pith (O-O). Total recovered radioactivity in the bark and pith was 44 898,9 and 12 445,7 dpm respectively. Mean e/i ratio was 3,61 : 1.

for the low-intensity experiments. In addition, of the total extracted ^{14}C-assimilate, only 0,1 % was associated with the bark and pith of daylight plants at termination of the experiments.

Increase in the time of exposure to $^{14}CO_2$ from 25 to 40 minutes (Figure 102) resulted in an increase in the e/i ration from 1,51 : 1 to 1,69 : 1. This is indicative of a greater proportion of the ^{14}C-assimilate being present in the external than internal phloem at the time of sampling after 40 minutes exposure. And while the curve of radioactivity (Figure 102) for the pith segments indicates that basipetal translocation in the internal phloem was possibly approaching a steady-state, that for the bark segments indicates a steady-state of basipetal translocation had been achieved in the external phloem.

After 40 minutes exposure more radioactibity was associated with the pith segments above the feeder node than below. In addition, considerably more total extractable ^{14}C-assimilate occurred in the bark and pith segments after 40 minutes exposure than after 25 minutes exposure: 14,78 % compared to 0,1 %.

After 150 minutes of steady-state feeding, the distribution of ^{14}C-assimilate decreased rapidly in the bark and pith above and below the feeder node (Figure 103). The e/i ratio of 3,61 : 1 indicates that much more ^{14}C-assimilate is present in the bark than pith after 150 minutes. Of the total extracted ^{14}C-assimilate, 7,5 % was associated with the bark and pith segments. Although this is a decrease from the percentag associated with the bark and pith segments after 40 minutes exposure (Figure 102), the decrease is likely due to translocation of ^{14}C-assimilates out of the 10 cm zone studied.

Bark-stripping experiments on lateral branches of mature axes (Figs. 104 and 105) revealed that the lateral branches had translocation profiles

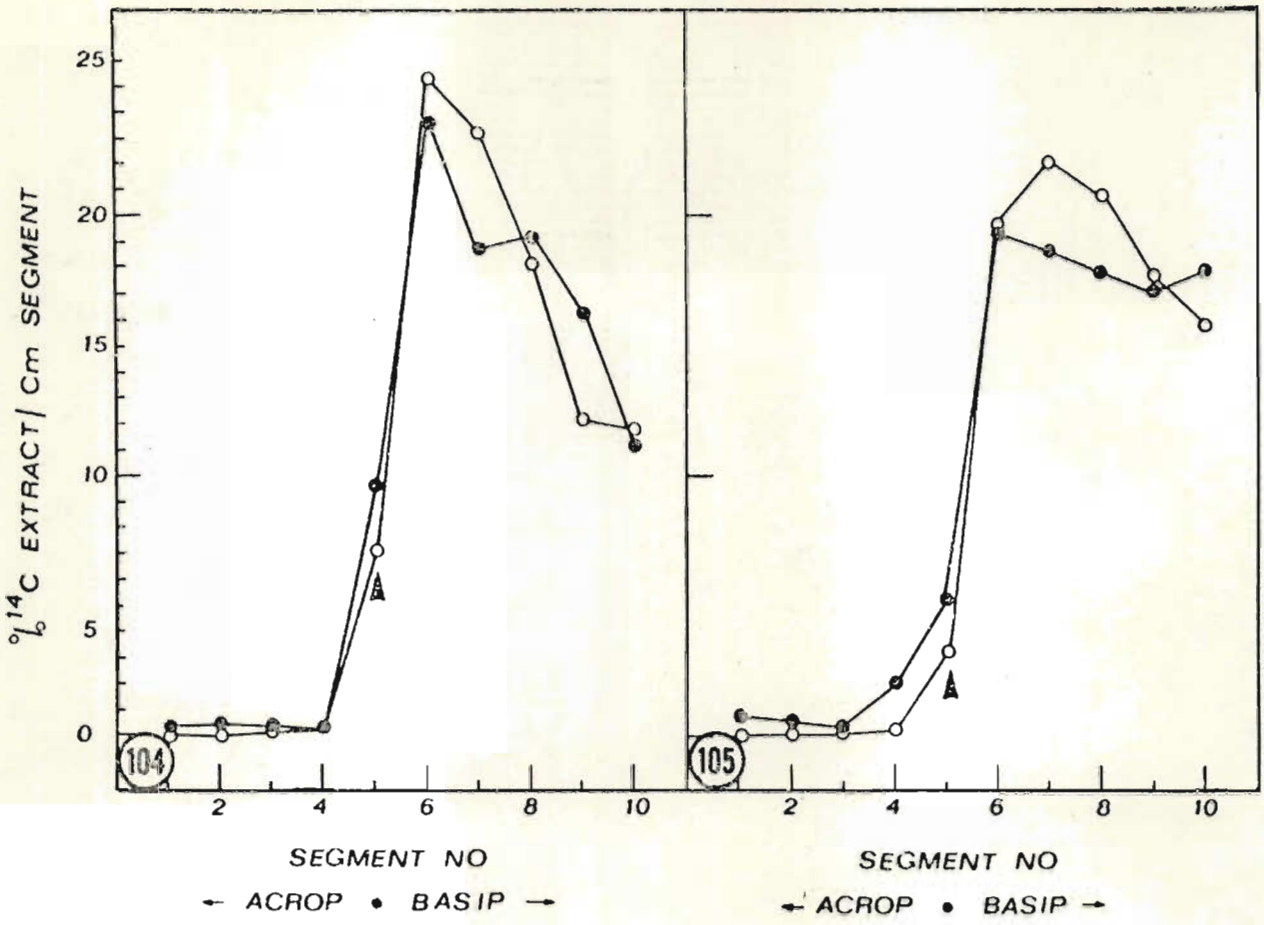
% ^{14}C EXTRACT / Cm SEGMENT
25
20
15
10
5
0
104
105
2
4
6
8
10
SEGMENT NO
← ACROP • BASIP →
SEGMENT NO
← ACROP • BASIP →

Figs. 104 and 105. Comparison of ^{14}C-assimilate distribution and translocation as a function of distance along a 10 cm portion of lateral branches of mature G. physocarpus. Figure 104 morphologically younger than that depicted in Figure 105. Continuous feeding for 25 minutes.

Figure 104. Distribution of assimilate in the bark (■-■) and pith (O-O). Total recovered radioactivity in the bark and pith was 59 728,0 and 18 095,0 dpm respectively. Mean e/i ration was 3,3 : 1.

Figure 105. Distribution of assimilate in the bark (■-■) and pith (O-O). Total recovered radioactivity in the bark and pith was 79 938,5 and 6 711,9. Mean e/i ratio was 11,91 : 1.

essentially similar to those of younger main stems, although the acropetal translocation component is almost nonexistent in these branches. In morphologically older laterals (Figure 10S) basipetal translocation appears depressed, compared to the younger laterals. In addition, the e/i ratio calculated for the older laterals (11,91 : 1) differs greatly from that calculated for the younger ones (3,03 : 1). The e/i ratio of the younger laterals compares favourably with the range for 20-week-old main stems.

6.1.3 Role of the External and Internal Phloem in Export/Import Relationships in Young and Mature Leaves

The anatomical investigation of the ontogeny of the primary phloem of G. physocarpus indicated that the uppermost four pairs of leaves of each shoot tip were served by external phloem only; that is, any adaxial phloem in the petioles and laminas of these leaves lacked mature sieve tubes. It is also pertinent to emphasize that by far the largest colonies of A. nerii were located on portions of stems - between nods 5 and 15 - which contained mature primary sieve tubes but lacked secondary vascular tissues.

Experiments were designed to study the role of the external and abaxial phloem in immature stems and leaves, respectively, in the transport of assimilates from mature, actively-exporting leaves of the mature axis and, concomitantly, to observe the effect of ringbarking of the external phloem on the import of assimilate by immature leaves. In these experiments, 20-week-old G. physocarpus plants were treated by severing the external phloem either above or below the feeder leaf. The amount of radioactivity which reached the apical portions of treated plants was compared to that recovered in similar portions of intact control plants.

The results of these experiments are recorded in Tables III to VI.

TABLE III

DISTRIBUTION OF ^{14}C-ASSIMILATE IN YOUNG LEAVES OF 20-WEEK-OLD *G. PHYSOCARPUS* AFTER 2,5 HOURS EXPOSURE OF A MATURE LEAF TO $^{14}CO_2$ [1]

		dpm	% of total dpm
LEAF PAIR N^{O}	2	1 732,8	8,8
	3	3 288,6	16,8
	4	2 414,8	12,3
	5	917,1	4,7
	6	4 686,2	23,9
sub total	2-6	13 039,5	66,4
	APEX	6 584,4	33,6
TOTAL:		19 623,9	100,0

[1] Mean of six replicates

The control plants (Table III) were fed $^{14}CO_2$ via a mature leaf (leaf nine counting from the apex down) for 2,5 hours, after which the pairs of leaves were removed and the ^{14}C-activity in them was determined. The data recorded in Table III represents the means of six replicates. Leaf pairs 2 - 6 contained 66,4 % of the total ethanol-soluble ^{14}C-assimilates, the rest of the shoot tip (including leaf pair 1) the remaining 33,6 %. It will be noted that considerable variation exists among the values for leaf pairs 2 and 5. The reason for these differences is not known. Perhaps the phyllotaxy may have had an influence upon the distribution of assimilates.

Ringbarking below the feeder leaf resulted in a very marked reduction in the amount of radioactivity accumulated in the young leaves (Table IV) compared with the controls. After 1,0 and 2,5 hours exposure to $^{14}CO_2$

the apical meristem and first leaf pair together only contained 0,8 and 11,5 % after 1,0 and 2,5 hours respectively, of the total ethanol-soluble ^{14}C-assimilate.

TABLE IV

DISTRIBUTION OF ^{14}C-ASSIMILATE IN YOUNG LEAVES OF 20-WEEK-OLD *G. PHYSOCARPUS*, RINGBARKED BELOW MATURE FEEDER LEAF.[1]

		1,0 h		2,5 h	
		dpm	% of total dpm	dpm	% of total dpm
LEAF PAIR N°	2	37,6	3,1	182,3	4,2
	3	39,3	3,2	1 347,3	31,3
	4	70,4	5,7	264,7	6,1
	5	181,7	14,8	712,9	16,5
	6	886,1	72,4	1 302,0	30,4
sub total, 2 - 6		1 215,1	99,1	3 815,2	88,5
APEX		9,9	0,8	493,4	11,5
TOTAL:		1 225,0	100,0	4 308,6	100,0

[1] Mean of six replicates.

Results of ringbarking above the feeder leaves are recorded in Table V. Less ^{14}C assimilate reached the shoot tips of these plants than those ringed below the feeder leaves. After 1,0 and 2,5 hours exposure to $^{14}CO_2$, the apical meristem and first leaf pair contained 4,8 and 10,4 % respectively, of the total ethanol-soluble ^{14}C-assimilate.

TABLE V

DISTRIBUTION OF ^{14}C-ASSIMILATE IN YOUNG LEAVES OF 20-WEEK-OLD *G. PHYSOCARPUS*, RINGBARKED ABOVE MATURE FEEDER LEAF.[1]

		1,0 h		2,5 h	
		dpm	% of total dpm	dpm	% of total dpm
LEAF PAIR N°	2	131,0	16,7	241,9	7,1
	3	48,7	6,2	243,0	7,1
	4	82,7	10,5	158,0	4,6
	5	48,7	6,2	1 214,5	35,5
	6	437,5	55,6	1 204,2	35,3
sub total, 2 - 6		748,5	95,2	3 062,1	89,6
APEX		38,1	4,8	354,7	10,4
TOTAL:		786,6	100,0	3 416,8	100,0

[1] Mean of six replicates

Table VI summarizes the effects of ringbarking above and below feeder leaves. Analysis of the amount of ^{14}C-assimilate reaching the apical regions of control and ringed plants revealed a reduction of 82,59 and 78,05 % for leaf pairs 2 - 6 of plants ringed above and below feeder leaves, compared with the amount of ^{14}C reaching similar leaves of control plants. The reduction for the apical meristems and first pair of leaves was even greater: 94,62 and 92,50 %.

TABLE VI

REDUCTION IN TOTAL ^{14}C-ASSIMILATE RECOVERED FROM APEX AND YOUNG LEAVES DUE TO RINGBARKING.[1]

	Ring position	2,5 h
REDUCTION IN APICIES COMPARED WITH INTACT CONTROLS (% OF CONTROLS)	below feeder	92,50
	above feeder	94,62
REDUCTION IN TOTAL RECOVERED ^{14}C (FOR LEAVES 2 - 6, % OF CONTROLS)	below feeder	78,05
	above feeder	82,59

[1]Data from Tables I - III.

The increase in percentage of radioactivity in leaf pairs five and six of ringbarked plants (Tables IV and V), compared to the controls (Table III) may be due in part to damage sustained by the external phloem during ringbarking. This damage may have resulted in assimilates being diverted to the internal phloem at the source. After diversion,

leaf pairs five and six, which contained both adaxial and abaxial phloem, could accumulate appreciably more ^{14}C-assimilate. The adaxial and abaxial phloem of these leaves contained mature, functional sieve tubes; the petioles of leaf pairs five and six contained more adaxial than abaxial sieve tubes. Interestingly, ringbarking below the feeder leaf resulted in a greater amount of ^{14}C-assimilate in leaf pair three than would be expected (Table IV). After 2,5 hours, 31,3 percent of the total extracted ^{14}C-assimilate was associated with leaf pair three. It is possible, that after diversion into the internal phloem, that the assimilate could have been rediverted to the abaxial phloem by means of the parenchymatous bridge which exists between the bark and pith in immature stems, especially near the apical meristem. It is notable that in plants ringbarked above the feeder, leaf pair three, after 2,5 hours exposure to $^{14}CO_2$, contained only 7,1 percent of the total extracted ^{14}C-assimilate. Diversion of the assimilate at the source in this instance, appears to be limited to the internal/adaxial phloem system only, ringbarking the external phloem above the feeder leaf exerts a much more marked effect on the ability of the external phloem to continue translocating assimilates than when the external phloem is ringed below the feeder leaf.

The calculated e/i ratio appears to favour the external phloem. This would seem to indicate that, under the experimental conditions, the external phloem translocates more ^{14}C-assimilate per unit time than does the internal phloem. However, any interpretation of these results must of necessity, take into account the anatomical and ultrastructural findings.

Per unit area, more mature, functional internal sieve tubes than external are to be found in stems which lack secondary tissue, and more adaxial

than abaxial sieve tubes in near-mature or mature leaves. At the ultrastructural level, very little callose was observed deposited around sieve plates and lateral sieve areas of the external and abaxial sieve elements. Those of the internal and abaxial phloem were always associated with varying amounts of callose. Callose deposition, other than dormancy callose, is considered to be a fixation artifact by phloem researchers who support a mass or pressure flow mechanism of assimilate translocation. The difference in the amount of callose observed in external/abaxial and internal/adaxial sieve elements does indicate a probable pressure difference between the sieve elements of the two systems. The heavier callose deposition associated with sieve plates and lateral sieve areas of internal/adaxial sieve elements, does indicate that prior to fixation, they were under a greater pressure than the external/abaxial sieve elements.

If the flow rate of assimilates is proportional to the pressure realised within the files of sieve tubes which constitute functional phloem (Canny, 1973), then the infered higher pressure existing in the internal/adaxial phloem would mean that the rate of translocation within the sieve tubes would be greater than the rate in the external/abaxial phloem. This would mean in effect, that appreciably more ^{14}C-assimilates would remain accumulated in the files of external/abaxial sieve tubes within the 10 cm stem segment due to the slower rate of translocation. Thus, the calculated e/i ratio would apparently favour the external phloem. The adaxial phloem could however, account for the greater proportion of assimilate exported from mature leaves, and the internal phloem for a greater proportion of the translocated assimilate in stems lacking secondary tissue per unit time.

Hall et al., (1971), reported that bark incisions of vigorously-growing Ricinus communis resulted in an increase in the rate of translocation of ^{14}C-assimilate in the phloem of treated compared to intact controls. Ringbarking the external phloem of G. physocarpus has been demonstrated to have little or no effect on the translocation of ^{14}C-assimilates within the internal phloem. The report of Hanstein (1864) that organic materials continued to move in the stems of plants which contained both external and internal phloem are confirmed by these results. Further, the results of the experiments reported here show conclusively that mechanical injury results in a very marked decrease in the recorded translocation of ^{14}C-assimilates within the external phloem; more noticeable in plants ringed above than below the feeder leaf. The results of the experiments demonstrate conclusively that the internal and external phloem are physiologically separate and that the internal phloem is capable of translocating assimilates independently of the external phloem.

6.2 Summary

Translocation of ^{14}C-assimilates within the external and internal phloem was investigated using feeding aphids, barkstripping, and ringbarking techniques. Compared with intact controls, ringbarking stems of plants on which colonies of the aphid were feeding, is shown to have no noticeable effect on the translocation of ^{14}C-assimilates within the internal phloem; such treatment has a very pronounced effect on translocation in the external phloem. The import of assimilates by immature leaves was found to be dependent on the external phloem being intact and undamaged. Ringbarking the stem, even 9 - 10 nodes below such young leaves resulted in a marked reduction in the amount of ^{14}C-assimilates reaching these leaves, one to 2,5 hours after initial exposure of the feeder leaf to $^{14}CO_2$.

The results are interpreted as indicating that the external and internal phloem are physiologically distinct from one another, and as being capable of independent translocation of assimilates.

7. CONCLUSIONS

Aphis nerii locates the internal and adaxial phloem strands of Gomphocarpus physocarpus with some degree of precision in most instances, especially where penetration was confined to those areas of the stem which were mature or nearly mature, but in which growth was mostly primary. During the course of penetration of the internal and adaxial phloem strands, the external and abaxial strands were often penetrated, or bypassed in close proximity by the aphid's stylets, without obvious signs of feeding.

A reason suggested by the configuration of the stylets and associated tracks for the lack of evidence of feeding on either external or abaxial phloem strands, was that their sieve tubes were more easily damaged by stylet penetration than were the internal and adaxial phloem sieve tubes, which would render the former non-functional. Interestingly enough, the external and abaxial phloem sieve elements exhibited less signs of protoplast damage caused by the manipulative techniques used during preparation for electron microscopy than the internal and adaxial sieve elements. Callose deposition around sieve plate and sieve area pores was minimal in plasmolysed external and abaxial sieve elements, compared with examples observed in thin sections of internal and adaxial sieve elements. The significance of the fixation artifacts cannot be overlooked in this instance, as viz., callose deposition and the general lack of P-protein (slime) plugs, were also generally conspicuous by their absence in obviously-plasmolysed external and abaxial sieve elements. Internal and adaxial sieve elements which were even mildly plasmolysed during fixation, exhibited partial plugging of sieve area and sieve plate pores. Indirectly then, the marked difference in the fixation images observed between external/abaxial compared with internal/adaxial phloem sieve elements is

a strong indicator that the former functions at a lower osmotic potential than the latter. Many authors state that the flow rate of assimilates is proportional to the osmotic potential realised within the files of sieve tubes which constitutes the functional phloem of all plant species (see Crafts and Crisp, 1971; and Canny, 1973, and literature cited therein). As a consequence, the ultrastructural examination of the primary phloem of Gomphocarpus yields indirect evidence supporting the hypothesis that the internal/adaxial phloem sieve tubes translocate more photosynthetic assimilate per unit time than the external/abaxial sieve tubes.

Light and electron microscope investigation of the ontogeny and differentiation of the primary phloem revealed that even though the external/abaxial phloem begins to differentiate prior to the internal/adaxial phloem the former matures more slowly than the latter. Between nodes three and four, the external and internal primary phloem sieve tubes are equal in number. The result of the early equalization in the numbers of sieve tubes per phloem strand, is that by nodes four and five (and to some extent, in petioles of leaf pairs four-five) there are more mature primary internal (and primary adaxial in leaf) sieve tubes per strand, compared with the primary external/abaxial phloem.

Ringbarking and aphid feeding experiments have provided sufficient evidence that the two phloem systems, viz. the external/abaxial and the internal/adaxial phloem are capable of translocating ^{14}C-assimilates independently. Translocation experiments have revealed that the translocation profile within the internal/adaxial phloem is unaffected by ringbarking the stem, above or below the mature leaf exposed to $^{14}CO_2$.

If the problem posed by the preferential feeding habit of Aphis nerii

is to be elucidated, then cognisance must be taken of the following:

Firstly, the internal/adaxial phloem is capable of unaffected translocation in plants which have severed external/abaxial phloem.

Secondly, the internal /adaxial phloem attains a more advanced stage of maturity earlier than the external/abaxial phloem.

Thirdly, the longevity of the internal/adaxial phloem procambial cells results in strands which contain proportionately more sieve tubes per strand at cessation of primary growth than the corresponding external/abaxial strands.

Fourthly, in petioles of mature leaves, the adaxial protophloem metaphloem sieve tubes, apart from being both longer and wider in cross-section, remain functional throughout the primary stages of growth, whereas most of the sieve plates of the abaxial protophloem sieve elements are associated with massive deposits of definitive callose during the latter stages of primary growth, thus effectively reducing even further the number of functional abaxial phloem sieve tubes per strand. This would result in a decreased ability to translocate assimilates via the abaxial phloem to the external phloem in the stem.

Independent translocation of assimilates by proportionately more sieve tubes, with a larger volume per sieve element, would, in all probability, result in translocation of a greaater proportion of the exported assimilate from the mature leaves to the stem. Hence Aphis nerii preferentially feeds on the internal and adaxial phloem of Gomphocarpus physocarpus.

8. REFERENCES

Adams, J.B. and F.W. Fyfe, 1970: Sterioscan views of some aphid mouthparts. Can. J. Zool. 48, 1033-1036.

Auclair, J.L., 1963: Aphid feeding and nutrition. Ann. Rev. Entomol. 8, 439-491.

Balch, R.E., 1952: Studies on the balsam wooly aphid Adelges piceae (Ratz.) and its effects on the balsam fir, Abies balsamea (L.) Mill. Dept. Agr. Can. Pub. 867.

Botha, C.E.J., C.H. Bornman, M. Carter, and J. Heeg, 1972: Transport studies on Gomphocarpus physocarpus: Observations of the feeding habit of Aphis nerii (B.de F.). Jour S. Afr. Bot. 38, 195-203.

Burr, F.A., and R.F. Evert, 1973: Some aspects of sieve-element structure and development in Selaginella krausiana. Protoplasma 28, 81-97.

Büsgen, M., 1891: Der Honingtau. Biologische studien an Pflanzen und Pflanzenlaüsen. Z. Naturwiss. 25, 339-428.

Buvat, R., 1963a: Infrastructure et differentiation des cellules criblées de Cucurbita pepo. Evolution du tonoplaste et signification du contenue cellulare final. Compt. Rend. Acad. Sci. (Paris) 250, 1528-1530.

_____, 1963b: Infrastructure et differentiation des cellules criblées de Cucurbita pepo. Relations entre la membranes plasmique du cytoplasm. Compt. Rend. Acad. Sci. (Paris) 257, 221-224.

Canny, M.J., 1973: Phloem Translocation. Cambridge University Press. 301p.

Crafts, A.S., and C.E. Crisp, 1971: Phloem Transport in Plants. W.H. Freeman and Co., San Francisco. 481p.

Cronshaw, J., and K. Esau, 1968: P-protein in the phloem of Cucurbita II. The P-protein of mature sieve elements. J. Cell. Biol. 38, 292-303.

Day, M.F., H. Irzykiewicz, and A. McKinnon, 1952: Observations on the feeding habit of the virus vector Orosius argentatus (Evans) and comparisons with certain other jassids. Aust. J. Sci. Res., Ser. Bul. 5 128-142.

Davidson, J., 1923: Biological studies of Aphis rumicus Linn. The penetration of plant tissues and the source of the food supply of aphids. Ann. Appl. Biol. 10, 35-54.

Duloy, M., F.V. Mercer, and N. Rathgeber, 1961: Studies in translocation II, Submicroscopic anatomy of the phloem. Aust. J. Biol. Sci. 14, 506-518.

Esau, K., 1938: Ontogeny and structure of the phloem of tobacco. Hilgardia 11, 343-424.

_____, 1969: The Phloem, Encyclopedia of plant anatomy, Volume 2. Gebrüder Borntraeger, Berlin.

_____, and V.I. Cheadle, 1958: Wall thickening in sieve elements. Proc. Natl. Acad. Sci. U.S. 44, 546-553.

Eschrich, W., 1966: Translokation ^{14}C-Markierter assimilate in licht und dunkeln bei Vicia faba. Planta (Berl.) 70, 99-124.

Evert, R.F., L. Murmanis, and I.B. Sachs, 1966: Another view of the ultrastructure of Cucurbita phloem. Ann. Bot. 30, 563-585.

_____, W. Eschrich, J.T. Medler, and F.J. Alfeiri, 1968: Observations of the penetration of linden branches by stylets of the aphid Longistigma caryae (Han.). Amer. J. Bot. 55, 860-874.

_____, and B.P. Deshpande, 1969: Electron microscope investigation of sieve element ontogeny and structure in Ulmus americana. Protoplasma 68, 403-432.

Evert, R.F., B.P. Deshpande, and S.E. Eichhorn, 1971: Lateral sieve area pores in woody dicotyledons. Canad. J. Bot. 49, 1509-1515.

_____, W, Eschrich, and S.E. Eichhorn, 1973a: P-protein distribution in mature sieve elements of Cucurbita maxima. Planta (Berl.) 109, 193-210.

_____, _____, and _____, 1973b: Observations on the penetration of barley leaves by the aphid, Rhopalosiphum maidis (Fitch) Protoplasma 77, 95-110.

Falk, H., 1969: Fusiform vesicles in plant cells. J. Cell. Biol. 43, 167-174.

Fader, N., and T.P. O'Brien, 1968: Plant microtechnique: Some principles and methods. Amer. J. Bot. 55, 123-142.

Forbes, A.R., 1969: The stylets of the green peach aphid Myzus persicae (Homoptera; Aphididae) Can. Ent. 101, 31-41.

_____, and D.B. Mullick, 1970: The stylets of the balsam wooly aphid Adelges piceae (Homoptera : Adelgidae). Can. Ent. 102, 1074-1082.

_____, and J. Raine, 1973: The stylets of the six-spotted leafhopper, Macrosteles fascifrons (Homoptera : Cicadellidae). Can. Ent. 105, 559-567.

Fritz, E., and W. Eschrich, 1970: ^{14}C-Microautoradiographie waterlöslicher Substanzen im Phloem. Planta (Berl.) 92, 267-281.

Hall, S.M., D.A. Baker, and J.A. Milburn, 1971: Phloem transport of ^{14}C-labelled assimilates in Ricinus. Planta (Berl.) 100, 200-207.

Hanstein, J., 1864: Die Milchsaftgefaese und verwandten Organe der Rinde. Berlin, Wiegandt & Hempel. Cited By Esau, 1969.

Jean, M., 1926: Essai sur lánatomie comparée du liber interna dans quelques familles de Dicotyledons. Etude des plantules. Botaniste Ber. 17, fasc. 5-6, 225864. Cited by Esau, 1969.

Kennedy, J.S., and T.E. Mittler, 1953: A method of obtaining phloem sap via the mouth parts of aphids. Nature 171, 528.

Kinsey, M.G. and D.L. McLean, 1967: Additional evidence that aphids ingest through an open stylet sheath. Ann. Entomol. Soc. Amer. 60, 1263-1265.

MacRobbie, E.A.C., 1971: Phloem translocation. Facts and mechanisms: a comparative survey. Biol. Rev. 46, 429-481.

Metcalfe, C.R., and L. Chalk, 1950: Anatomy of the Dicotyledons, Vol. II p. 917-925. Oxford Clarendon Press.

Miles, P.W., D.L. McLean, and M.G. Kinsey, 1964: Evidence that two species of aphid ingest food through an open stylet sheath. Experimenta 20, 582.

Mittler, T.E., 1957: Studies on the feeding and nutrition of Tuberolachnus salignus (Gmelin) Homoptera Aphidididae 1. The uptake of phloem sap. J. Exp. Biol. 34, 334-341.

Northcote, D.H., and F.B.P. Wooding, 1966: Development of sieve tubes in Acer pseudoplatanus. Proc. Roy. Soc. (London) B. 163, 524-536.

Painter, R.H., 1928: Notes on the injury to plant cells by chinch bug feeding. Ann. Entomol. Soc. Amer. 21, 232-242.

Parrish, W.B., 1967: The origin, morphology, and interpretation of aphid stylets (Homoptera) Ann. Ent. Soc. Amer. 60, 273-276.

Reynolds, E.S., 1963: The use of lead citrate at high pH as an electron-opaque stain in electron microscopy. J. Cell. Biol. 17, 208-212.

Sass, J.E., 1958: Botanical Microtechnique. 3rd ed. Ames: Iowa State College Press.

Sheldrake, A.R., 1972: Auxin transport in secondary tissues. Jour. Exp. Bot. 24, 87-96.

Smith, K.M., 1926: A comparative study of the feeding methods of certain Hemiptera and the resulting effects upon the plant tissue, with special reference to the potato plant. Ann. App. Biol. 13, 109-139.

Tripp. P., and P.R. Gorham, 1968: Bidirectional translocation of sugars in sieve tubes of squash plants. Plant Physiol. 43, 877-882.

Van Hoof, H.A., 1958: Onderzoekingen over de biologische overdracht van een non-persistent virus. Med. No. 161, Van Putten en Dortmeijer, Alkmar, Holland, 19 p. Cited by Auclair, 1963.

Warmbrodt, R.D., and R.F. Evert, 1974: Structure and development of the sieve element in the stem of Lycopodium lucidulum. Amer. J. Bot. 61, 267-277.

Weatherley, P.E., A.J. Peel, and G.P. Hill, 1958: The physiology of the sieve tube. Preliminary experiments using aphid mouth parts. Jour. Exp. Bot. 10, 1-16.

_____, and R.C.P. Johnson, 1968: The form and function of the sieve tubes: A problem in reconciliation. Int. Rev. Cytol. 24, 149-192.

Webb, J.A., and P.R. Gorham, 1964: Translocation of photosynthetically assimilated ^{14}C in strait-necked squash. Plant Physiol. 39, 663-672.

Wooding, F.B.P., and D.H. Northcote, 1965: Association of the endoplasmic reticulum and the plastids in Acer and Pinus. Amer. J. Bot. 52, 526-531.

Zimmermann, M.H., 1961: Movement of organic substances in trees. Science 133, 73-79.

_____, 1963: How sap moves in trees. Scientific American 208, 132-142.

9. ACKNOWLEDGEMENTS

I am grateful to Professor Ray F. Evert, of the Department of Botany, University of Wisconsin-Madison U.S.A., for his unfailing enthusiasm, encouragement and advice given during the course of this investigation, and for his constructive criticism of the research, which was a constant guiding force. I wish to express my sincere thanks to Mr. Danny Walmsley, National Institute for Water Research, for the many hours given to discussion and criticism of the research, and for his generous technical assistance over the last three years. My sincere thanks to Mrs. Mary Carter, late of the Department of Botany, for cheerful and willing help with the operation of the scanning electron microscope. Mrs. Margaret G. Gilliland, Mr. Vijay Bandu and Mr. Phil Evers, Electron Microscope Unit, University of Natal, to whom I am indebted for their cheerful and always enthusiastic assistance in the preparation of transmission electron microscope specimens, and for photographic assistance. Dr. Charles M. Breen and Dr. A.R.A. Noel of the Department of Botany, University of Natal, are acknowledged for advice and discussion of sections of the thesis. My sincere thanks to my wife, Vivien for encouragement, discussion and criticis of the manuscript, and for help in proof reading the final draft of the thesis. In this connection, I wish to thank Miss. Valerie Butler, Department of Botany, University of Natal, Pietermaritzburg, for comments on the structural organization and presentation of the material. Sincere thanks are due to my supervisor, Professor Chris H. Bornman, Department of Botany, University of Natal, Pietermaritzburg, for the generous financial aid awarded, the technical assistance which he made available to me, and for the use of Departmental facilities, during the course of this research project without which much of the work could not have been accomplished. Finally, thank you to Mrs. Jenny Granger for typing this manuscript.